WCAP-16093-NP
Revision 2

July 2007

Analysis of Capsule U from the South Texas Project Nuclear Operating Company, South Texas Unit 2 Reactor Vessel Radiation Surveillance Program

WCAP-16093-NP, Revision 2

Analysis of Capsule U from the South Texas Project Nuclear Operating Company, South Texas Unit 2 Reactor Vessel Radiation Surveillance Program

B. N. Burgos*

July 2007

Approved by: J. S. Carlson, Manager*
Primary Component Asset Management

** Electronically approved records are authenticated in the Electronic Document Management System.*

Westinghouse Electric Company LLC
Energy Systems
P.O. Box 355
Pittsburgh, PA 15230-0355

TABLE OF CONTENTS

LIST OF TABLES iv

LIST OF FIGURES vi

PREFACE viii

EXECUTIVE SUMMARY ix

1 SUMMARY OF RESULTS 1-1

2 INTRODUCTION 2-1

3 BACKGROUND 3-1

4 DESCRIPTION OF PROGRAM 4-1

5 TESTING OF SPECIMENS FROM CAPSULE U 5-1
- 5.1 OVERVIEW 5-1
- 5.2 CHARPY V-NOTCH IMPACT TEST RESULTS 5-3
- 5.3 TENSILE TEST RESULTS 5-5
- 5.4 1/2T COMPACT TENSION SPECIMEN TESTS 5-5

6 RADIATION ANALYSIS AND NEUTRON DOSIMETRY 6-1
- 6.1 INTRODUCTION 6-1
- 6.2 DISCRETE ORDINATES ANALYSIS 6-2
- 6.3 NEUTRON DOSIMETRY 6-5
- 6.4 CALCULATIONAL UNCERTAINTIES 6-6

7 SURVEILLANCE CAPSULE WITHDRAWAL SCHEDULE 7-1

8 REFERENCES 8-1

APPENDIX A VALIDATION OF THE RADIATION TRANSPORT MODELS BASED ON NEUTRON DOSIMETRY MEASUREMENTS A-0

APPENDIX B LOAD-TIME RECORDS FOR CHARPY SPECIMEN TESTS B-0

APPENDIX C CHARPY V-NOTCH PLOTS FOR CAPSULE U USING SYMMETRIC HYPERBOLIC TANGENT CURVE-FITTING METHOD C-0

APPENDIX D SOUTH TEXAS UNIT 2 SURVEILLANCE PROGRAM CREDIBILITY EVALUATION D-0

LIST OF TABLES

Table 4-1 Chemical Composition (wt %) of the South Texas Unit 2 Reactor Vessel Surveillance Materials (Unirradiated) 4-3

Table 4-2 Heat Treatment History of the South Texas Unit 2 Reactor Vessel Surveillance Materials 4-4

Table 5-1 Charpy V-Notch Data for the South Texas Unit 2 Intermediate Shell Plate R2507-1 Irradiated to a Fluence of 2.40 x 10^{19} n/cm^2 (E > 1.0 MeV) (Longitudinal Orientation) 5-6

Table 5-2 Charpy V-Notch Data for the South Texas Unit 2 Intermediate Shell Plate R2507-1 Irradiated to a Fluence of 2.40 x 10^{19} n/cm^2 (E > 1.0 MeV) (Transverse Orientation) 5-7

Table 5-3 Charpy V-notch Data for the South Texas Unit 2 Surveillance Weld Material Irradiated to a Fluence of 2.40 x 10^{19} n/cm^2 (E> 1.0 MeV) 5-8

Table 5-4 Charpy V-notch Data for the South Texas Unit 2 Heat-Affected-Zone (HAZ) Material Irradiated to a Fluence of 2.40 x 10^{19} n/cm^2 (E> 1.0 MeV) 5-9

Table 5-5 Instrumented Charpy Impact Test Results for the South Texas Unit 2 Intermediate Shell Plate R2507-1 Irradiated to a Fluence of 2.40 x 10^{19} n/cm^2 (E> 1.0 MeV) (Longitudinal Orientation) 5-10

Table 5-6 Instrumented Charpy Impact Test Results for the South Texas Unit 2 Intermediate Shell Plate R2507-1 Irradiated to a Fluence of 2.40 x 10^{19} n/cm^2 (E> 1.0 MeV) (Transverse Orientation) 5-11

Table 5-7 Instrumented Charpy Impact Test Results for the South Texas Unit 2 Surveillance Weld Metal Irradiated to a Fluence of 2.40 x 10^{19} n/cm^2 (E> 1.0 MeV) 5-12

Table 5-8 Instrumented Charpy Impact Test Results for the South Texas Unit 2 Heat-Affected-Zone (HAZ) Metal Irradiated to a Fluence of 2.40 x 10^{19} n/cm^2 (E> 1.0MeV) 5-13

Table 5-9 Effect of Irradiation to 2.40 x 10^{19} n/cm^2 (E> 1.0 MeV) on the Capsule U Notch Toughness Properties of the South Texas Unit 2 Reactor Vessel Surveillance Materials 5-14

Table 5-10 Comparison of the South Texas Unit 2 Surveillance Material 30 ft-lb Transition Temperature Shifts and Upper Shelf Energy Decreases with Regulatory Guide 1.99, Revision 2, Predictions 5-15

LIST OF TABLES (Cont.)

Table 5-11 Tensile Properties of the South Texas Unit 2 Capsule U Reactor Vessel Surveillance Materials Irradiated to 2.40 x 10^{19} n/cm^2 (E> 1.0MeV) 5-16

Table 6-1 Calculated Neutron Exposure Rates and Integrated Exposures At The Surveillance Capsule Center 6-13

Table 6-2 Calculated Azimuthal Variation of Maximum Exposure Rates and Integrated Exposures at the Reactor Vessel Clad/Base Metal Interface 6-17

Table 6-3 Calculated Integrated Exposures for Key Vessel Plate and Weld Materials At The Reactor Vessel Clad/Base Metal Interface 6-21

Table 6-4 Relative Radial Distribution Of Neutron Fluence (E > 1.0 MeV) Within The Reactor Vessel Wall 6-23

Table 6-5 Relative Radial Distribution Of Iron Atom Displacements (dpa) Within The Reactor Vessel Wall 6-23

Table 6-6 Calculated Fast Neutron Exposure of Surveillance Capsules Withdrawn from South Texas Project Unit 2 6-24

Table 6-7 Calculated Surveillance Capsule Lead Factors 6-24

Table 7-1 Recommended Surveillance Capsule Withdrawal Schedule 7-1

LIST OF FIGURES

Figure 4-1 Arrangement of Surveillance Capsules in the South Texas Unit 2 Reactor Vessel 4-5

Figure 4-2 Capsule U Diagram Showing the Location of Specimens, Thermal Monitors, and Dosimeters 4-6

Figure 5-1 Charpy V-Notch Impact Energy vs. Temperature for South Texas Unit 2 Reactor Vessel Intermediate Shell Plate R2507-1 (Longitudinal Orientation) 5-17

Figure 5-2 Charpy V-Notch Lateral Expansion vs. Temperature for South Texas Unit 2 Reactor Vessel Intermediate Shell Plate R2507-1 (Longitudinal Orientation) 5-18

Figure 5-3 Charpy V-Notch Percent Shear vs. Temperature for South Texas Unit 2 Reactor Vessel Intermediate Shell Plate R2507-1 (Longitudinal Orientation) 5-19

Figure 5-4 Charpy V-Notch Impact Energy vs. Temperature for South Texas Unit 2 Reactor Vessel Intermediate Shell Plate R2507-1 (Transverse Orientation) 5-20

Figure 5-5 Charpy V-Notch Lateral Expansion vs. Temperature for South Texas Unit 2 Reactor Vessel Intermediate Shell Plate R2507-1 (Transverse Orientation) 5-21

Figure 5-6 Charpy V-Notch Percent Shear vs. Temperature for South Texas Unit 2 Reactor Vessel Intermediate Shell Plate R2507-1 (Transverse Orientation) 5-22

Figure 5-7 Charpy V-Notch Impact Energy vs. Temperature for South Texas Unit 2 Reactor Vessel Weld Metal 5-23

Figure 5-8 Charpy V-Notch Lateral Expansion vs. Temperature for South Texas Unit 2 Reactor Vessel Weld Metal. 5-24

Figure 5-9 Charpy V-Notch Percent Shear vs. Temperature for South Texas Unit 2 Reactor Vessel Weld Metal 5-25

Figure 5-10 Charpy V-Notch Impact Energy vs. Temperature for South Texas Unit 2 Reactor Vessel Heat-Affected-Zone Material 5-26

Figure 5-11 Charpy V-Notch Lateral Expansion vs. Temperature for South Texas Unit 2 Reactor Vessel Heat-Affected-Zone Material 5-27

Figure 5-12 Charpy V-Notch Percent Shear vs. Temperature for South Texas Unit 2 Reactor Vessel Heat-Affected-Zone Material 5-28

Figure 5-13 Charpy Impact Specimen Fracture Surfaces for South Texas Unit 2 Reactor Vessel Intermediate Shell Plate R2507-1 (Longitudinal Orientation) 5-29

LIST OF FIGURES (Cont.)

Figure 5-14 Charpy Impact Specimen Fracture Surfaces for South Texas Unit 2 Reactor Vessel Intermediate Shell Plate R2507-1 (Transverse Orientation) 5-30

Figure 5-15 Charpy Impact Specimen Fracture Surfaces for South Texas Unit 2 Reactor Vessel Weld Metal. 5-31

Figure 5-16 Charpy Impact Specimen Fracture Surfaces for South Texas Unit 2 Reactor Vessel Heat-Affected-Zone Metal 5-32

Figure 5-17 Tensile Properties for South Texas Unit 2 Reactor Vessel Intermediate Shell Plate R2507-1 (Longitudinal Orientation) 5-33

Figure 5-18 Tensile Properties for South Texas Unit 2 Reactor Vessel Intermediate Shell Plate R2507-1 (Transverse Orientation) 5-34

Figure 5-19 Tensile Properties for South Texas Unit 2 Reactor Vessel Weld Metal 5-35

Figure 5-20 Fractured Tensile Specimens from South Texas Unit 2 Reactor Vessel Intermediate Shell Plate R2507-1 (Longitudinal Orientation) 5-36

Figure 5-21 Fractured Tensile Specimens from South Texas Unit 2 Reactor Vessel Intermediate Shell Plate R2507-1 (Transverse Orientation) 5-37

Figure 5-22 Fractured Tensile Specimens from South Texas Unit 2 Reactor Vessel Weld Metal 5-38

Figure 5-23 Engineering Stress-Strain Curves for South Texas Unit 2 Intermediate Shell Plate R2507-1 Tensile Specimens HL-1, HL-2 and HL-3 (Longitudinal Orientation) 5-39

Figure 5-24 Engineering Stress-Strain Curves for South Texas Unit 2 Intermediate Shell Plate R2507-1 Tensile Specimens HT-1, HT-2 and HT-3 (Transverse Orientation) 5-41

Figure 5-25 Engineering Stress-Strain Curves for Weld Metal Tensile Specimens HW-2, HW-2 and HW-3 5-43

Figure 6-1 South Texas Project Unit 2 r,θ Reactor Geometry
- 12.5° Neutron Pad at the Core Midplane 6-8
- 20.0° Neutron Pad at the Core Midplane 6-9
- 22.5° Neutron Pad at the Core Midplane 6-10

Figure 6-2 South Texas Project Unit 2 r,z Reactor Geometry
- with Neutron Pad 6-11
- without Neutron Pad 6-12

PREFACE

Revision 2 has been technically reviewed by:

Reviewer (Revision 2): F.C. Gift*

RECORD OF REVISIONS

Revision 0: Original Issue

Revision 1: Appendix D text was updated to reflect the correct plant name. This change was editorial in nature only.

Revision 2: Additional formatting changes were made to be consistent with the current standards of EDMS. These changes were editorial in nature only.

** Electronically approved records are authenticated in the Electronic Document Management System.*

EXECUTIVE SUMMARY

The purpose of this report is to document the results of the testing of surveillance Capsule U from South Texas Unit 2. Capsule U was removed at 10.31 EFPY and post irradiation mechanical tests of the Charpy V-notch and tensile specimens were performed. A fluence evaluation utilizing the recently released neutron transport and dosimetry cross-section libraries was derived from the ENDF/B-VI data-base. Capsule U received a fluence of 2.40×10^{19} n/cm^2 (E > 1.0 MeV) after irradiation to 10.31 EFPY. The peak clad/base metal interface vessel fluence after 10.31 EFPY of plant operation was 7.52×10^{18} n/cm^2 (E > 1.0 MeV).

This evaluation lead to the following conclusions: 1) The measured 30 ft-lb shift in transition temperature values of the intermediate shell plate R2507-1 contained in capsule U (longitudinal) is less than the Regulatory Guide 1.99, Revision 2[1], predictions. 2) The measured 30 ft-lb shift in transition temperature values of the intermediate shell plate R2507-1 contained in capsule U (transverse) is greater than the Regulatory Guide 1.99, Revision 2, predictions. However, the shift value is less than two sigma allowance by Regulatory Guide 1.99, Revision 2. 3) The measured 30 ft-lb shift in transition temperature values of the weld metal contained in capsule U is less than the Regulatory Guide 1.99, Revision 2, predictions. 4) The measured percent decrease in upper shelf energy for all the surveillance materials of Capsules U contained in the South Texas Unit 2 surveillance program are less than the Regulatory Guide 1.99, Revision 2 predictions. 5) All beltline materials exhibit a more than adequate upper shelf energy level for continued safe plant operation and are predicted to maintain an upper shelf energy greater than 50 ft-lb throughout the current license (34 EFPY) as required by 10CFR50, Appendix G [2]. 6) The South Texas Unit 2 surveillance data was found to be credible. This evaluation can be found in Appendix D.

Lastly, a brief summary of the Charpy V-notch testing can be found in Section 1. All Charpy V-notch data was plotted using a symmetric hyperbolic tangent curve fitting program.

1 SUMMARY OF RESULTS

The analysis of the reactor vessel materials contained in surveillance Capsule U, the third capsule removed and tested from the South Texas Unit 2 reactor pressure vessel, led to the following conclusions:

- The Charpy V-notch data presented in WCAP-14978[3] were based on a re-plot of all capsule data from WCAP-9967[4] and WCAP-13182[5] using CVGRAPH, Version 4.1, which is a symmetric hyperbolic tangent curve-fitting program. The results presented herein only for the Capsule U test results, which are also based on using CVGRAPH, Version 4.1. This report also shows the composite plots that show the results from the previous capsules. Appendix C presents the CVGRAPH, Version 4.1, Charpy V-notch plots and the program input data.

- Capsule U received an average fast neutron fluence (E> 1.0 MeV) of 2.40×10^{19} n/cm^2 after 10.31 effective full power years (EFPY) of plant operation.

- Irradiation of the reactor vessel intermediate shell plate R2507-1 Charpy specimens, oriented with the longitudinal axis of the specimen parallel to the major working direction (longitudinal orientation), resulted in an irradiated 30 ft-lb transition temperature of -10.49°F and an irradiated 50 ft-lb transition temperature of 21.74°F. This results in a 30 ft-lb transition temperature increase of 27.48°F and a 50 ft-lb transition temperature increase of 29.02°F for the longitudinal oriented specimens.

- Irradiation of the reactor vessel intermediate shell plate R2507-1 Charpy specimens, oriented with the longitudinal axis of the specimen perpendicular to the major working direction (transverse orientation), resulted in an irradiated 30 ft-lb transition temperature of 22.23°F and an irradiated 50 ft-lb transition temperature of 65.3°F. This results in a 30 ft-lb transition temperature increase of 40.18°F and a 50 ft-lb transition temperature increase of 47.2°F for the longitudinal oriented specimens.

- Irradiation of the weld metal (heat number 90209) Charpy specimens resulted in an irradiated 30 ft-lb transition temperature of 5.88°F and an irradiated 50 ft-lb transition temperature of 33.53°F. This results in a 30 ft-lb transition temperature increase of 20.64°F and a 50 ft-lb transition temperature increase of 21.47°F.

- Irradiation of the weld Heat-Affected-Zone (HAZ) metal Charpy specimens resulted in an irradiated 30 ft-lb transition temperature of -95.05°F and an irradiated 50 ft-lb transition temperature of -50.42°F. This results in a 30 ft-lb transition temperature increase of 21.84°F and a 50 ft-lb transition temperature increase of 33.77°F.

- The average upper shelf energy of the intermediate shell plate R2507-1 (longitudinal orientation) resulted in no energy decrease after irradiation. This results in an irradiated average upper shelf energy of 138 ft-lb for the longitudinal oriented specimens.

- The average upper shelf energy of the Intermediate Shell Plate R2507-1 (transverse orientation) resulted in no energy decrease after irradiation. This results in an irradiated average upper shelf energy of 98 ft-lb for the longitudinal oriented specimens.

- The average upper shelf energy of the weld metal Charpy specimens resulted in an average energy decrease of 1 ft-lb after irradiation. This results in an irradiated average upper shelf energy of 97 ft-lb for the weld metal specimens.

- The average upper shelf energy of the weld HAZ metal Charpy specimens resulted in an average energy decrease of 26 ft-lb after irradiation. This results in an irradiated average upper shelf energy of 129 ft-lb for the weld HAZ metal.

- A comparison, as presented in Table 5-10, of the South Texas Unit 2 reactor vessel surveillance material test results with the Regulatory Guide 1.99, Revision 2[1] predictions led to the following conclusions:

  — The measured 30 ft-lb shift in transition temperature value of the intermediate shell plate R2507-1 contained in capsule U (longitudinal) is less than the Regulatory Guide 1.99, Revision 2, predictions.

  — The measured 30 ft-lb shift in transition temperature value of the intermediate shell plate R2507-1 contained in capsule U (transverse) is greater than the Regulatory Guide 1.99, Revision 2, predictions. However, the shift value is less than the two sigma allowance by Regulatory Guide 1.99, Revision 2.

  — The measured 30 ft-lb shift in transition temperature value of the weld metal contained in capsule U is less than the Regulatory Guide 1.99, Revision 2, predictions.

  — The measured percent decrease in upper shelf energy for all the surveillance materials of Capsules U contained in the South Texas Unit 2 surveillance program are less than the Regulatory Guide 1.99, Revision 2 predictions.

- All beltline materials exhibit a more than adequate upper shelf energy level for continued safe plant operation and are predicted to maintain an upper shelf energy greater than 50 ft-lb throughout the end of the current license (34 EFPY) as required by 10CFR50, Appendix G [2].

- The calculated end-of-license (34 EFPY) neutron fluence (E> 1.0 MeV) at the core midplane for the South Texas Unit 2 reactor vessel using the Regulatory Guide 1.99, Revision 2 attenuation formula (i.e., Equation #3 in the guide) are as follows:

Calculated: Vessel inner radius* = 2.36×10^{19} n/cm^2

Vessel 1/4 thickness = 1.41×10^{19} n/cm^2

Vessel 3/4 thickness = 4.99×10^{18} n/cm^2

*Clad/base metal interface. (Interpolated From Table 6-2)

2 INTRODUCTION

This report presents the results of the examination of Capsule U, the third capsule removed from the reactor in the continuing surveillance program which monitors the effects of neutron irradiation on the South Texas Project Nuclear Operating Company, South Texas Unit 2 reactor pressure vessel materials under actual operating conditions.

The surveillance program for the South Texas Project Nuclear Operating Company South Texas Unit 2 reactor pressure vessel materials was designed and recommended by the Westinghouse Electric Corporation. A description of the surveillance program and the pre-irradiation mechanical properties of the reactor vessel materials are presented in WCAP-9967, "Houston Lighting & Power Company South Texas Project Unit No. 2 Reactor Vessel Radiation Surveillance Program"[4]. The surveillance program was planned to cover the 40-year design life of the reactor pressure vessel and was based on ASTM E185-79, "Standard Practice for Conducting Surveillance Tests for Light-Water Cooled Nuclear Power Reactor Vessels."[17] Capsule U was removed from the reactor after 10.31 EFPY of exposure and shipped to the Westinghouse Science and Technology Department Hot Cell Facility, where the post-irradiation mechanical testing of the Charpy V-notch impact and tensile surveillance specimens was performed.

This report summarizes the testing of and the post-irradiation data obtained from surveillance capsule U removed from the South Texas Project Nuclear Operating Company South Texas Unit 2 reactor vessel and discusses the analysis of the data.

3 BACKGROUND

The ability of the large steel pressure vessel containing the reactor core and its primary coolant to resist fracture constitutes an important factor in ensuring safety in the nuclear industry. The beltline region of the reactor pressure vessel is the most critical region of the vessel because it is subjected to significant fast neutron bombardment. The overall effects of fast neutron irradiation on the mechanical properties of low alloy, ferritic pressure vessel steels such as SA533 Grade B Class 1 (base material of the South Texas Unit 2 reactor pressure vessel beltline) are well documented in the literature. Generally, low alloy ferritic materials show an increase in hardness and tensile properties and a decrease in ductility and toughness during high-energy irradiation.

A method for ensuring the integrity of reactor pressure vessels has been presented in "Fracture Toughness Criteria for Protection Against Failure," Appendix G to Section XI of the ASME Boiler and Pressure Vessel Code [7]. The method uses fracture mechanics concepts and is based on the reference nil-ductility transition temperature (RT_{NDT}).

RT_{NDT} is defined as the greater of either the drop weight nil-ductility transition temperature (NDTT per ASTM E-208[6]) or the temperature 60°F less than the 50 ft-lb (and 35-mil lateral expansion) temperature as determined from Charpy specimens oriented perpendicular (transverse) to the major working direction of the plate. The RT_{NDT} of a given material is used to index that material to a reference stress intensity factor curve (K_{Ic} curve) which appears in Appendix G to the ASME Code[7]. The K_{Ic} curve is a lower bound of static fracture toughness results obtained from several heats of pressure vessel steel. When a given material is indexed to the K_{Ic} curve, allowable stress intensity factors can be obtained for this material as a function of temperature. Allowable operating limits can then be determined using these allowable stress intensity factors.

RT_{NDT} and, in turn, the operating limits of nuclear power plants can be adjusted to account for the effects of radiation on the reactor vessel material properties. The changes in mechanical properties of a given reactor pressure vessel steel, due to irradiation, can be monitored by a reactor vessel surveillance program, such as the South Texas Unit 2 reactor vessel radiation surveillance program[4], in which a surveillance capsule is periodically removed from the operating nuclear reactor and the encapsulated specimens tested. The increase in the average Charpy V-notch 30 ft-lb temperature (ΔRT_{NDT}) due to irradiation is added to the initial RT_{NDT}, along with a margin (M) to cover uncertainties, to adjust the RT_{NDT} (ART) for radiation embrittlement. This ART (RT_{NDT} initial + M + ΔRT_{NDT}) is used to index the material to the K_{Ic} curve and, in turn, to set operating limits for the nuclear power plant that take into account the effects of irradiation on the reactor vessel materials.

4 DESCRIPTION OF PROGRAM

Six surveillance capsules for monitoring the effects of neutron exposure on the South Texas Unit 2 reactor pressure vessel core region (beltline) materials were inserted in the reactor vessel prior to initial plant start-up. The six capsules were positioned in the reactor vessel between the neutron pads and the vessel wall as shown in Figure 4-1. The vertical center of the capsules is opposite the vertical center of the core. The capsules contain specimens made from intermediate shell plate R2507-1, weld metal fabricated with weld wire Type B4, Heat Number 90209 and Linde Type 124 flux, Lot Number 1061, which is identical to that used in the actual fabrication of the intermediate to lower shell circumferential weld seam and lower shell longitudinal weld seams. The surveillance weld was fabricated with the same heat of weld wire as all beltline region welds and is therefore representative of all of the reactor vessel beltline region welds.

Capsule U was removed after 10.31 effective full power years (EFPY) of plant operation. This capsule contained Charpy V-notch, tensile, and 1/2T-CT fracture mechanics specimens made from Intermediate Shell Plate R2507-1 and submerged arc weld metal representative of all the reactor vessel beltline region weld seams. In addition, this capsule contained Charpy V-notch specimens from the weld Heat-Affected-Zone (HAZ) metal of plate R2507-1.

Test material obtained from the intermediate shell course plate (after thermal heat treatment and forming of the plate) was taken at least one plate thickness from the quenched edges of the plate. All test specimens were machined from the ¼ thickness location of the plate after performing a simulated post-weld stress-relieved treatment on the test material and also from weld and heat-affected-zone metal of a stress-relieved weldment joining intermediate shell plate R2507-1 and adjacent intermediate shell plate R2507-2. All heat-affected-zone specimens were obtained from the weld heat-affected-zone of the Intermediate Shell Plate R2507-1.

Charpy V-notch impact specimens from intermediate shell plate R2507-1 were machined in the longitudinal orientation (longitudinal axis of the specimen parallel to the major working direction) and also in the transverse orientation (longitudinal axis of the specimen perpendicular to the major working direction). The core region weld Charpy impact specimens were machined from the weldment such that the long dimension of each Charpy specimen was perpendicular to the weld direction. The notch of the weld metal Charpy specimens was machined such that the direction of crack propagation in the specimen was in the welding direction.

Tensile specimens from intermediate shell plate R2507-1 were machined in both the longitudinal and transverse orientations. Tensile specimens from the weld metal were oriented with the long dimension of the specimen perpendicular to the weld direction.

Compact tension test specimens from intermediate shell plate R2507-1 were machined in the longitudinal and transverse orientations. Compact tension test specimens from the weld metal were machined perpendicular to the weld direction with the notch oriented in the direction of welding. All specimens were fatigue pre-cracked according to ASTM E399.

The chemical composition and heat treatment of the unirradiated surveillance materials are presented in Tables 4-1 and 4-2, respectively. The data in Table 4-1 and 4-2 was obtained from the unirradiated surveillance program report, WCAP-9967, Appendix A.

Capsule U contained dosimeter wires of pure iron, copper, nickel, and aluminum-0.15 weight percent cobalt (cadmium-shielded and unshielded). In addition, cadmium shielded dosimeters of neptunium (Np^{237}) and uranium (U^{238}) were placed in the capsule to measure the integrated flux at specific neutron energy levels.

The capsule contained thermal monitors made from two low-melting-point eutectic alloys and sealed in Pyrex tubes. These thermal monitors were used to define the maximum temperature attained by the test specimens during irradiation. The composition of the two eutectic alloys and their melting points are as follows:

2.5% Ag, 97.5% Pb	Melting Point: 579°F (304°C)
1.5% Ag, 1.0% Sn, 97.5% Pb	Melting Point: 590°F (310°C)

The arrangement of the various mechanical specimens, dosimeters and thermal monitors contained in Capsule U is shown in Figure 4-2.

Table 4-1 Chemical Composition (wt%) of the South Texas Unit 2 Reactor Vessel Surveillance Materials (Unirradiated)(a)

Element	Intermediate Shell Plate R2507-1	Weld Metal (b)
C	0.220	0.120
Mn	1.550	1.450
P	0.006	0.010
S	0.012	0.011
Si	0.210	0.380
Ni	0.650	0.150
Mo	0.560	0.530
Cr	0.050	0.120
Cu	0.040	0.010
Al	0.021	0.012
Co	0.011	0.013
Pb	<0.001	0.001
W	<0.010	0.005
Ti	<0.010	<0.010
Zr	0.001	<0.001
V	0.002	<0.002
Sn	<0.001	<0.001
As	0.014	0.003
Cb	<0.010	<0.001
N_2	0.009	0.004
B	<0.001	<0.001

Notes:

(a) Data obtained from WCAP-9967 and duplicated herein for completeness.

(b) Weld wire Type B4, Heat Number 90209, Flux Type Linde 124, and Flux Lot Number 1061. Surveillance weldment is from a weld between the intermediate shell plates R2507-1 and R2507-2 and is identical to the intermediate to lower shell circumferential weld seam and the lower shell longitudinal weld seams.

Table 4-2 Heat Treatment History of the South Texas Unit 2 Reactor Vessel Surveillance Materials[a]

Material	Temperature (°F)	Time	Coolant
Intermediate Shell Plate R2507-1	Austenitized @ 1600 ± 25	4 hrs.	Water-Quench
	Tempered @ 1225 ± 25	4 hrs.	Air-cooled
	Stress Relieved[b] @ 1150 ± 50	10 hrs. 30 min.	Furnace Cooled
Weld Metal (heat # 90146)	Stress Relieved[b] @ 1150 ± 50	8 hrs.	Furnace Cooled

Notes:

(a) This table was taken from WCAP-9967[4].

(b) The stress relief heat treatment received by the surveillance test plate and weldment have been simulated.

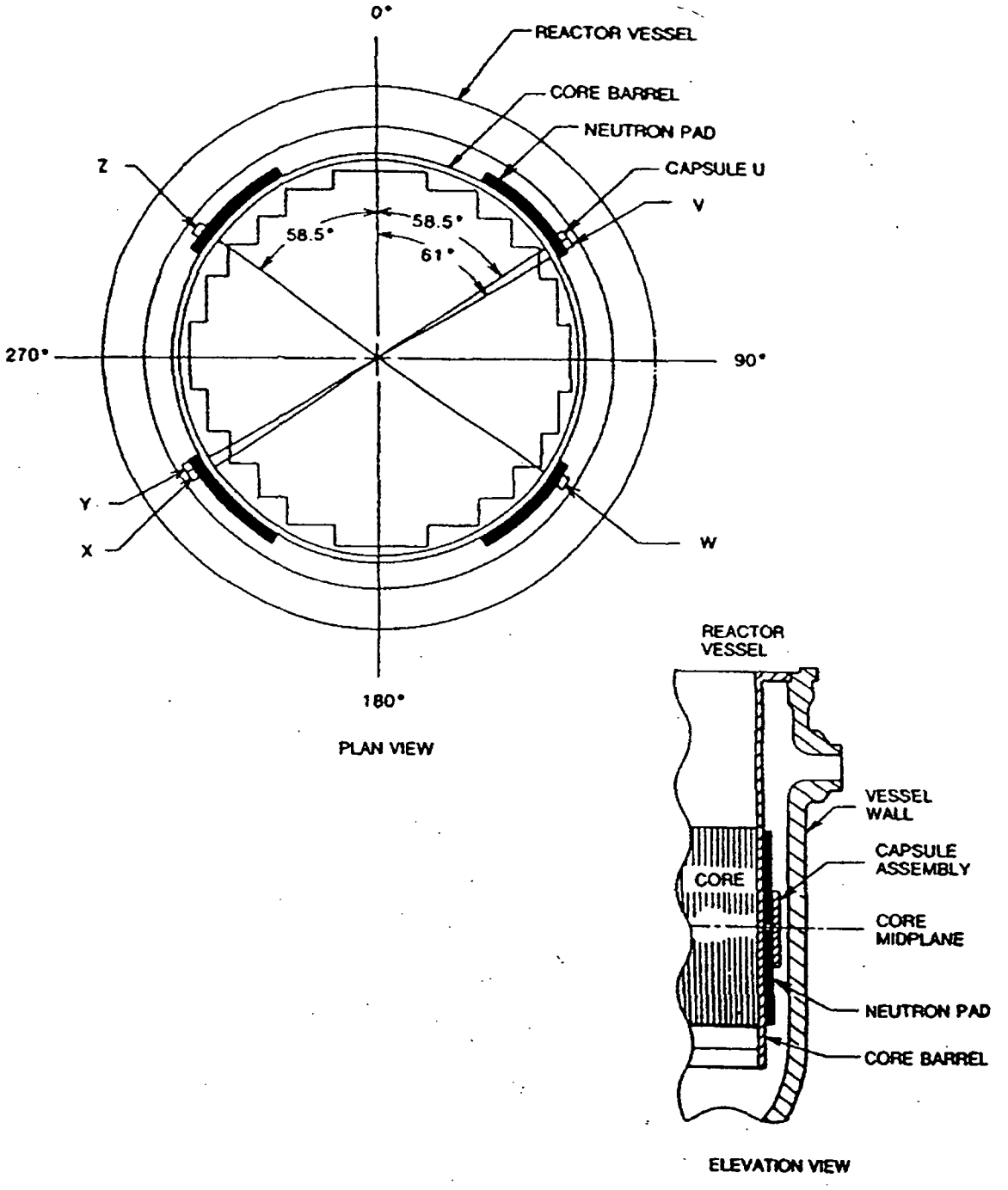

Figure 4-1 Arrangement of Surveillance Capsules in the South Texas Unit 2 Reactor Vessel

LEGEND:

HL - INTERMEDIATE SHELL PLATE R2507-1 (LONGITUDINAL)

HT - INTERMEDIATE SHELL PLATE R2507-1 (TRANSVERSE)

HW - WELD METAL

HH - HEAT-AFFECTED-ZONE MATERIAL

CAPSULE U

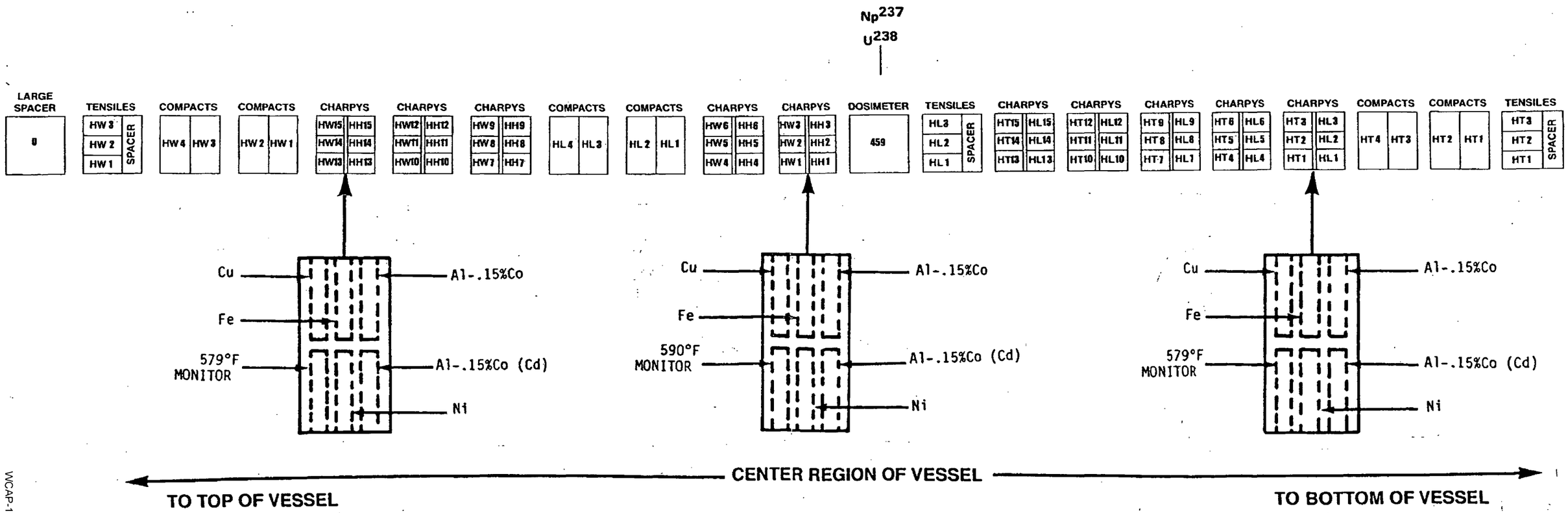

Figure 4-2 Capsule U Diagram Showing The Location of Specimens, Thermal Monitors, and Dosimeters

5 TESTING OF SPECIMENS FROM CAPSULE U

5.1 OVERVIEW

The post-irradiation mechanical testing of the Charpy V-notch impact specimens and tensile specimens was performed in the Remote Metallographic Facility (RMF) at the Westinghouse Research and Technology Park. Testing was performed in accordance with 10CFR50, Appendices G and H[2], ASTM Specification E185-82[8], and Westinghouse Procedure RMF 8402[9], Revision 2 as modified by Westinghouse RMF Procedures 8102[10], Revision 1, and 8103[11], Revision 1.

Upon receipt of the capsule at the hot cell laboratory, the specimens and spacer blocks were carefully removed, inspected for identification number, and checked against the master list in WCAP-9967[4]. No discrepancies were found.

Examination of the two low-melting point 579°F (304°C) and 590°F (310°C) eutectic alloys indicated no melting of either type of thermal monitor. Based on this examination, the maximum temperature to which the test specimens were exposed was less than 579°F (304°C).

The Charpy impact tests were performed per ASTM Specification E23-98[12] and RMF Procedure 8103, Rev. 1, on a Tinius-Olsen Model 74, 358J machine. The tup (striker) of the Charpy impact test machine is instrumented with a GRC 930-I instrumentation system, feeding information into an IBM-compatible computer. With this system, load-time and energy-time signals can be recorded in addition to the standard measurement of Charpy energy (E_D). From the load-time curve (Appendix B), the load of general yielding (P_{GY}), the time to general yielding (t_{GY}), the maximum load (P_M), and the time to maximum load (t_M) can be determined. Under some test conditions, a sharp drop in load indicative of fast fracture was observed. The load at which fast fracture was initiated is identified as the fast fracture load (P_F), and the load at which fast fracture terminated is identified as the arrest load (P_A).

The energy at maximum load (E_M) was determined by comparing the energy-time record and the load-time record. The energy at maximum load is approximately equivalent to the energy required to initiate a crack in the specimen. Therefore, the propagation energy for the crack (E_p) is the difference between the total energy to fracture (E_D) and the energy at maximum load (E_M).

The yield stress (σ_Y) was calculated from the three-point bend formula having the following expression:

$$\sigma_Y = (P_{GY} * L) / [B * (W - a)^2 * C] \quad (1)$$

where: L = distance between the specimen supports in the impact machine
B = the width of the specimen measured parallel to the notch
W = height of the specimen, measured perpendicularly to the notch
a = notch depth

The constant C is dependent on the notch flank angle (ϕ), notch root radius (ρ) and the type of loading (i.e., pure bending or three-point bending). In three-point bending, for a Charpy specimen in which $\phi = 45°$ and $\rho = 0.010$ inch, Equation 1 is valid with C = 1.21. Therefore, (for L = 4W),

$$\sigma_Y = (P_{GY} * L) / [B * (W - a)^2 * 1.21] = (3.305 * P_{GY} * W) / [B * (W - a)^2] \quad (2)$$

For the Charpy specimen, B = 0.394 inch, W = 0.394 inch and a = 0.079 inch. Equation 2 then reduces to:

$$\sigma_Y = 33.3 * P_{GY} \quad (3)$$

where σ_y is in units of psi and P_{GY} is in units of lbs. The flow stress was calculated from the average of the yield and maximum loads, also using the three-point bend formula.

The symbol A in columns 4, 5, and 6 of Tables 5-5 through 5-8 is the cross-section area under the notch of the Charpy specimens:

$$A = B * (W - a) = 0.1241 \text{ sq.in.} \quad (4)$$

Percent shear was determined from post-fracture photographs using the ratio-of-areas methods in compliance with ASTM Specification E23-98 and A370-97a[13]. The lateral expansion was measured using a dial gage rig similar to that shown in the same specification.

Tensile tests were performed on a 20,000-pound Instron, split-console test machine (Model 1115) per ASTM Specification E8-99[14] and E21-92 (1998)[15], and Procedure RMF 8102, Rev. 1. All pull rods, grips, and pins were made of Inconel 718. The upper pull rod was connected through a universal joint to improve axiality of loading. The tests were conducted at a constant crosshead speed of 0.05 inches per minute throughout the test.

Extension measurements were made with a linear variable displacement transducer extensometer. The extensometer knife-edges were spring-loaded to the specimen and operated through specimen failure. The extensometer gage length was 1.00 inch. The extensometer is rated as Class B-2 per ASTM E83-93[16].

Elevated test temperatures were obtained with a three-zone electric resistance split-tube furnace with a 9-inch hot zone. All tests were conducted in air. Because of the difficulty in remotely attaching a thermocouple directly to the specimen, the following procedure was used to monitor specimen temperatures. Chromel-Alumel thermocouples were positioned at the center and at each end of the gage section of a dummy specimen and in each tensile machine griper. In the test configuration, with a slight load on the specimen, a plot of specimen temperature versus upper and lower tensile machine griper and controller temperatures was developed over the range from room temperature to 550°F. During the actual testing, the grip temperatures were used to obtain desired specimen temperatures. Experiments have indicated that this method is accurate to $\pm$2°F.

The yield load, ultimate load, fracture load, total elongation, and uniform elongation were determined directly from the load-extension curve. The yield strength, ultimate strength, and fracture strength were calculated using the original cross-sectional area. The final diameter and final gage length were determined from post-fracture photographs. The fracture area used to calculate the fracture stress (true stress at fracture) and percent reduction in area was computed using the final diameter measurement.

5.2 CHARPY V-NOTCH IMPACT TEST RESULTS

The results of the Charpy V-notch impact tests performed on the various materials contained in Capsule U, which received a fluence of 2.40 x 10^{19} n/cm^2(E> 1.0 MeV) in 10.31 EFPY of operation, are presented in Tables 5-1 through 5-8 and are compared with unirradiated results[4] as shown in Figures 5-1 through 5-12.

The transition temperature increases and upper shelf energy decreases for the Capsule U materials are summarized in Table 5-9 and led to the following results:

- Irradiation of the reactor vessel intermediate shell plate R2507-1 Charpy specimens, oriented with the longitudinal axis of the specimen parallel to the major working direction (longitudinal orientation), resulted in an irradiated 30 ft-lb transition temperature of –10.49°F and an irradiated 50 ft-lb transition temperature of 21.74°F. This results in a 30 ft-lb transition temperature increase of 27.48°F and a 50 ft-lb transition temperature increase of 29.02°F for the longitudinal oriented specimens.

- Irradiation of the reactor vessel intermediate shell plate R2507-1 Charpy specimens, oriented with the longitudinal axis of the specimen perpendicular to the major working direction (transverse orientation), resulted in an irradiated 30 ft-lb transition temperature of 22.23°F and an irradiated 50 ft-lb transition temperature of 65.3°F. This results in a 30 ft-lb transition temperature increase of 40.18°F and a 50 ft-lb transition temperature increase of 47.2°F for the longitudinal oriented specimens.

- Irradiation of the weld metal (heat number 90209) Charpy specimens resulted in an irradiated 30 ft-lb transition temperature of 5.88°F and an irradiated 50 ft-lb transition temperature of 33.53°F. This results in a 30 ft-lb transition temperature increase of 20.64°F and a 50 ft-lb transition temperature increase of 21.47°F.

- Irradiation of the weld Heat-Affected-Zone (HAZ) metal Charpy specimens resulted in an irradiated 30 ft-lb transition temperature of –95.05°F and an irradiated 50 ft-lb transition temperature of –50.42°F. This results in a 30 ft-lb transition temperature increase of 21.84°F and a 50 ft-lb transition temperature increase of 33.77°F.

- The average upper shelf energy of the intermediate shell plate R2507-1 (longitudinal orientation) resulted in no energy decrease after irradiation. This results in an irradiated average upper shelf energy of 138 ft-lb for the longitudinal oriented specimens.

- The average upper shelf energy of the Intermediate Shell Plate R2507-1 (transverse orientation) resulted in no energy decrease after irradiation. This results in an irradiated average upper shelf energy of 98 ft-lb for the longitudinal oriented specimens.

- The average upper shelf energy of the weld metal Charpy specimens resulted in an average energy decrease of 1 ft-lb after irradiation. This results in an irradiated average upper shelf energy of 97 ft-lb for the weld metal specimens.

- The average upper shelf energy of the weld HAZ metal Charpy specimens resulted in an average energy decrease of 26 ft-lb after irradiation. This results in an irradiated average upper shelf energy of 129 ft-lb for the weld HAZ metal.

- A comparison, as presented in Table 5-10, of the South Texas Unit 2 reactor vessel surveillance material test results with the Regulatory Guide 1.99, Revision 2[1] predictions led to the following conclusions:

  — The measured 30 ft-lb shift in transition temperature of the intermediate shell plate R2507-1 contained in capsule U (longitudinal) is less than the Regulatory Guide 1.99, Revision 2, predictions.

  — The measured 30 ft-lb shift in transition temperature of the intermediate shell plate R2507-1 contained in capsule U (transverse) is greater than the Regulatory Guide 1.99, Revision 2, predictions. However, the shift value is less than two sigma allowance by Regulatory Guide 1.99, Revision 2.

  — The measured 30 ft-lb shift in transition temperature of the weld metal contained in capsule U is less than the Regulatory Guide 1.99, Revision 2, predictions.

  — The measured percent decrease in upper shelf energy for all the surveillance materials of Capsules U contained in the South Texas Unit 2 surveillance program are less than the Regulatory Guide 1.99, Revision 2 predictions.

All beltline materials exhibit a more than adequate upper shelf energy level for continued safe plant operation and are predicted to maintain an upper shelf energy greater than 50 ft-lb throughout the end of the current license (34 EFPY) as required by 10CFR50, Appendix G [2].

The fracture appearance of each irradiated Charpy specimen from the various surveillance Capsule U materials is shown in Figures 5-13 through 5-16 and shows an increasingly ductile or tougher appearance with increasing test temperature.

The load-time records for individual instrumented Charpy specimen tests are shown in Appendix B.

The Charpy V-notch data presented in WCAP-14978[3] were based on a re-plot of all capsule data from WCAP-9967[4] and WCAP-13182[5] using CVGRAPH, Version 4.1, which is a symmetric hyperbolic tangent curve-fitting program. The results presented herein only for the Capsule U test results, which are also based on using CVGRAPH, Version 4.1. This report also shows the composite plots that show the results from the previous capsules. Appendix C presents the CVGRAPH, Version 4.1, Charpy V-notch plots and the program input data for Capsule U.

5.3 TENSILE TEST RESULTS

The results of the tensile tests performed on the various materials contained in Capsule U irradiated to 2.40 x 10^{19} n/cm^2 (E> 1.0 MeV) are presented in Table 5-11 and are compared with unirradiated results[4] as shown in Figures 5-17 and 5-19.

The results of the tensile tests performed on the intermediate shell plate R2507-1 (longitudinal orientation) indicated that irradiation to 2.40 x 10^{19} n/cm^2 (E> 1.0 MeV) caused approximately a 6 to 10 ksi increase in the 0.2 percent offset yield strength and approximately a 7 ksi increase in the ultimate tensile strength when compared to unirradiated data[4]. See Figure 5-17.

The results of the tensile tests performed on the intermediate shell plate R2507-1 (transverse orientation) indicated that irradiation to 2.40 x 10^{19} n/cm^2 (E> 1.0 MeV) caused approximately a 4 to 6 ksi increase in the 0.2 percent offset yield strength and approximately a 4 to 6 ksi increase in the ultimate tensile strength when compared to unirradiated data[4]. See Figure 5-18.

The results of the tensile tests performed on the surveillance weld metal indicated that irradiation to 2.40 x 10^{19} n/cm^2 (E> 1.0 MeV) caused approximately a 2 ksi increase in the 0.2 percent offset yield strength and approximately a 2 to 3 ksi increase in the ultimate tensile strength when compared to unirradiated data[4]. See Figure 5-19.

The fractured tensile specimens for the intermediate shell plate R2507-1 material are shown in Figures 5-20 and 5-21, while the fractured tensile specimens for the surveillance weld metal are shown in Figure 5-22. The engineering stress-strain curves for the tensile tests are shown in Figures 5-23 through 5-25.

5.4 1/2T COMPACT TENSION SPECIMEN TESTS

Per the surveillance capsule testing contract, the 1/2T Compact Tension Specimens were not tested and are being stored at the Westinghouse Research and Technology Park Hot Cell facility.

Table 5-1 Charpy V-notch Data for the South Texas Unit 2 Intermediate Shell Plate R2507-1 Irradiated to a Fluence of 2.40×10^{19} n/cm^2 (E > 1.0 MeV) - (Longitudinal Orientation)

Sample	Temperature		Impact Energy		Lateral Expansion		% Shear
Number	°F	°C	ft-lbs	Joules	mils	mm	%
HL14	-50	-46	7	9	1	0.03	2
HL7	-25	-32	28	38	15	0.38	10
HL6	0	-18	22	30	11	0.28	15
HL1	10	-12	46	62	28	0.71	15
HL8	20	-7	58	79	35	0.89	25
HL9	40	4	60	81	37	0.94	30
HL12	50	10	68	92	40	1.02	40
HL15	75	24	107	145	63	1.60	75
HL13	100	38	105	142	65	1.65	85
HL3	125	52	105	142	70	1.78	85
HL10	150	66	127	172	75	1.91	100
HL11	175	79	127	172	78	1.98	90
HL5	200	93	144	195	82	2.08	100
HL4	225	107	143	194	81	2.06	100
HL2	250	121	133	180	78	1.98	100

Table 5-2 Charpy V-notch Data for the South Texas Unit 2 Intermediate Shell Plate R2507-1 Irradiated to a Fluence of 2.40×10^{19} n/cm^2 (E > 1.0 MeV) (Transverse Orientation)

Sample	Temperature		Impact Energy		Lateral Expansion		Shear
Number	°F	°C	ft-lbs	Joules	mils	mm	%
HT11	-75	-59	2	3	0	0.00	2
HT3	-50	-46	10	14	1	0.03	5
HT4	-25	-32	24	33	10	0.25	10
HT6	0	-18	22	30	11	0.28	10
HT7	25	-4	32	43	18	0.46	15
HT8	50	10	35	47	20	0.51	20
HT10	60	16	50	68	30	0.76	25
HT12	75	24	59	80	31	0.79	35
HT9	100	38	64	87	44	1.12	60
HT2	125	52	79	107	51	1.30	80
HT14	150	66	79	107	50	1.27	85
HT1	190	88	101	137	67	1.70	100
HT13	225	107	102	138	63	1.60	100
HT15	250	121	108	146	66	1.68	100
HT5	275	135	104	141	69	1.75	100

Table 5-3 Charpy V-notch Data for the South Texas Unit 2 Surveillance Weld Metal Irradiated to a Fluence of 2.40 x 10^{19} n/cm^2 (E> 1.0 MeV)

Sample	Temperature		Impact Energy		Lateral Expansion		Shear
Number	°F	°C	ft-lbs	Joules	mils	mm	%
HW6	-75	-59	4	5	0	0.00	10
HW15	-50	-46	10	14	3	0.08	15
HW9	-25	-32	17	23	10	0.25	25
HW10	0	-18	28	38	20	0.51	45
HW12	10	-12	28	38	20	0.51	40
HW8	30	-1	41	56	25	0.64	65
HW3	50	10	72	98	50	1.27	75
HW4	50	10	64	87	45	1.14	70
HW14	75	24	74	100	51	1.30	85
HW2	125	52	94	127	64	1.63	95
HW5	150	66	86	117	62	1.57	95
HW7	200	93	91	123	63	1.60	98
HW13	225	107	97	132	67	1.70	98
HW11	250	121	96	130	71	1.80	100
HW1	275	135	104	141	70	1.78	100

Table 5-4 Charpy V-notch Data for the South Texas Unit 2 Heat-Affected-Zone (HAZ) Material Irradiated to a Fluence of 2.40×10^{19} n/cm^2 (E> 1.0 MeV)

Sample	Temperature		Impact Energy		Lateral Expansion		Shear
Number	°F	°C	Ft-lbs	Joules	mils	mm	%
HH3	-200	-129	6	8	0	0.00	2
HH2	-150	-101	7	9	1	0.03	2
HH4	-125	-87	13	18	4	0.10	5
HH7	-108	-78	30	41	11	0.28	10
HH14	-75	-59	52	71	18	0.46	15
HH5	-50	-46	36	49	15	0.38	35
HH11	-25	-32	56	76	26	0.66	55
HH10	0	-18	90	122	52	1.32	80
HH8	25	-4	130	176	75	1.91	100
HH15	50	10	61	83	35	0.89	55
HH9	75	24	96	130	53	1.35	70
HH12	125	52	115	156	65	1.65	100
HH6	150	66	114	155	53	1.35	100
HH13	175	79	144	195	73	1.85	100
HH1	200	93	143	194	76	1.93	100

Table 5-5 Instrumented Charpy Impact Test Results for the South Texas Unit 2 Intermediate Shell Plate R2507-1 Irradiated to a Fluence of 2.40 x 10^{19} n/cm^2 (E>1.0 MeV) (Longitudinal Orientation)

Sample No.	Test Temp. (°F)	Charpy Energy E_D (ft-lb)	Normalized Energies (ft-lb/in^2)			Yield Load P_{GY} (lb)	Time to Yield t_{GY} (msec)	Max Load P_M (lb)	Time to Max t_M (msec)	Fast Fract Load P_F (lb)	Arrest Load P_A (lb)	Yield Stress σ_Y (ksi)	Flow Stress (ksi)
			Charpy E_D/A	Max. E_M/A	Prop. E_P/A								
HL14	-50	7	56	35	21	3405	0.14	3548	0.16	3538	0	113	116
HL7	-25	28	226	194	32	3487	0.15	4533	0.44	4533	0	116	134
HL6	0	22	177	63	114	3284	0.14	4125	0.21	3856	274	109	123
HL1	10	46	371	316	55	3393	0.15	4533	0.66	4530	0	113	132
HL8	20	58	467	331	136	3596	0.15	4668	0.67	4549	0	120	138
HL9	40	60	483	320	164	3346	0.14	4516	0.68	4431	0	111	131
HL12	50	68	548	314	234	3329	0.15	4417	0.68	4158	262	111	129
HL15	75	107	862	323	539	3326	0.14	4490	0.69	3367	955	111	130
HL13	100	105	846	313	533	3232	0.15	4398	0.68	2956	1418	108	127
HL3	125	105	846	321	525	3235	0.15	4395	0.70	2869	1106	108	127
HL10	150	127	1023	304	720	3047	0.14	4254	0.68	n/a	n/a	101	122
HL11	175	127	1023	303	720	3053	0.14	4282	0.69	1132	617	102	122
HL5	200	144	1160	299	862	3064	0.15	4282	0.68	n/a	n/a	102	122
HL4	225	143	1152	298	855	2873	0.16	4206	0.70	n/a	n/a	96	118
HL2	250	133	1072	322	750	2975	0.15	4230	0.74	n/a	n/a	99	120

Table 5-6 Instrumented Charpy Impact Test Results for the South Texas Unit 2 Intermediate Shell Plate R2507-1 Irradiated to a Fluence of 2.40×10^{19} n/cm^2 (E>1.0 MeV) (Transverse Orientation)

Sample No.	Test Temp. (°F)	Charpy Energy E_D (ft-lb)	Normalized Energies (ft-lb/in^2)			Yield Load P_{GY} (lb)	Time to Yield t_{GY} (msec)	Max. Load P_M (lb)	Time to Max. t_M (msec)	Fast Fract. Load P_F (lb)	Arrest Load P_A (lb)	Yield Stress σ_Y (ksi)	Flow Stress (ksi)
			Charpy E_D/A	Max. E_M/A	Prop. E_P/A								
HT11	-75	2	16	9	8	1098	0.09	1190	0.10	1173	0	37	38
HT3	-50	10	81	44	37	3847	0.15	4034	0.17	4034	0	128	131
HT4	-25	24	193	155	38	3474	0.14	4384	0.37	4379	0	116	131
HT6	0	22	177	66	111	3384	0.14	4259	0.22	4194	0	113	127
HT7	25	32	258	193	65	3496	0.14	4472	0.44	4472	0	116	133
HT8	50	35	282	186	96	3313	0.14	4287	0.44	4273	591	110	127
HT10	60	50	403	226	177	3345	0.14	4387	0.52	4358	425	111	129
HT12	75	59	475	325	150	3402	0.15	4518	0.69	4433	389	113	132
HT9	100	64	516	309	207	3323	0.15	4403	0.67	4373	1204	111	129
HT2	125	79	637	304	333	3184	0.15	4355	0.67	4180	2169	106	126
HT14	150	79	637	299	337	3151	0.14	4262	0.67	3915	1313	105	123
HT1	190	101	814	284	530	3007	0.14	4072	0.66	n/a	n/a	100	118
HT13	225	102	822	290	532	3041	0.14	4171	0.66	n/a	n/a	101	120
HT15	250	108	870	284	586	2934	0.14	4124	0.67	n/a	n/a	98	118
HT5	275	104	838	288	550	2862	0.17	4004	0.70	n/a	n/a	95	114

Table 5-7 Instrumented Charpy Impact Test Results for the South Texas Unit 2 Surveillance Weld Metal Irradiated to a Fluence of 2.40×10^{19} n/cm^2 (E>1.0 MeV)

Sample No.	Test Temp. (°F)	Charpy Energy E_D (ft-lb)	Normalized Energies (ft-lb/in²)			Yield Load P_{GY} (lb)	Time to Yield t_{GY} (msec)	Max. Load P_M (lb)	Time to Max. t_M (msec)	Fast Fract. Load P_F (lb)	Arrest Load P_A (lb)	Yield Stress σ_Y (ksi)	Flow Stress (ksi)
			Charpy E_D/A	Max. E_M/A	Prop. E_P/A								
HW6	-75	4	32	16	17	1929	0.11	2031	0.12	2009	0	64	66
HW15	-50	10	81	40	40	3631	0.14	3915	0.16	3903	0	121	126
HW9	-25	17	137	46	90	3741	0.15	4049	0.18	4035	784	125	130
HW10	0	28	226	63	163	3504	0.14	4216	0.21	4216	1616	117	129
HW12	10	28	226	146	79	3516	0.14	4347	0.36	4332	488	117	131
HW8	30	41	330	72	258	3621	0.17	4196	0.24	4196	2650	121	130
HW3	50	72	580	231	349	3437	0.15	4385	0.52	4086	1576	114	130
HW4	50	64	516	229	287	3355	0.15	4376	0.52	4219	1347	112	129
HW14	75	74	596	221	375	3322	0.15	4396	0.50	4171	2403	111	129
HW2	125	94	757	294	464	3177	0.15	4185	0.66	2960	2164	106	123
HW5	150	86	693	286	407	3127	0.14	4194	0.65	3236	2704	104	122
HW7	200	91	733	211	522	3142	0.14	4208	0.50	2698	2225	105	122
HW13	225	97	782	286	496	3030	0.14	4104	0.66	2816	2475	101	119
HW11	250	96	774	290	484	2948	0.14	4133	0.66	n/a	n/a	98	118
HW1	275	104	838	272	566	2878	0.15	3902	0.67	n/a	n/a	96	113

Table 5-8 Instrumented Charpy Impact Test Results for the South Texas Unit 2 Heat-Affected-Zone (HAZ) Metal Irradiated to a Fluence of 2.40 x 10^{19} n/cm^2 (E>1.0 MeV)

Sample No.	Test Temp. (°F)	Charpy Energy E_D (ft-lb)	Normalized Energies (ft-lb/in^2) Charpy E_D/A	Max. E_M/A	Prop. E_p/A	Yield Load P_{GY} (lb)	Time to Yield t_{GY} (msec)	Max. Load P_M (lb)	Time to Max. t_M (msec)	Fast Fract. Load P_F (lb)	Arrest Load P_A (lb)	Yield Stress σ_Y (ksi)	Flow Stress (ksi)
HH3	-200	6	48	20	28	2642	0.13	2642	0.13	2639	0	88	88
HH2	-150	7	56	49	7	3771	0.27	3771	0.27	3761	0	126	126
HH4	-125	13	105	69	35	4740	0.17	5230	0.21	5204	0	158	166
HH7	-108	30	242	200	42	4167	0.19	4949	0.44	4937	0	139	152
HH14	-75	52	419	264	155	4067	0.16	4941	0.52	4825	0	135	150
HH5	-50	36	290	75	215	4131	0.16	4808	0.22	4743	771	138	149
HH11	-25	56	451	247	204	3911	0.15	4754	0.50	4690	1746	130	144
HH10	0	90	725	239	486	3661	0.15	4684	0.51	4107	1832	122	139
HH8	25	130	1047	350	698	3947	0.21	4760	0.72	n/a	n/a	131	145
HH15	50	61	491	246	245	3886	0.15	4777	0.51	4630	1833	129	144
HH9	75	96	774	330	443	3678	0.15	4800	0.66	3979	3027	122	141
HH12	125	115	927	325	601	3405	0.15	4594	0.68	n/a	n/a	113	133
HH6	150	114	919	326	592	3430	0.16	4529	0.69	n/a	n/a	114	133
HH13	175	144	1160	326	835	3452	0.15	4492	0.69	n/a	n/a	115	132
HH1	200	143	1152	319	833	3258	0.16	4476	0.70	n/a	n/a	108	129

Table 5-9 Effect of Irradiation to 2.40 x 10^{19} n/cm^2 (E>1.0 MeV) on the Capsule U Notch Toughness Properties of the South Texas Unit 2 Reactor Vessel Surveillance Materials

Material	Average 30 (ft-lb)[a] Transition Temperature (°F)			Average 35 mil Lateral[b] Expansion Temperature (°F)			Average 50 ft-lb[a] Transition Temperature (°F)			Average Energy Absorption[a] at Full Shear (ft-lb)		
	Unirradiated	Irradiated	ΔT_{30}	Unirradiated	Irradiated	ΔT	Unirradiated	Irradiated	ΔT_{50}	Unirradiated	Irradiated	ΔE
Intermediate Shell Plate R2507-1 (Long.)	-37.97	-10.49	27.48	-0.9	32.43	33.33	-7.27	21.74	29.02	138	140	+2
Intermediate Shell Plate R2507-1 (Trans.)	-17.95	22.23	40.18	25.62	81.98	56.35	18.1	65.3	47.2	98	104	+6
Weld Metal (Heat # 90209)	-14.76	5.88	20.64	9.76	35.43	25.66	12.06	33.53	21.47	98	97	-1
HAZ Metal	-116.9	-95.05	21.84	-60.75	-21.39	39.36	-84.2	-50.42	33.77	155	129	-26

a. "Average" is defined as the value read from the curve fit through the data points of the Charpy tests (see Figures 5-1, 5-4, 5-7 and 5-10).

b. "Average" is defined as the value read from the curve fit through the data points of the Charpy tests (see Figures 5-2, 5-5, 5-8 and 5-11).

Table 5-10 Comparison of the South Texas Unit 2 Surveillance Material 30 ft-lb Transition Temperature Shifts and Upper Shelf Energy Decreases with Regulatory Guide 1.99, Revision 2, Predictions

Material	Capsule	Fluence[d] ($\times 10^{19}$ n/cm^2, E > 1.0 MeV)	30 ft-lb Transition Temperature Shift		Upper Shelf Energy Decrease	
			Predicted (°F)[a]	Measured (°F)[b]	Predicted (%)[a]	Measured (%)[b]
Intermediate Shell Plate R2507-1 (Longitudinal)	V	0.23	15.60	16.39	14	0
	Y	1.21	27.30	33.96	20	4
	U	2.40	32.24	27.48	23	0
Intermediate Shell Plate R2507-1 (Transverse)	V	0.23	15.60	11.86	14	0
	Y	1.21	27.30	35.26	20	0
	U	2.40	32.24	40.18	23	0
Surveillance Program Weld Metal	V	0.23	14.70	0[c]	14	5
	Y	1.21	25.73	4.08	20	0
	U	2.40	30.38	20.64	23	1
Heat Affected Zone Material	V	0.23	---	0[c]	---	12
	Y	1.21	---	54.2	---	12
	U	2.40	---	21.84	---	17

Notes:

(a) Based on Regulatory Guide 1.99, Revision 2, methodology using the mean weight percent values of copper and nickel of the surveillance material.

(b) Calculated using measured Charpy data plotted using CVGRAPH, Version 4.1 (See Appendix C)

(c) Values are based on the definition of upper shelf energy given in ASTM E185-82.

(d) The fluence values presented here are the calculated values, not the best estimate values.

(e) Due to the scatter in the capsule V weld and HAZ Charpy test results, a true Hyperbolic Tangent Curve fit resulted in ΔT_{30} values of –7.6°F and –0.76°F, respectively, when compared to unirradiated Charpy test data. Physically this should not happen. Hence, based on engineering judgement a value of 0°F will be used in RT_{NDT} calculations.

Table 5-11 Tensile Properties of the South Texas Unit 2 Capsule U Reactor Vessel Surveillance Materials Irradiated to 2.40 x 10^{19} n/cm^2 (E > 1.0 MeV)

Material	Sample Number	Test Temp. (°F)	0.2% Yield Strength (ksi)	Ultimate Strength (ksi)	Fracture Load (kip)	Fracture Stress (ksi)	Fracture Strength (ksi)	Uniform Elongation (%)	Total Elongation (%)	Reduction in Area (%)
Inter. Shell Plate R2507-1 (Long.)	HL 2	75	75.5	96.3	3.1	167.4	62.1	11.3	24.9	63
	HL 1	300	72.7	89.8	2.9	171.4	58.9	9.0	19.0	66
	HL 3	550	66.0	93.5	3.2	166.3	64.2	11.0	22.1	61
Inter. Shell Plate R2507-1 (Trans.)	HT 3	75	74.4	94.8	3.2	173.5	64.4	10.5	22.0	63
	HT 2	300	67.5	86.7	3.3	157.6	66.8	9.7	19.5	58
	HT 1	550	65.4	91.1	4.0	139.4	81.1	9.0	14.0	42
Weld Metal	HW 1	75	77.8	91.8	2.8	186.0	57.2	11.8	24.5	69
	HW 3	300	72.3	87.0	2.9	192.8	58.1	9.0	20.8	70
	HW 2	550	71.6	91.6	3.2	163.0	64.4	10.2	21.4	61

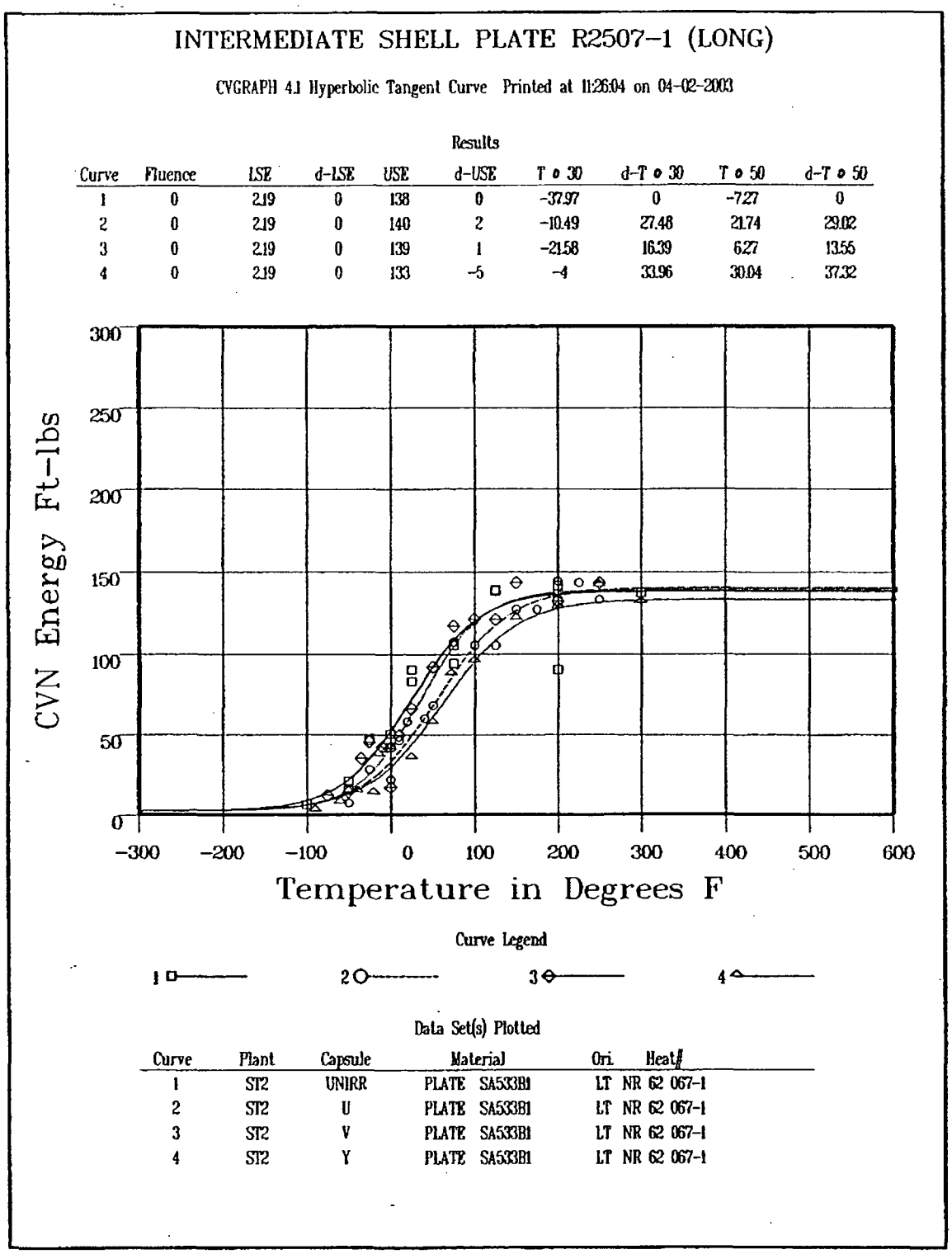

Figure 5-1 Charpy V-Notch Impact Energy vs. Temperature for South Texas Unit 2 Reactor Vessel Intermediate Shell Plate R2507-1 (Longitudinal Orientation)

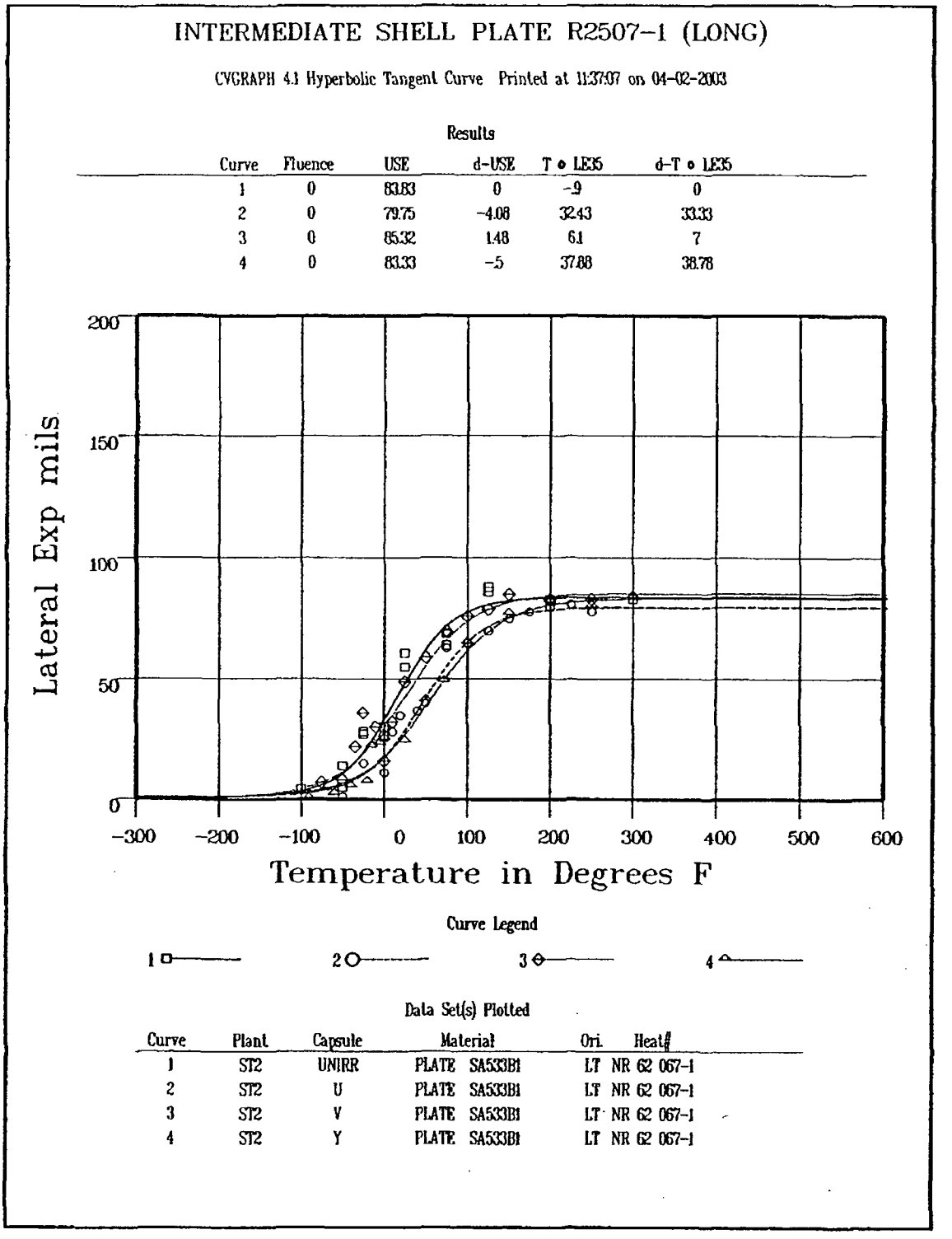

Figure 5-2 Charpy V-Notch Lateral Expansion vs. Temperature for South Texas Unit 2 Reactor Vessel Intermediate Shell Plate R2507-1 (Longitudinal Orientation)

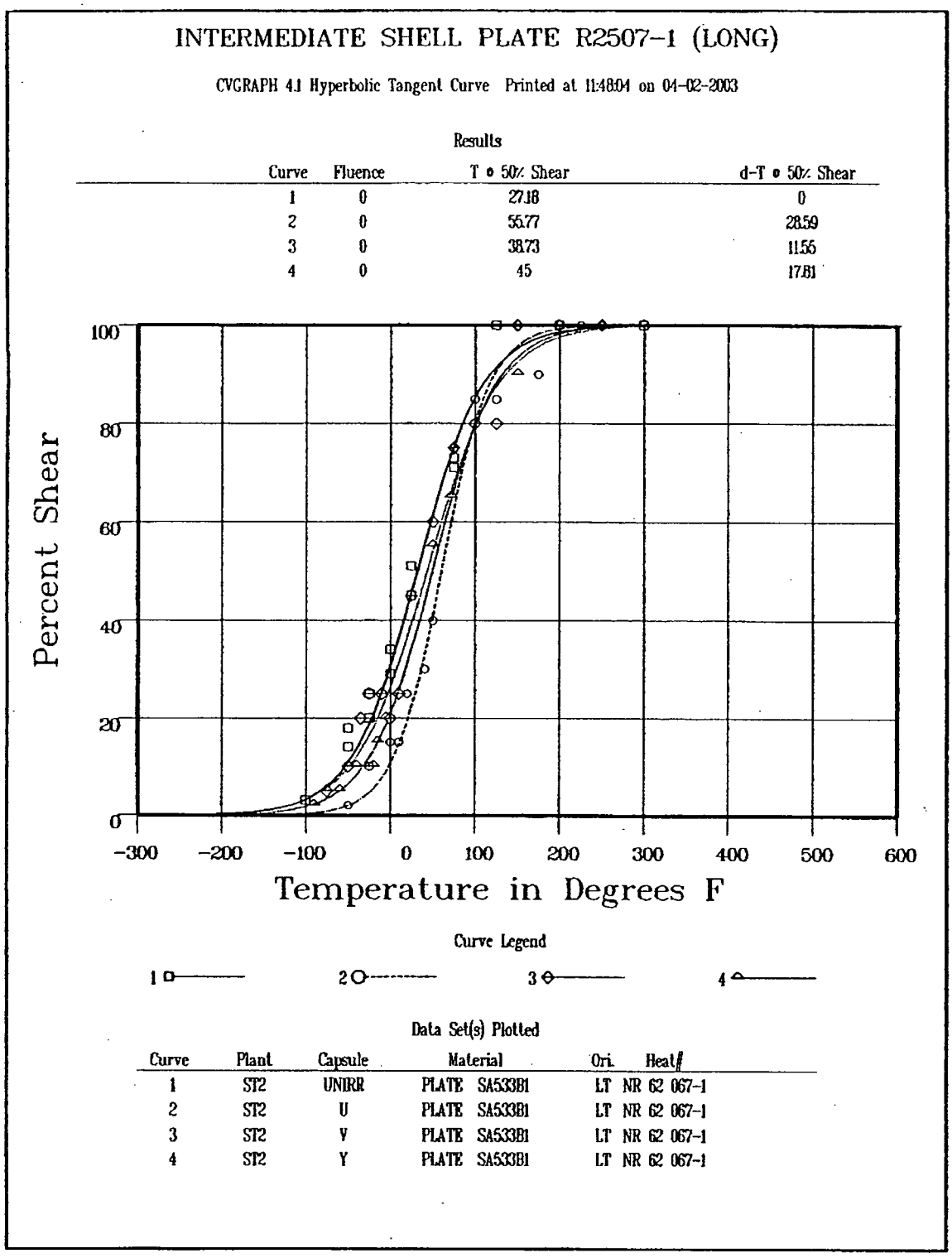

Figure 5-3 Charpy V-Notch Percent Shear vs. Temperature for South Texas Unit 2 Reactor Vessel Intermediate Shell Plate R2507-1 (Longitudinal Orientation)

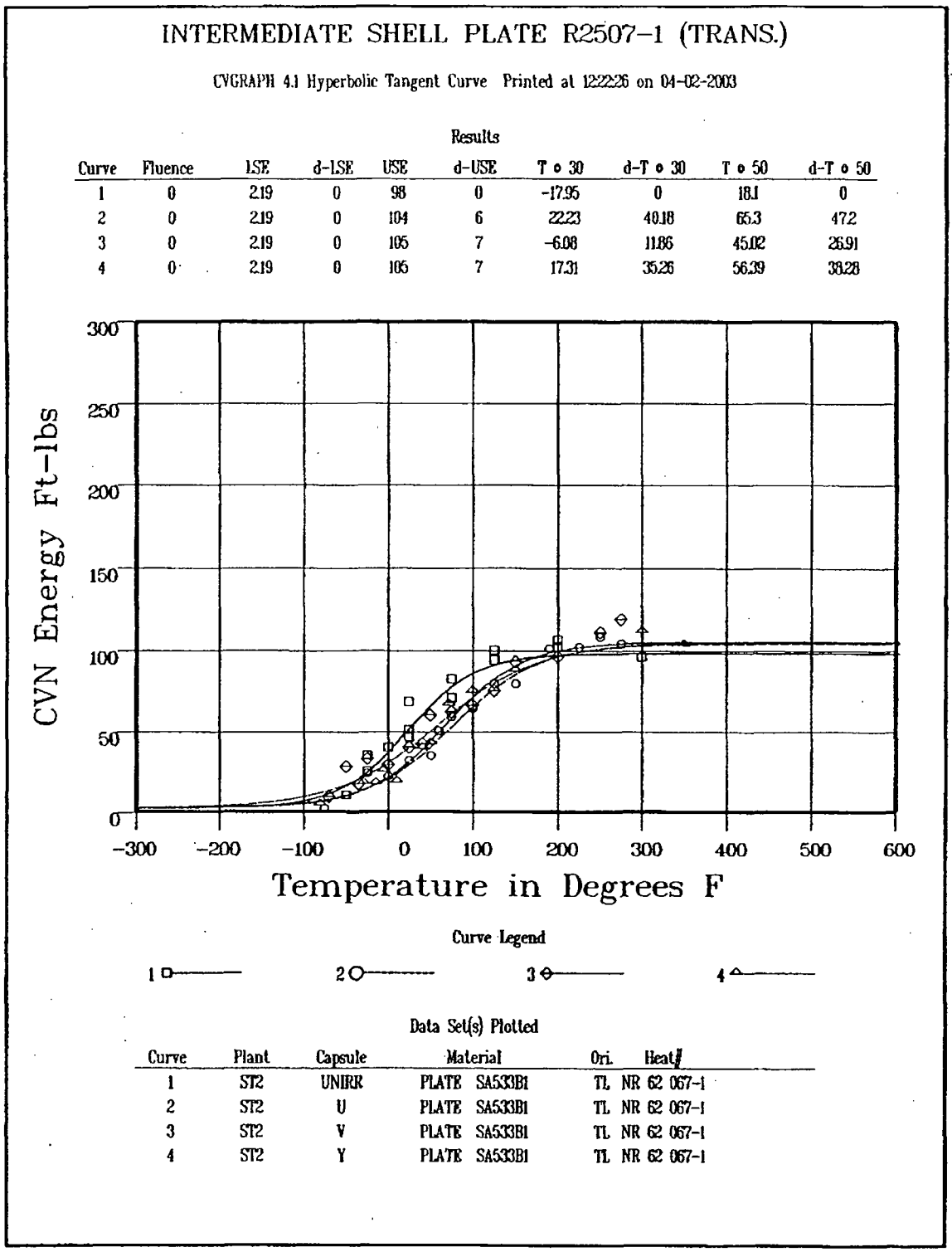

Figure 5-4 Charpy V-Notch Impact Energy vs. Temperature for South Texas Unit 2 Reactor Vessel Intermediate Shell Plate R2507-1 (Transverse Orientation)

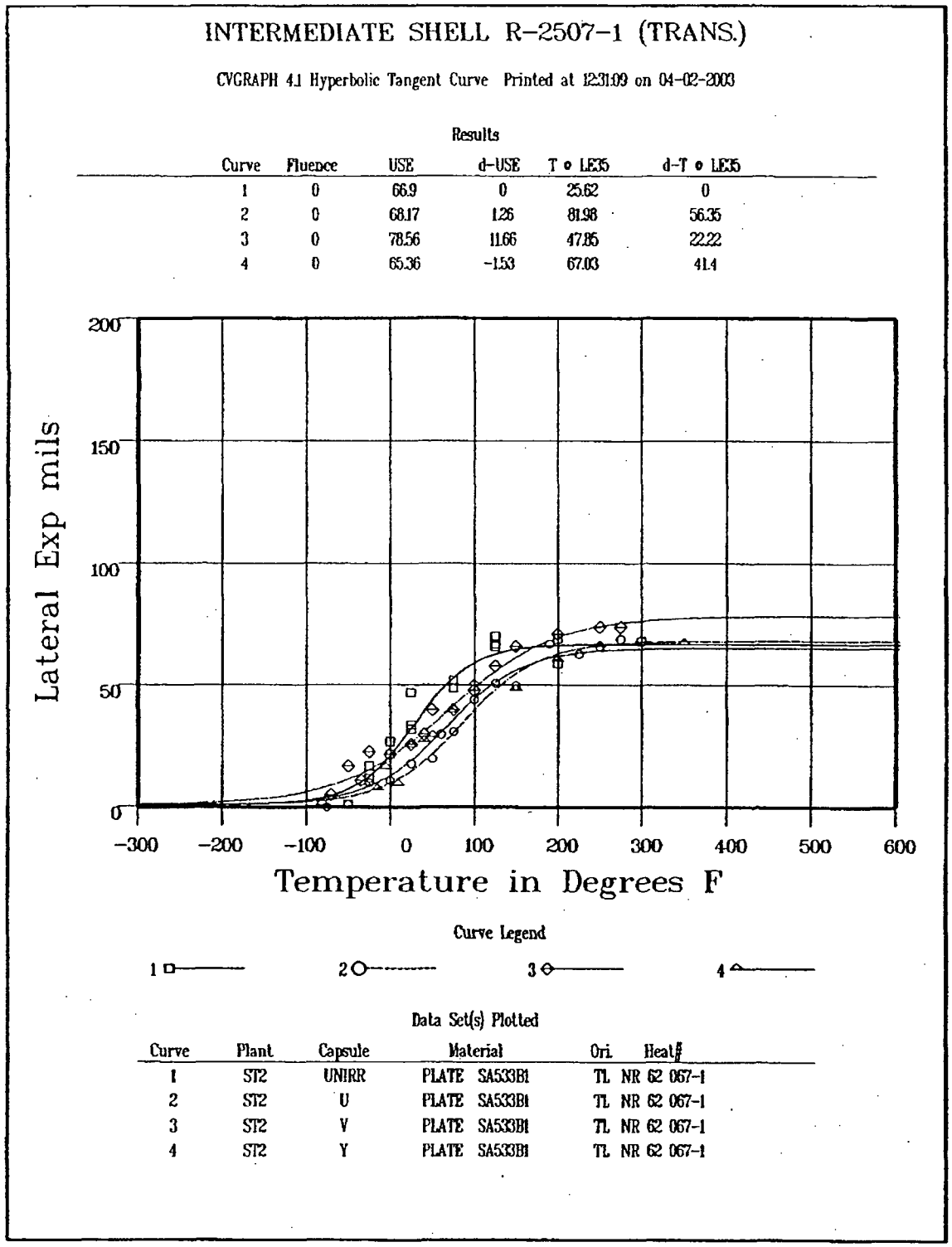

Figure 5-5 Charpy V-Notch Lateral Expansion vs. Temperature for South Texas Unit 2 Reactor Vessel Intermediate Shell Plate R2507-1 (Transverse Orientation)

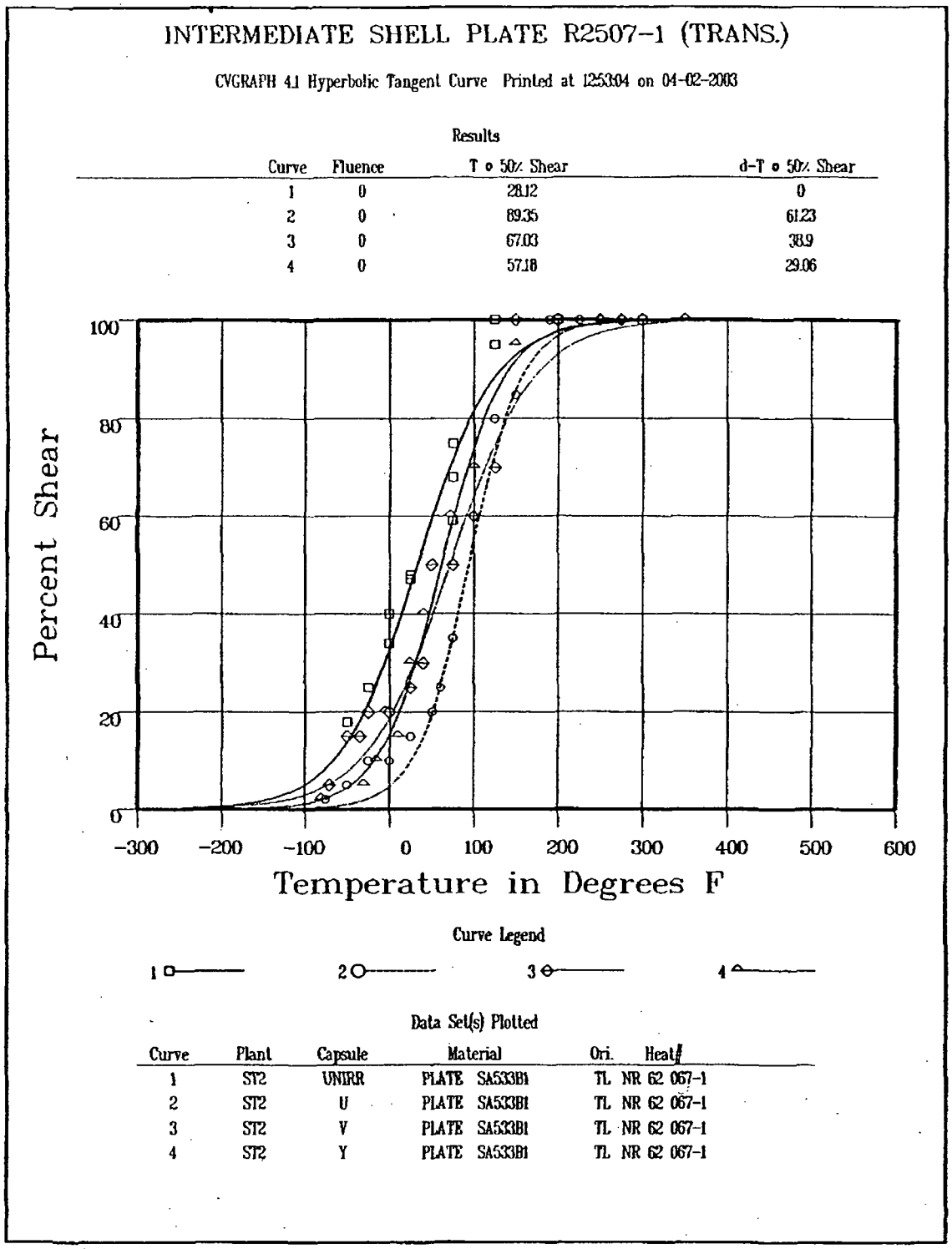

Figure 5-6 Charpy V-Notch Percent Shear vs. Temperature for South Texas Unit 2 Reactor Vessel Intermediate Shell Plate R2507-1 (Transverse Orientation)

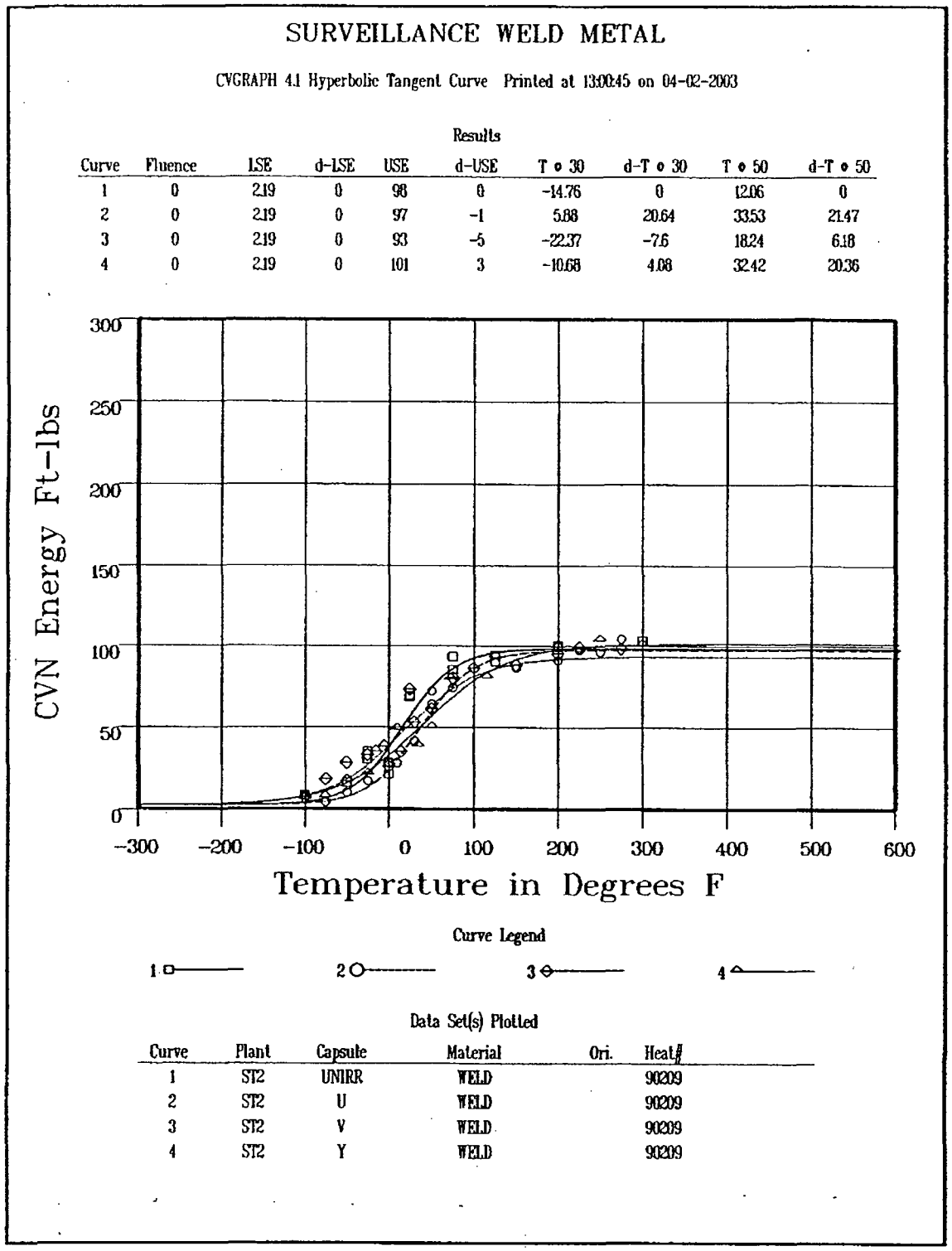

Figure 5-7 Charpy V-Notch Impact Energy vs. Temperature for South Texas Unit 2 Reactor Vessel Weld Metal

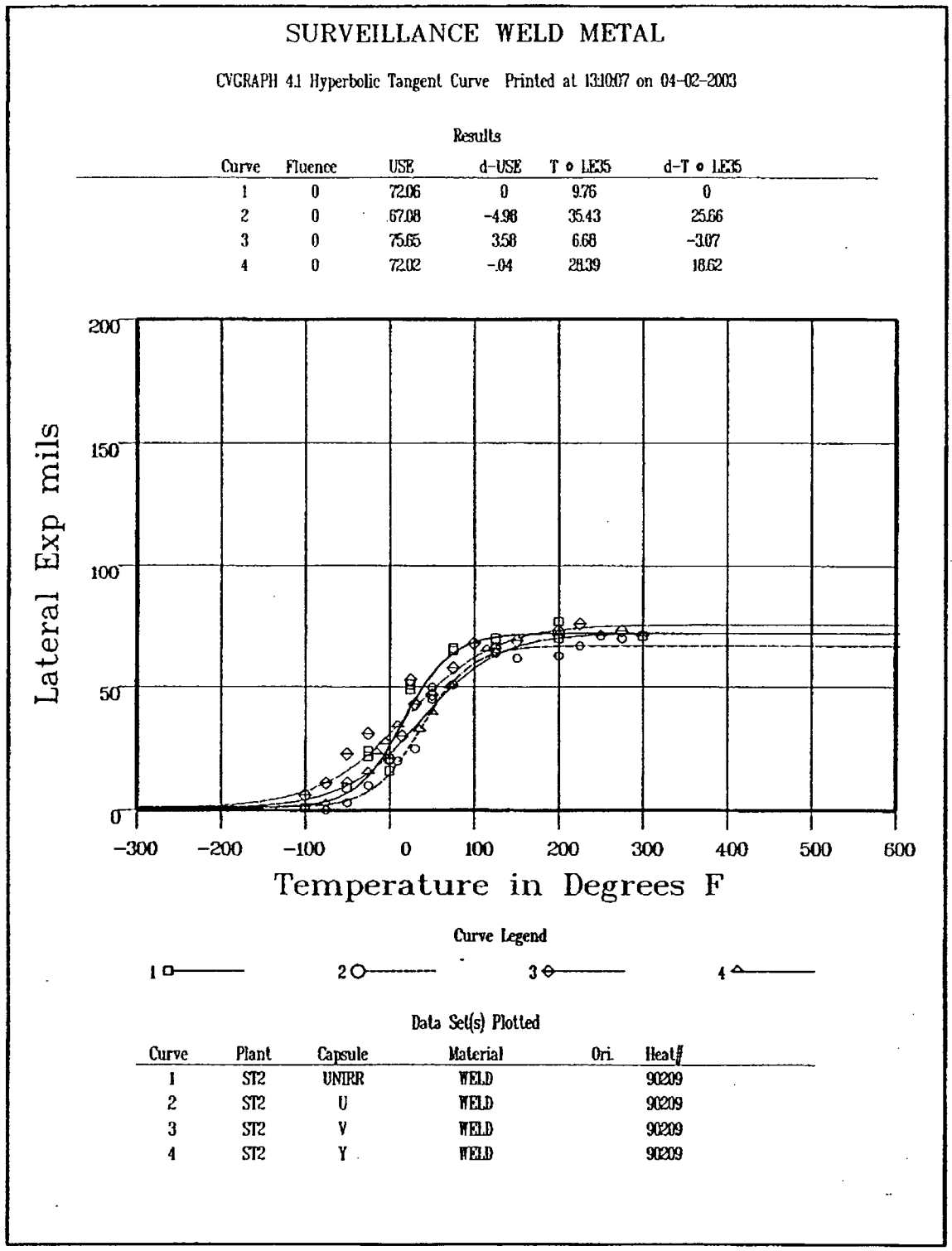

Figure 5-8 Charpy V-Notch Lateral Expansion vs. Temperature for South Texas Unit 2 Reactor Vessel Weld Metal

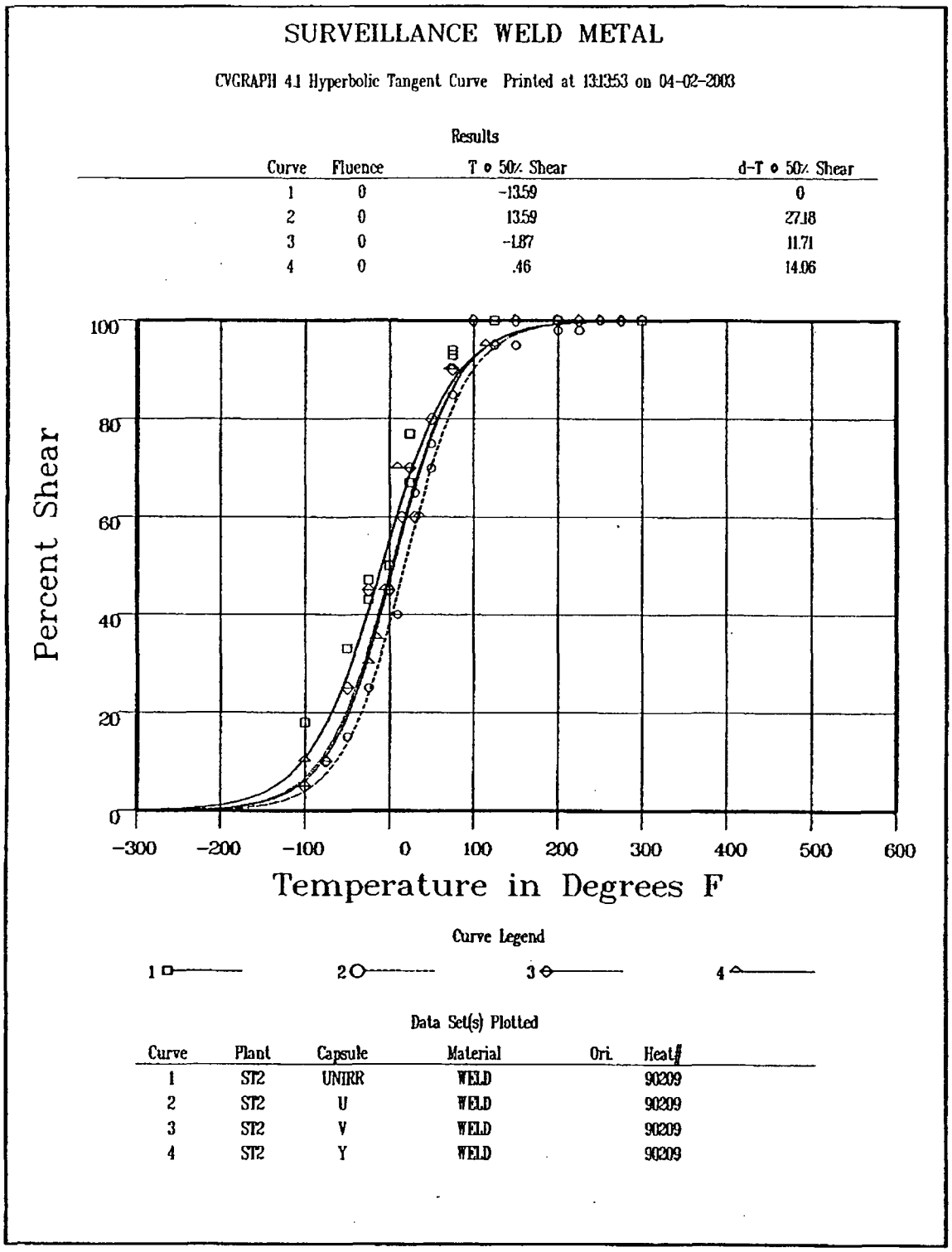

Figure 5-9 Charpy V-Notch Percent Shear vs. Temperature for South Texas Unit 2 Reactor Vessel Weld Metal

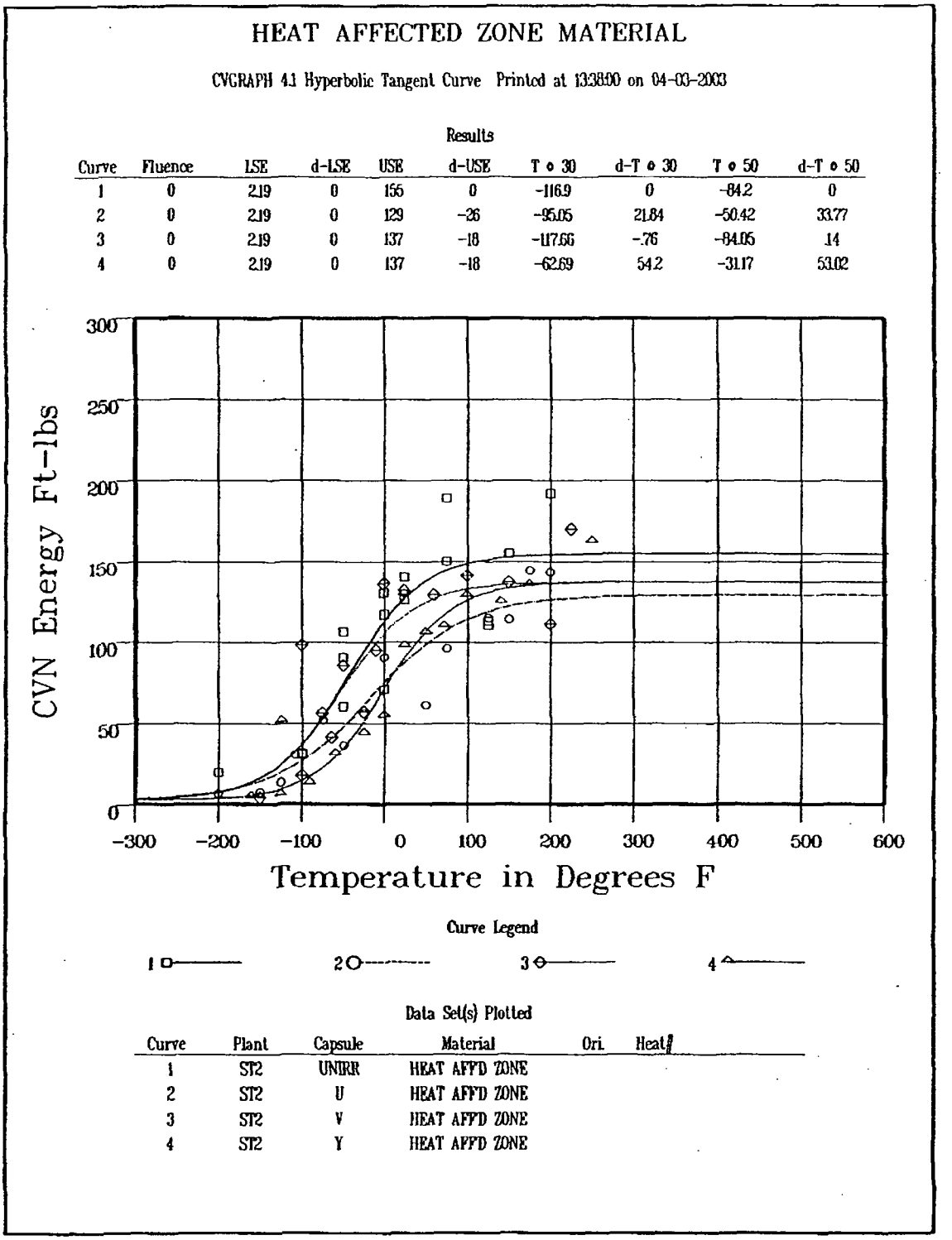

Figure 5-10 Charpy V-Notch Impact Energy vs. Temperature for South Texas Unit 2 Reactor Vessel Heat-Affected-Zone Material

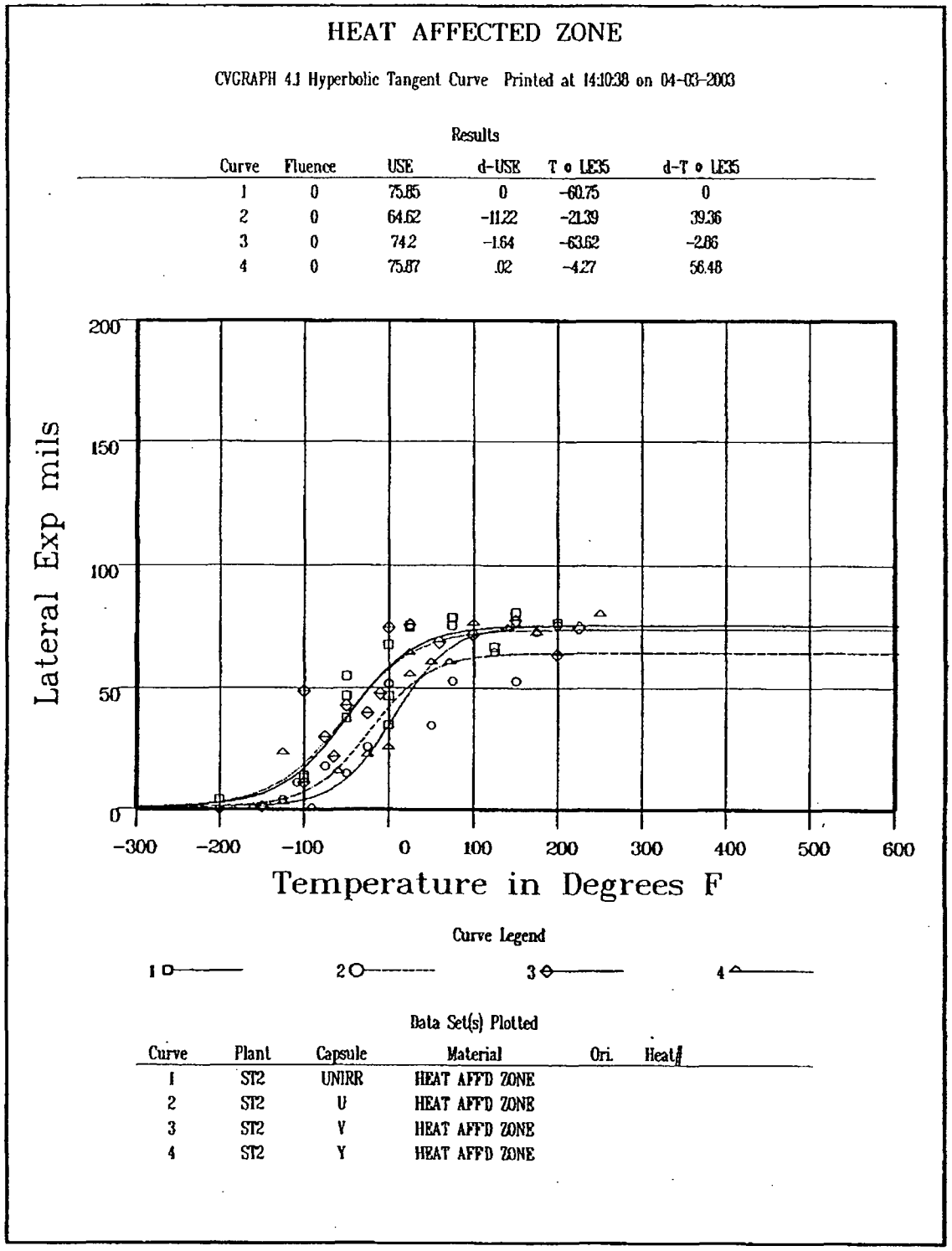

Figure 5-11 Charpy V-Notch Lateral Expansion vs. Temperature for South Texas Unit 2 Reactor Vessel Heat-Affected-Zone Material

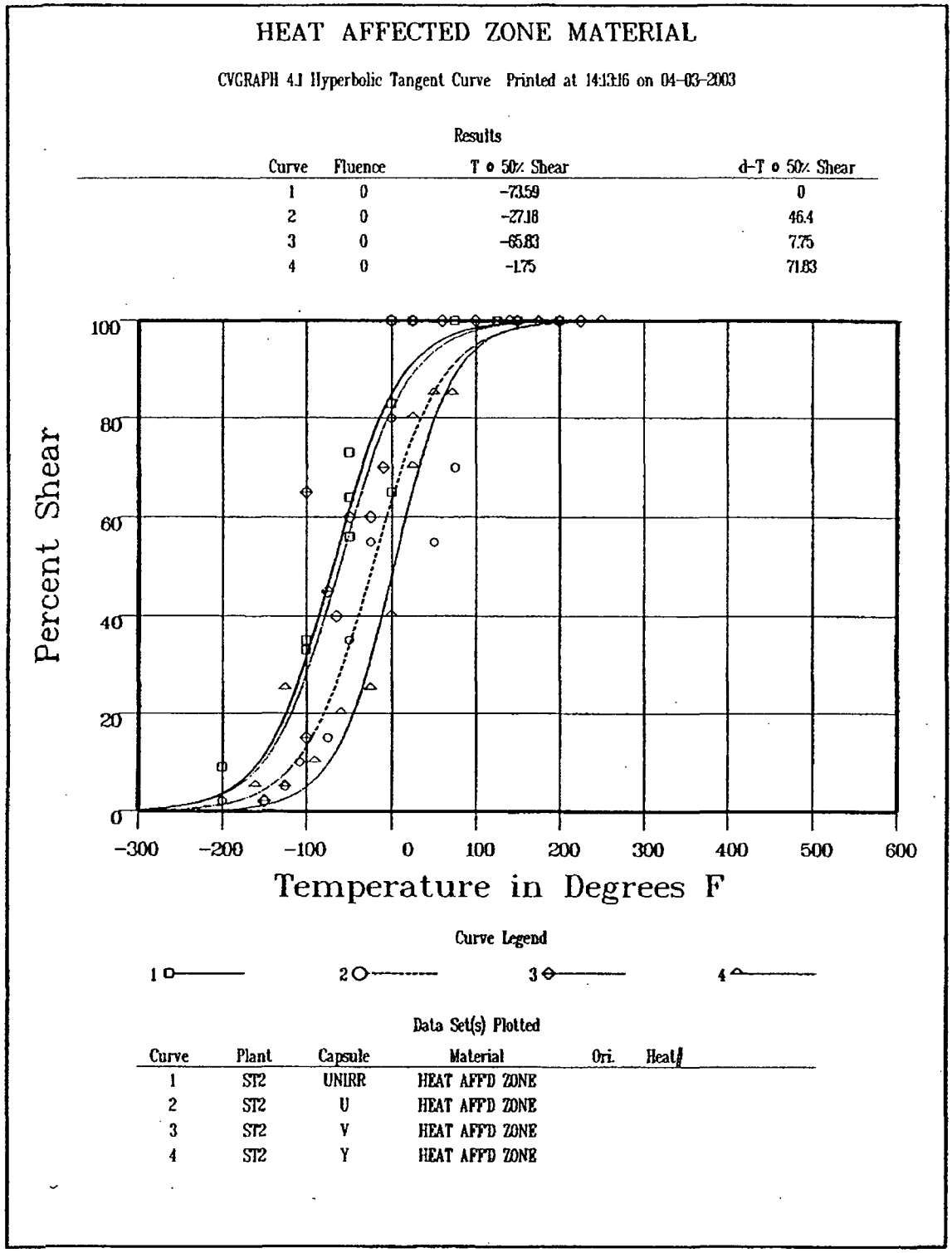

Figure 5-12 Charpy V-Notch Percent Shear vs. Temperature for South Texas Unit 2 Reactor Vessel Heat-Affected-Zone Material

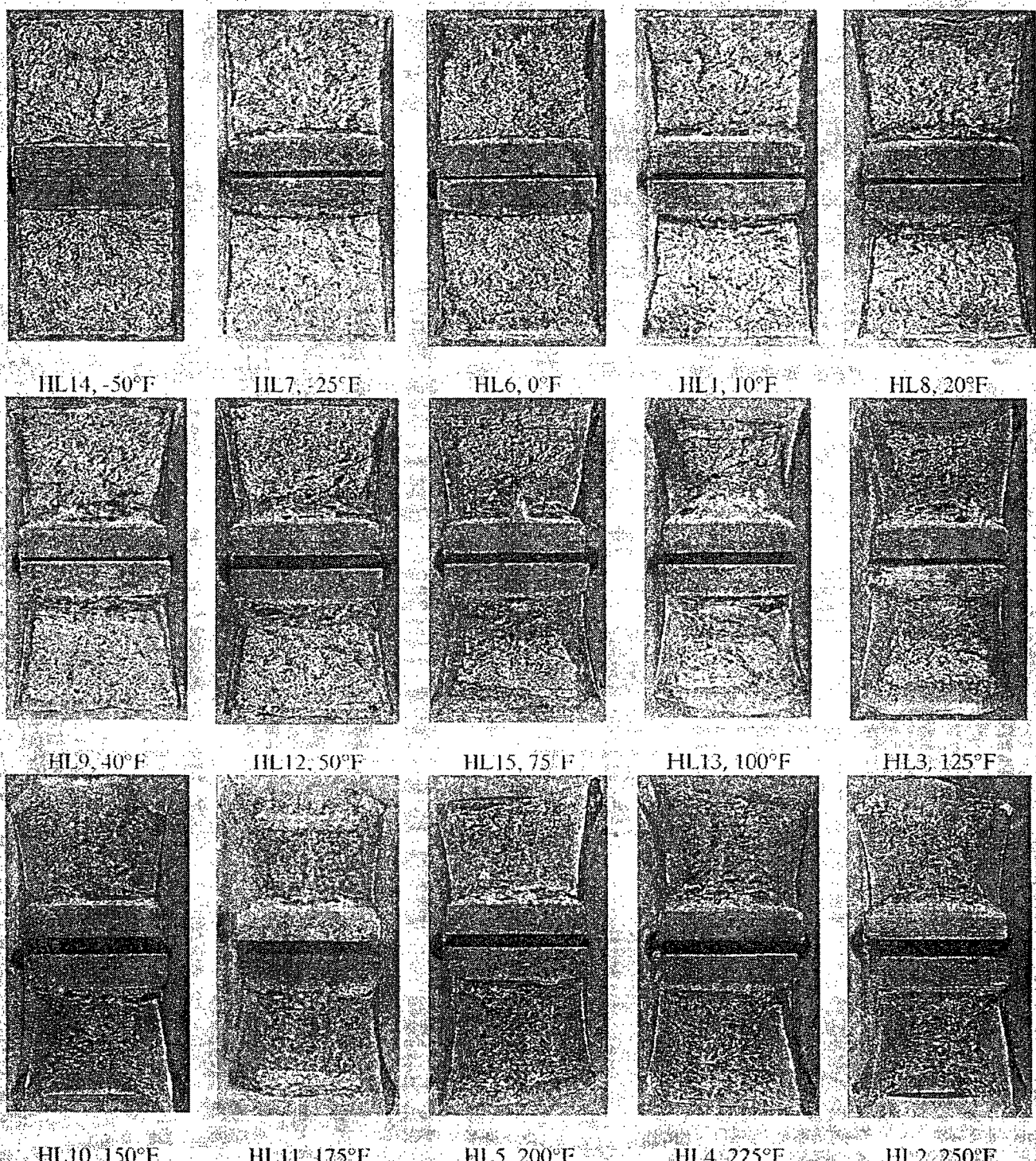

Figure 5-13 Charpy Impact Specimen Fracture Surfaces for South Texas Unit 2 Reactor Vessel Intermediate Shell Plate R2507-1 (Longitudinal Orientation)

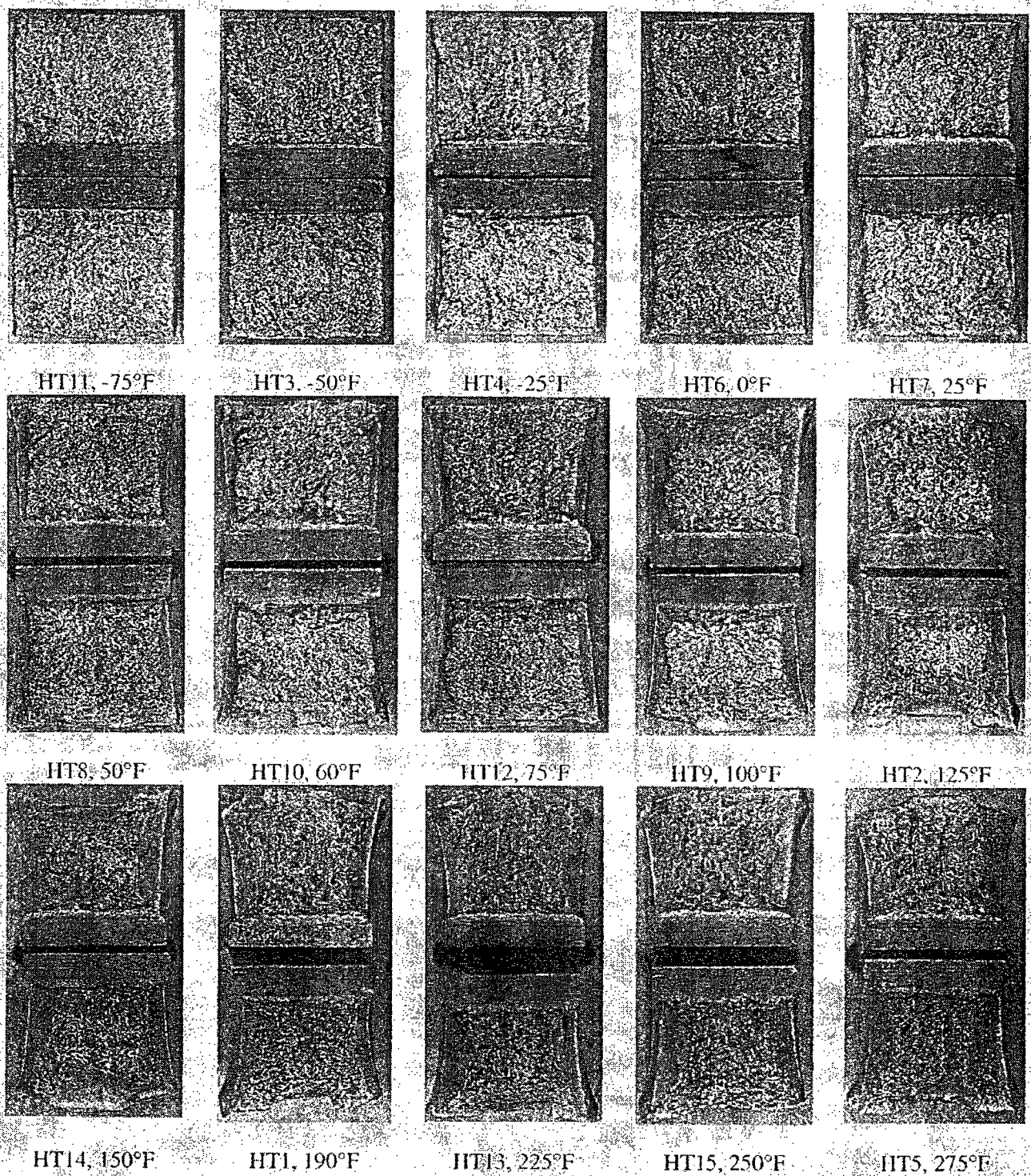

Figure 5-14 Charpy Impact Specimen Fracture Surfaces for South Texas Unit 2 Reactor Vessel Intermediate Shell Plate R2507-1 (Transverse Orientation)

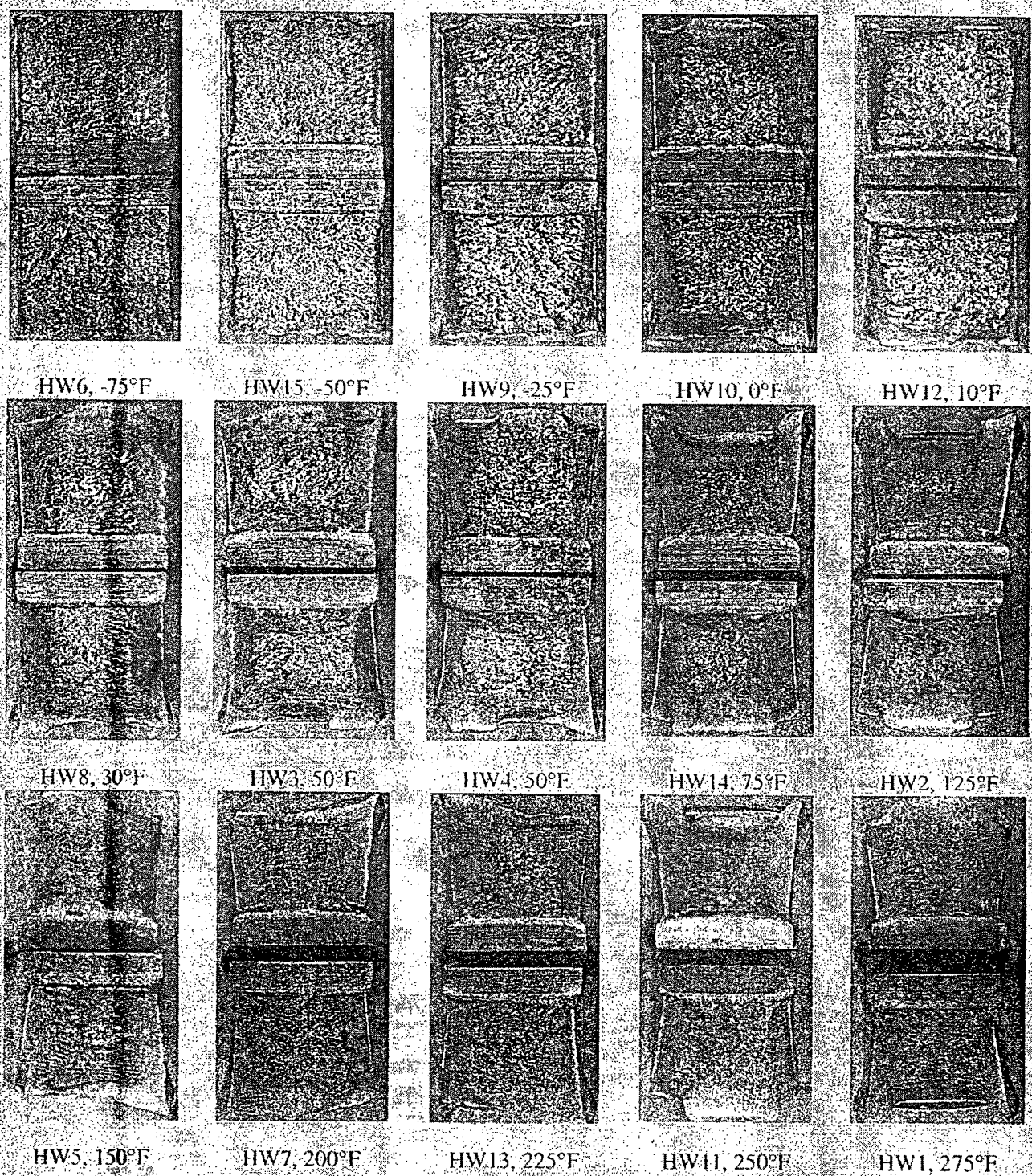

Figure 5-15 Charpy Impact Specimen Fracture Surfaces for South Texas Unit 2 Reactor Vessel Weld Metal

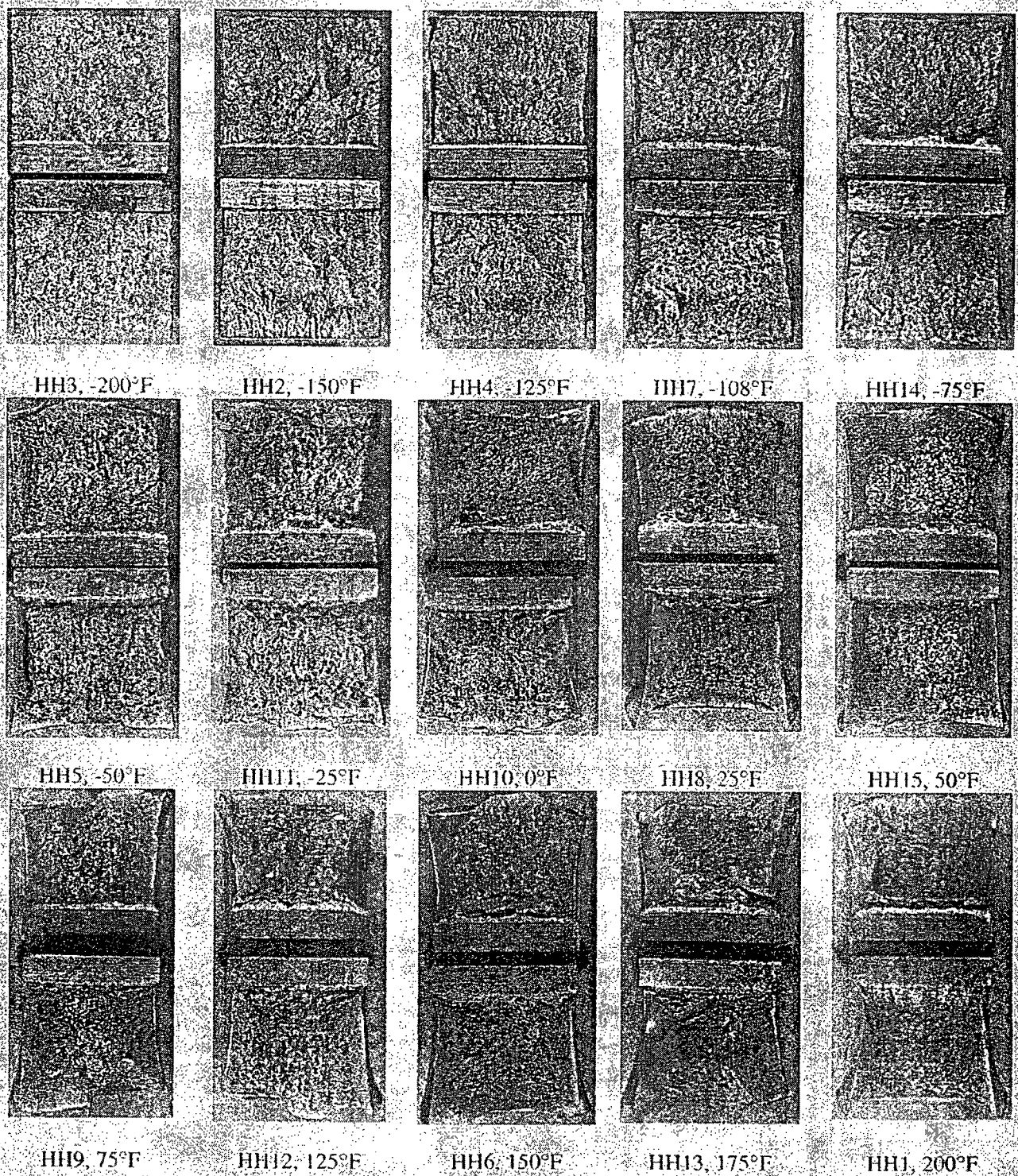

Figure 5-16 Charpy Impact Specimen Fracture Surfaces for South Texas Unit 2 Reactor Vessel Heat-Affected-Zone Metal

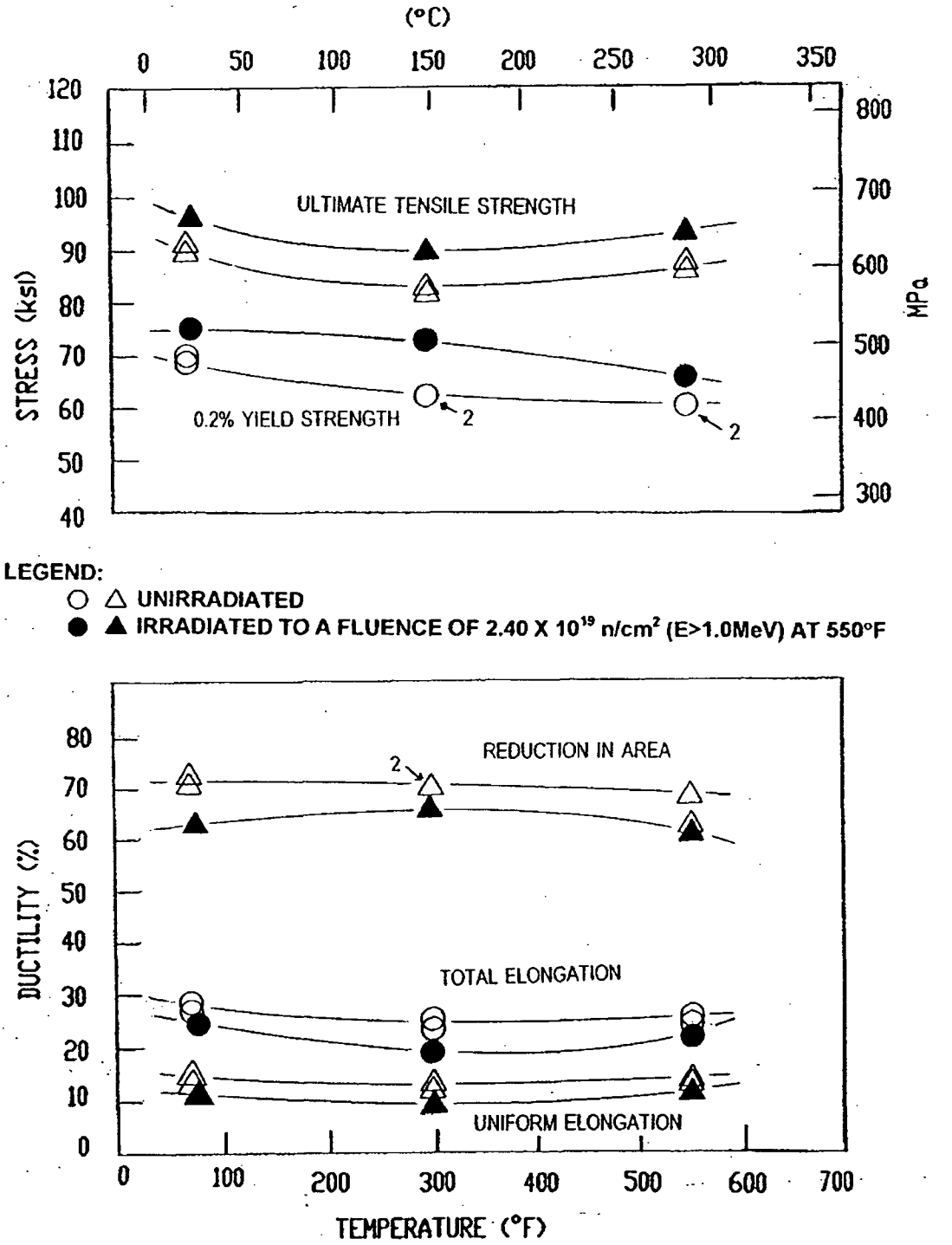

Figure 5-17 Tensile Properties for South Texas Unit 2 Reactor Vessel Intermediate Shell Plate R2507-1 (Longitudinal Orientation)

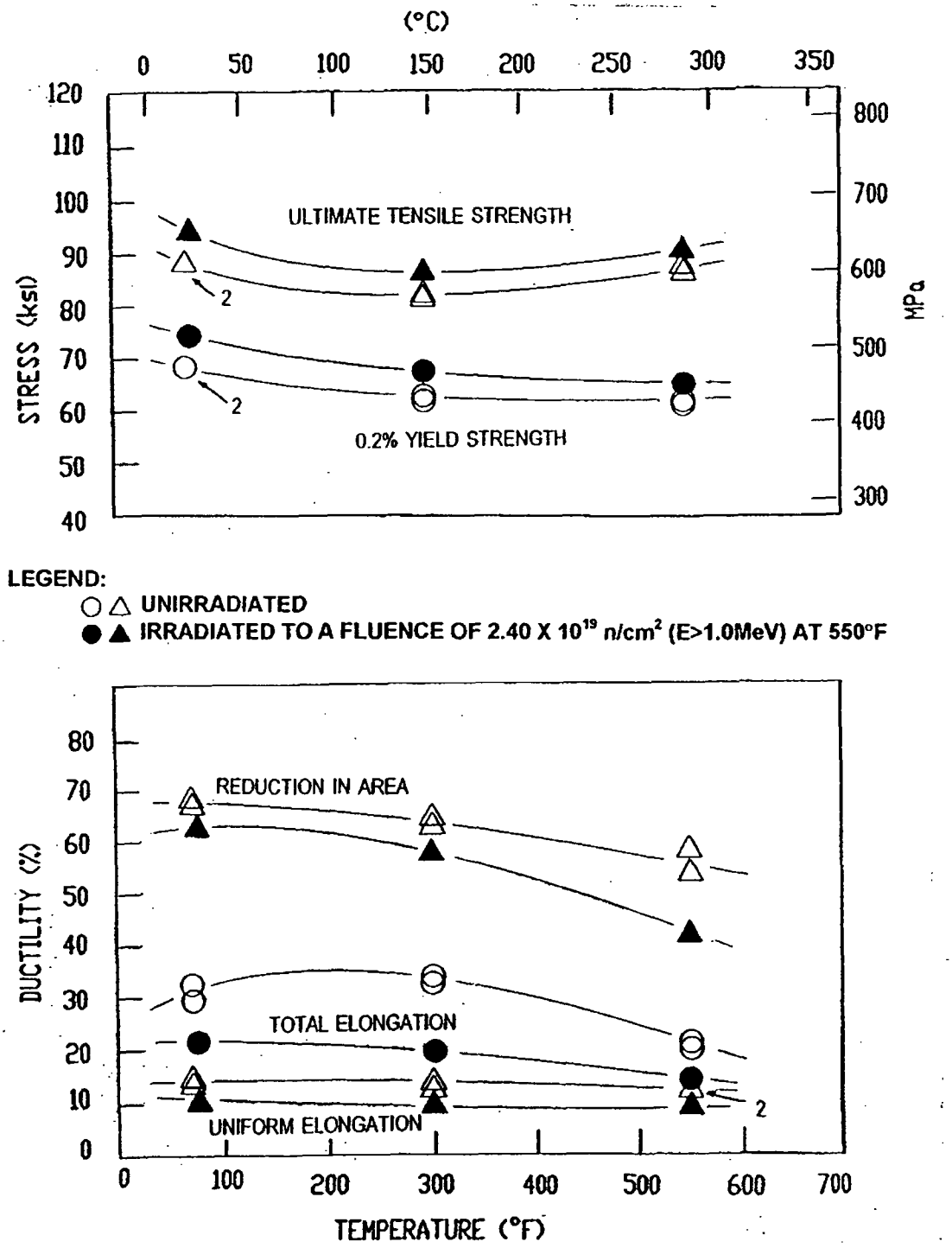

Figure 5-18 Tensile Properties for South Texas Unit 2 Reactor Vessel Intermediate Shell Plate R2507-1 (Transverse Orientation)

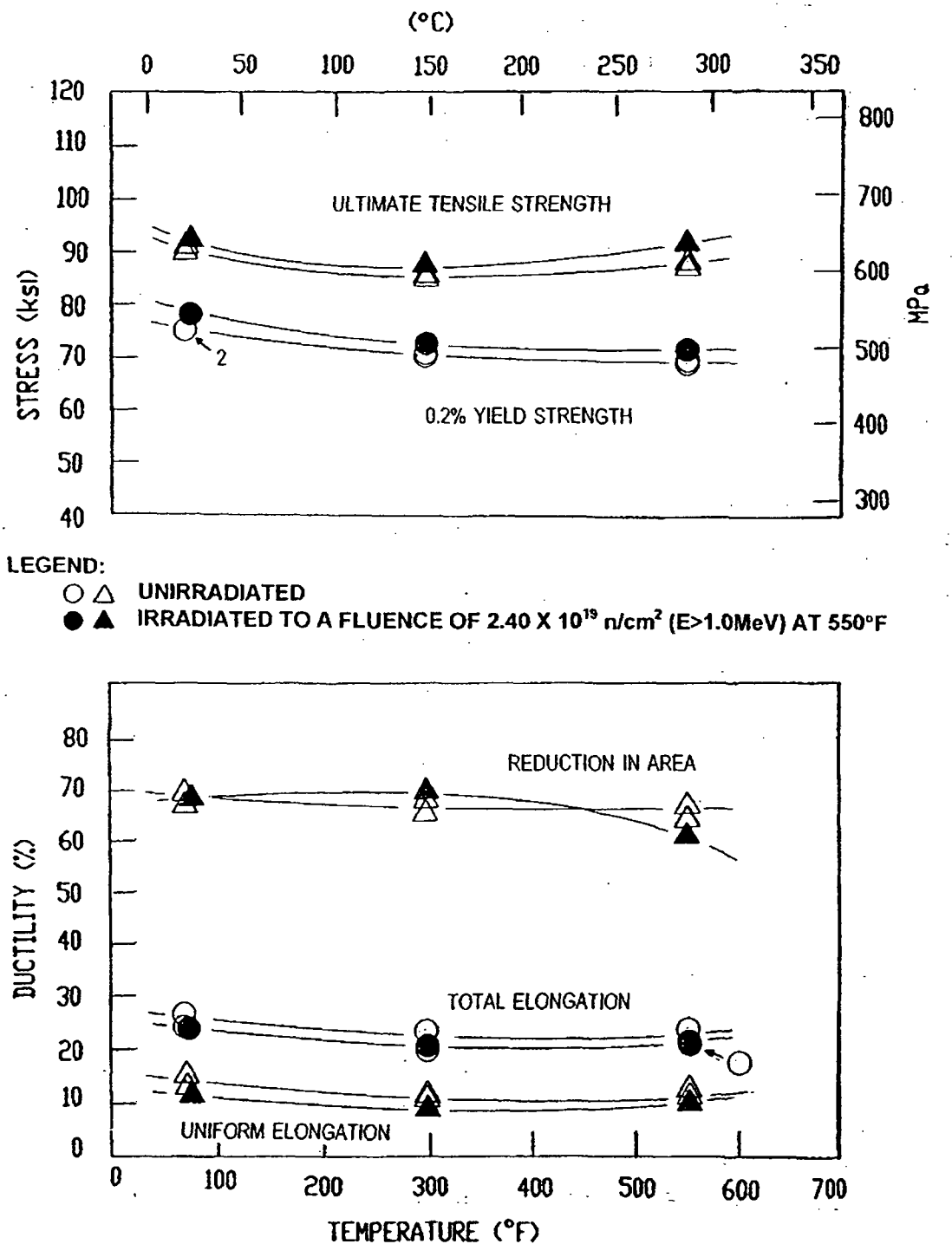

Figure 5-19 Tensile Properties for South Texas Unit 2 Reactor Vessel Weld Metal

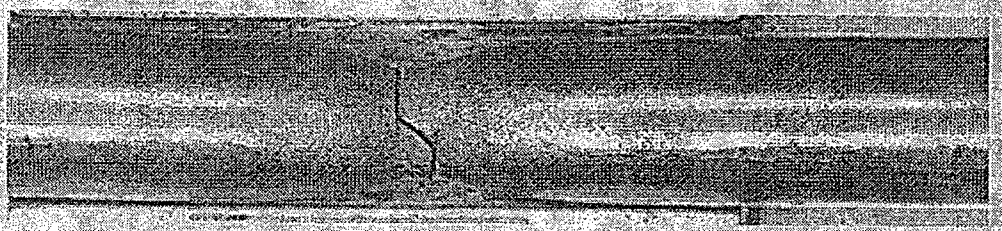

Specimen HL2 Tested at 75°F

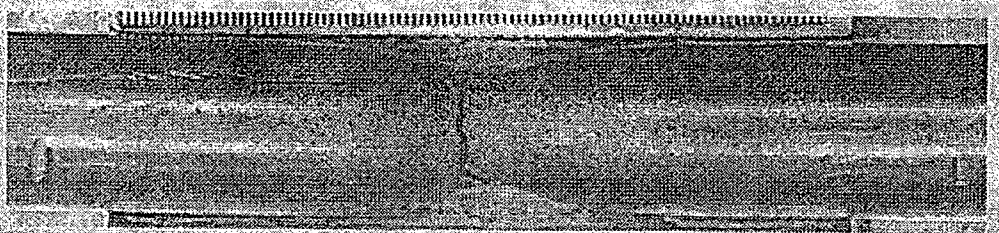

Specimen HL1 Tested at 300°F

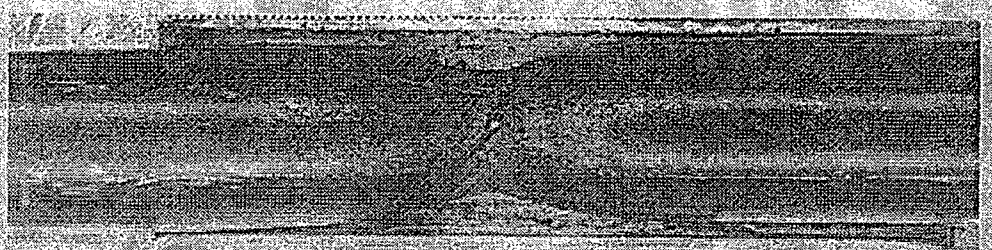

Specimen HL3 Tested at 550°F

Figure 5-20 Fractured Tensile Specimens from South Texas Unit 2 Reactor Vessel Lower Shell Plate R2508-3 (Longitudinal Orientation)

Specimen HT3 Tested at 75°F

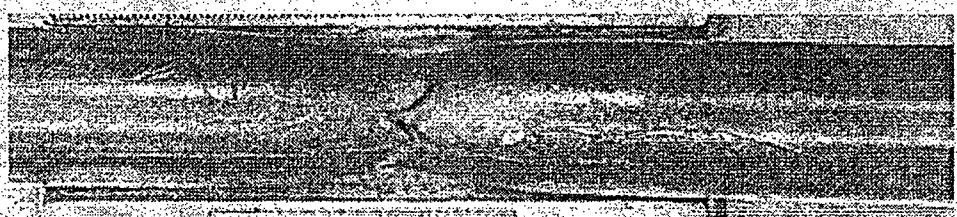

Specimen HT2 Tested at 300°F

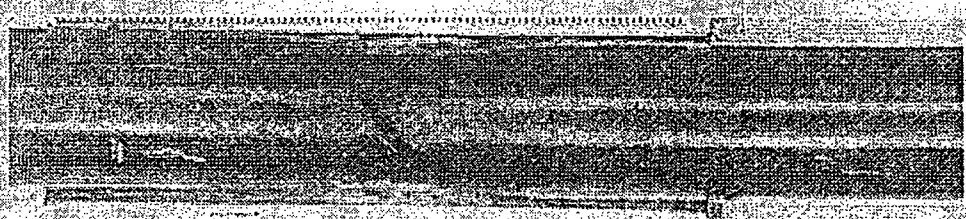

Specimen HT1 Tested at 550°F

Figure 5-21 Fractured Tensile Specimens from South Texas Unit 2 Reactor Vessel Lower Shell Plate R2508-3 (Transverse Orientation)

Specimen HW1 Tested at 75°F

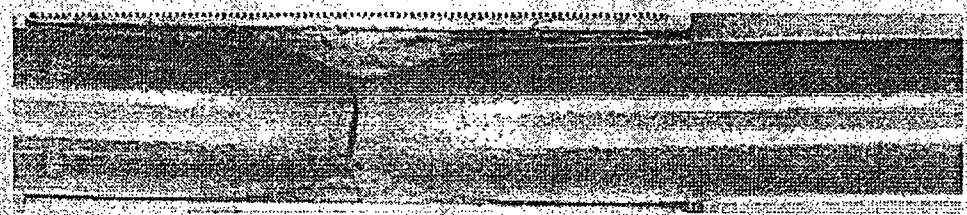

Specimen HW3 Tested at 300°F

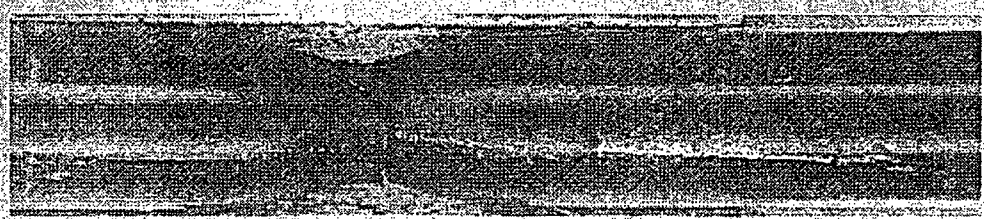

Specimen HW2 Tested at 550°F

Figure 5-22 Fractured Tensile Specimens from South Texas Unit 2 Reactor Vessel Weld Metal

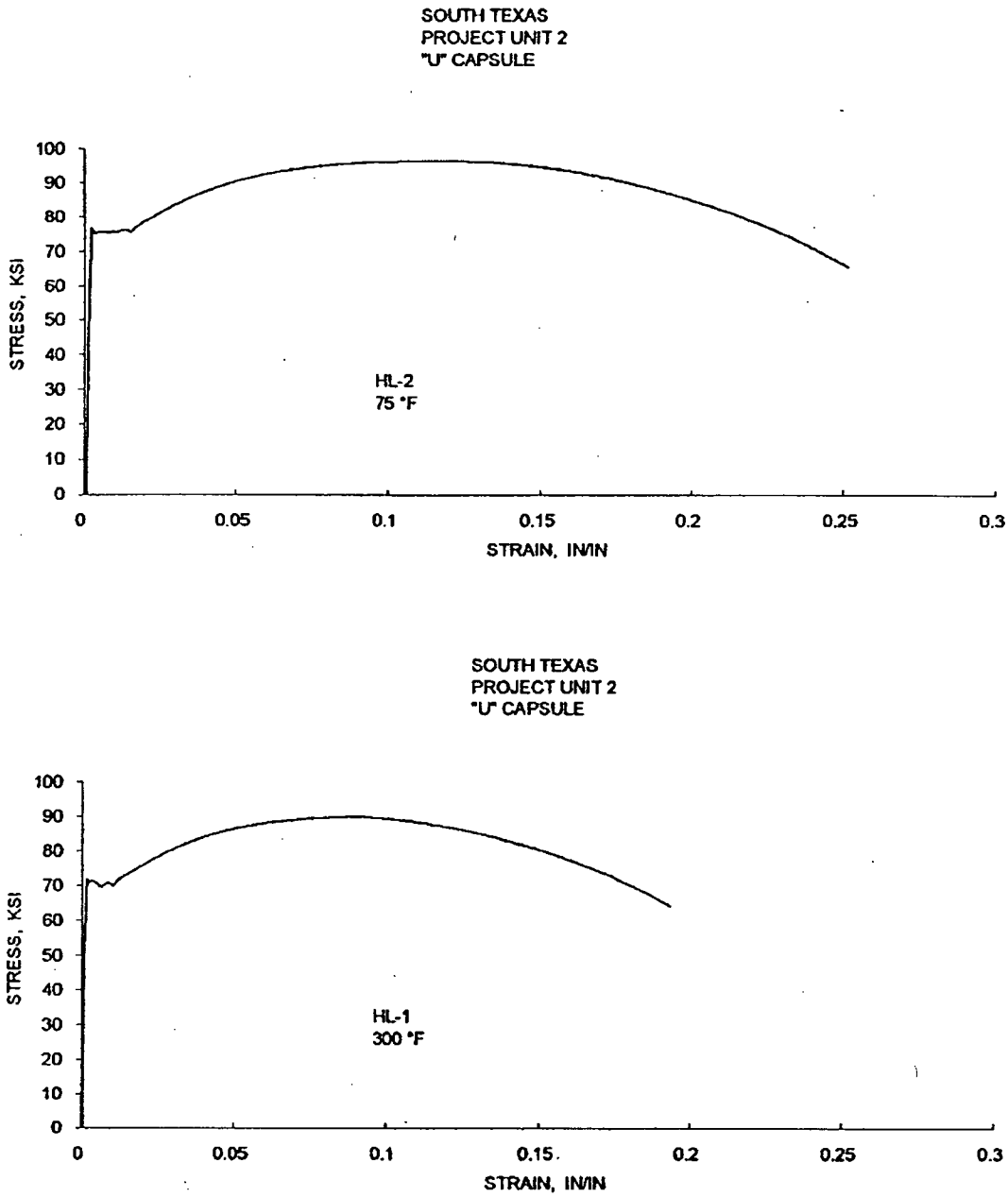

Figure 5-23 Engineering Stress-Strain Curves for South Texas Unit 2 Intermediate Shell Plate R2507-1 Tensile Specimens HL-1, HL-2 and HL-3 (Longitudinal Orientation)

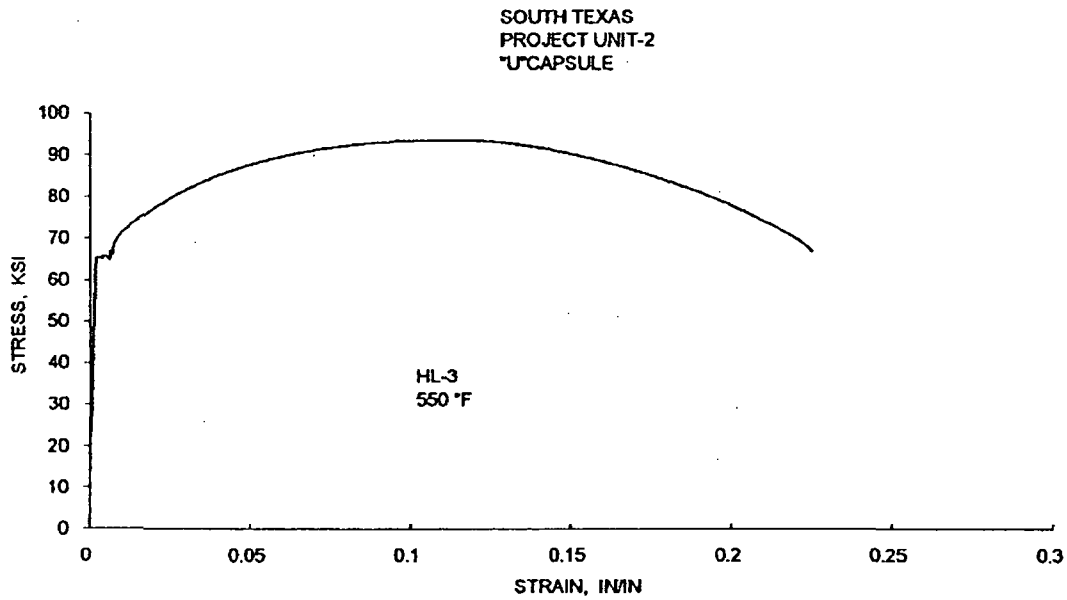

Figure 5-23 - Continued

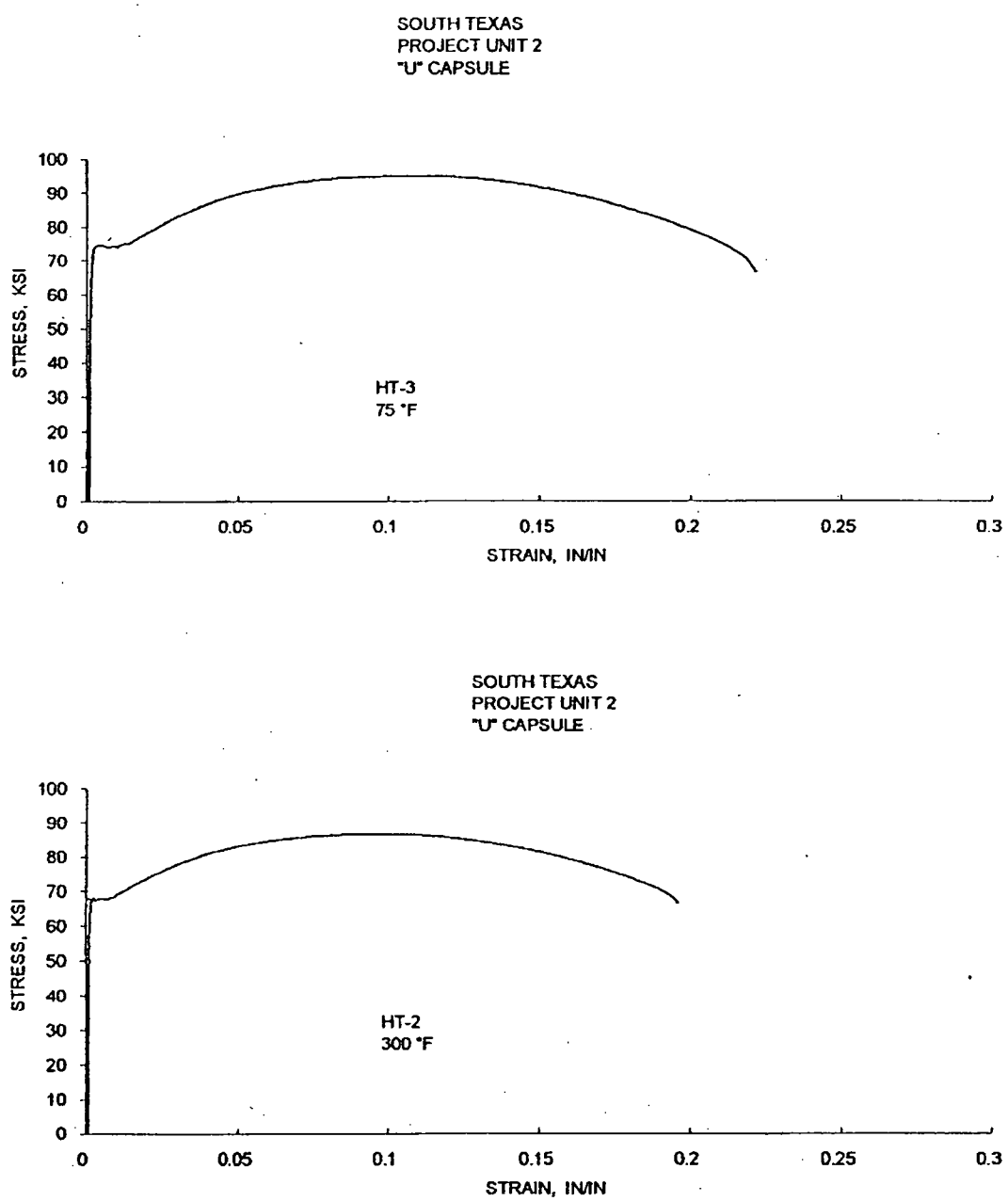

Figure 5-24 Engineering Stress-Strain Curves for South Texas Unit 2 Intermediate Shell Plate R2507-1 Tensile Specimens HT-1, HT-2 and HT-3 (Transverse Orientation)

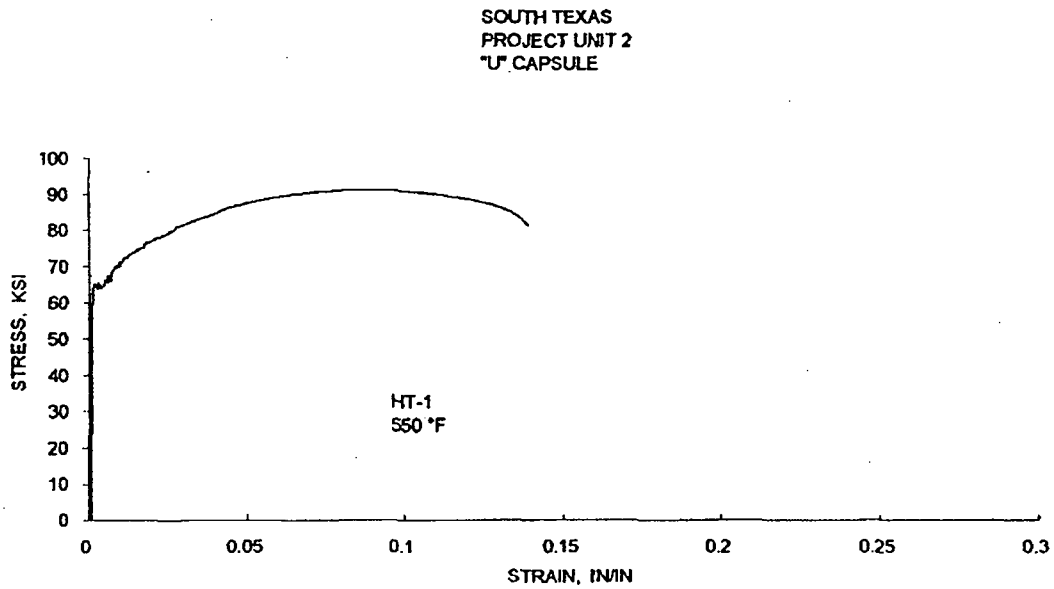

Figure 5-24 - Continued

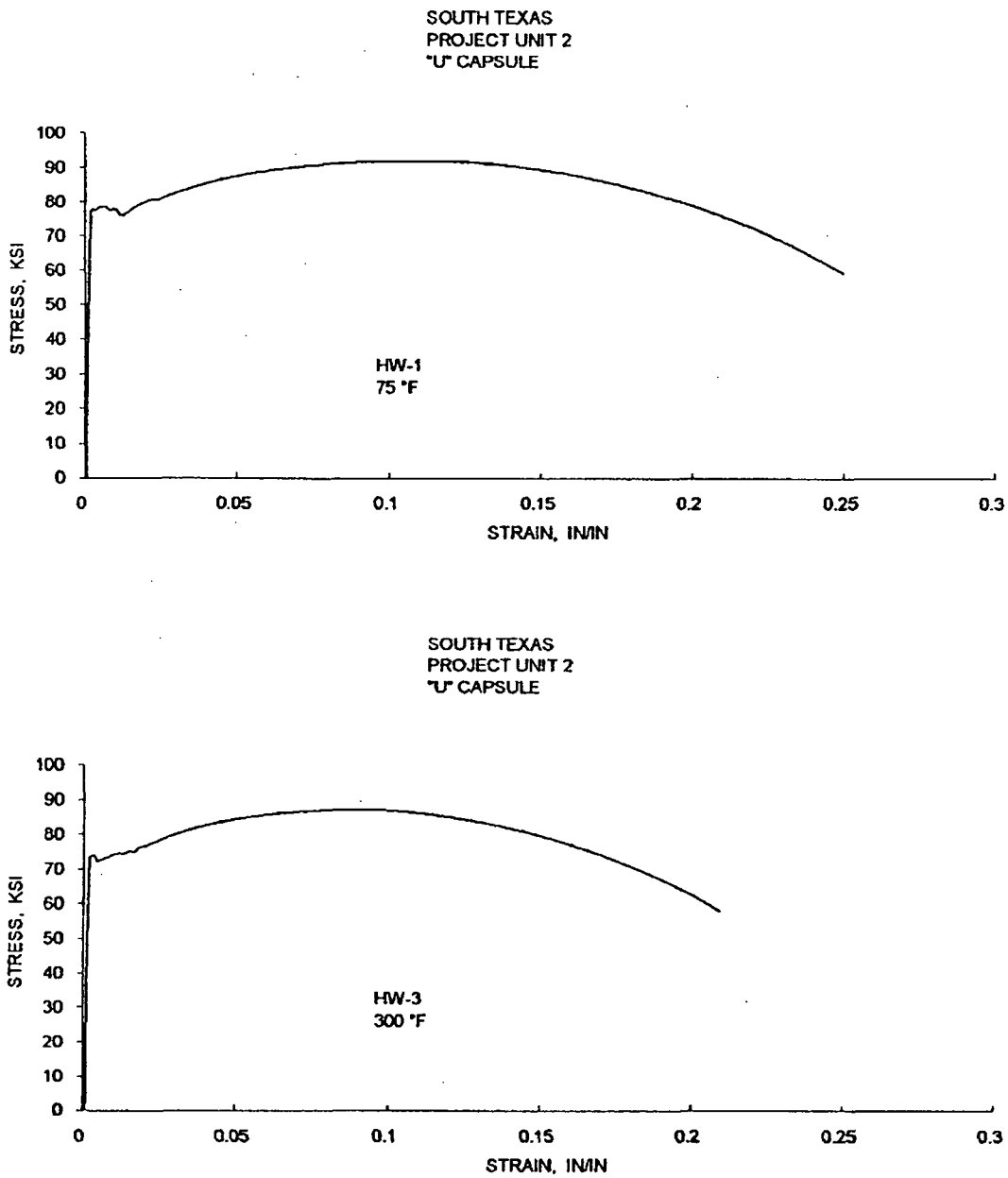

Figure 5-25 Engineering Stress-Strain Curves for Weld Metal Tensile Specimens HW-1, HW-2 and HW-3

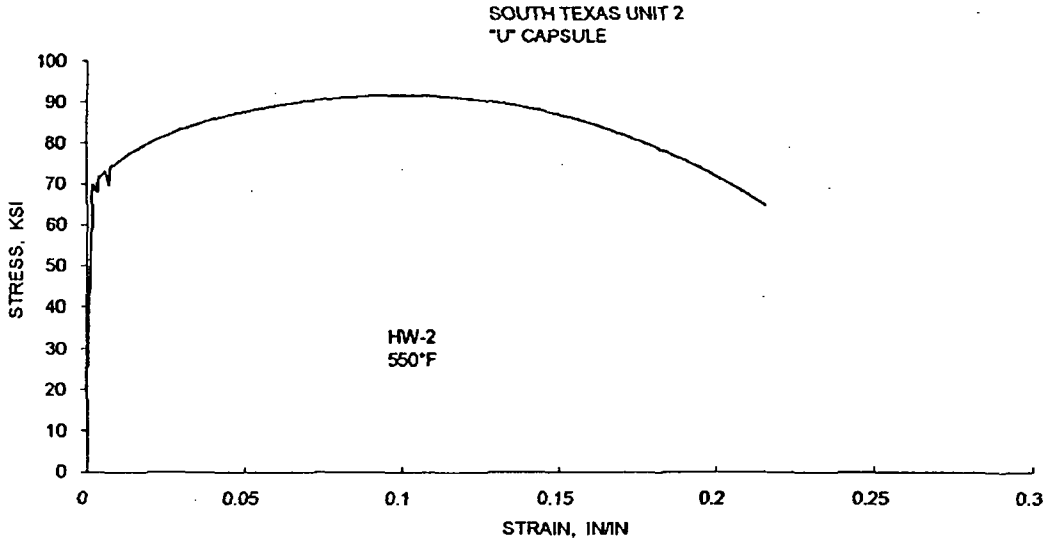

Figure 5-25 - Continued

6 RADIATION ANALYSIS AND NEUTRON DOSIMETRY

6.1 INTRODUCTION

This section describes a discrete ordinates S_n transport analysis performed for the South Texas Project Unit 2 reactor to determine the neutron radiation environment within the reactor pressure vessel and surveillance capsules. In this analysis, fast neutron exposure parameters in terms of fast neutron fluence (E > 1.0 MeV) and iron atom displacements (dpa) were established on a plant and fuel cycle specific basis. An evaluation of the most recent dosimetry sensor set from Capsule U, withdrawn at the end of the ninth plant operating cycle, is provided. In addition, to provide an up-to-date data base applicable to the South Texas Project Unit 2 reactor, sensor sets from previously withdrawn capsules (V and Y) were re-analyzed using the current dosimetry evaluation methodology. These dosimetry updates are presented in Appendix A of this report. Comparisons of the results from these dosimetry evaluations with the analytical predictions served to validate the plant specific neutron transport calculations. These validated calculations subsequently formed the basis for providing projections of the neutron exposure of the reactor pressure vessel for operating periods extending to 54 Effective Full Power Years (EFPY). These projections also account for a plant uprating, from 3800 MWt to 3853 MWt, which began at the onset of the tenth operating cycle.

The use of fast neutron fluence (E > 1.0 MeV) to correlate measured material property changes to the neutron exposure of the material has traditionally been accepted for the development of damage trend curves as well as for the implementation of trend curve data to assess the condition of the vessel. In recent years, however, it has been suggested that an exposure model that accounts for differences in neutron energy spectra between surveillance capsule locations and positions within the vessel wall could lead to an improvement in the uncertainties associated with damage trend curves and improved accuracy in the evaluation of damage gradients through the reactor vessel wall.

Because of this potential shift away from a threshold fluence toward an energy dependent damage function for data correlation, ASTM Standard Practice E853, "Analysis and Interpretation of Light-Water Reactor Surveillance Results," recommends reporting displacements per iron atom (dpa) along with fluence (E > 1.0 MeV) to provide a database for future reference. The energy dependent dpa function to be used for this evaluation is specified in ASTM Standard Practice E693, "Characterizing Neutron Exposures in Iron and Low Alloy Steels in Terms of Displacements per Atom." The application of the dpa parameter to the assessment of embrittlement gradients through the thickness of the reactor vessel wall has already been promulgated in Revision 2 to Regulatory Guide 1.99, "Radiation Embrittlement of Reactor Vessel Materials."

All of the calculations and dosimetry evaluations described in this section and in Appendix A were based on the latest available nuclear cross-section data derived from ENDF/B-VI and made use of the latest available calculational tools. Furthermore, the neutron transport and dosimetry evaluation methodologies follow the guidance and meet the requirements of Regulatory Guide 1.190, "Calculational and Dosimetry Methods for Determining Pressure Vessel Neutron Fluence."[19] Additionally, the methods used to develop the calculated pressure vessel fluence are consistent with the NRC approved methodology described in WCAP-14040-NP-A, "Methodology Used to Develop Cold Overpressure Mitigating System Setpoints and RCS Heatup and Cooldown Limit Curves," January 1996.[20] The specific calculational methods applied are also consistent with those described in WCAP-15557, "Qualification of the Westinghouse Pressure Vessel Neutron Fluence Evaluation Methodology."[21]

6.2 DISCRETE ORDINATES ANALYSIS

A plan view of the South Texas Project Unit 2 reactor geometry at the core midplane is shown in Figure 4-1. Six irradiation capsules attached to the neutron pad are included in the reactor design that constitutes the reactor vessel surveillance program. The capsules are located at azimuthal angles of 58.5°, 61°, 121.5°, 238.5°, 241°, and 301.5° as shown in Figure 4-1. These full-core positions correspond to the following octant symmetric capsule locations represented in Figure 6-1: 29° from the core cardinal axis (for the 61° and 241° dual surveillance capsule holder locations) and 31.5° from the core cardinal axes (for the 121.5° and 301.5° single surveillance capsule holder locations, and for the 58.5° and 238.5° dual surveillance capsule holder locations). The stainless steel specimen containers are 1.182-inch by 1-inch and are approximately 56 inches in height. The containers are positioned axially such that the test specimens are centered on the core midplane, thus spanning the central 5 feet of the 14-foot high reactor core.

From a neutronic standpoint, the surveillance capsules and associated support structures are significant. The presence of these materials has a marked effect on both the spatial distribution of neutron flux and the neutron energy spectrum in the water annulus between the neutron pads and the reactor vessel. In order to determine the neutron environment at the test specimen location, the capsules themselves must be included in the analytical model.

In performing the fast neutron exposure evaluations for the South Texas Project Unit 2 reactor vessel and surveillance capsules, a series of fuel cycle specific forward transport calculations were carried out using the following three-dimensional flux synthesis technique:

$$\phi(r,\theta,z) = \phi(r,\theta) * \frac{\phi(r,z)}{\phi(r)}$$

where $\phi(r,\theta,z)$ is the synthesized three-dimensional neutron flux distribution, $\phi(r,\theta)$ is the transport solution in r,θ geometry, $\phi(r,z)$ is the two-dimensional solution for a cylindrical reactor model using the actual axial core power distribution, and $\phi(r)$ is the one-dimensional solution for a cylindrical reactor model using the same source per unit height as that used in the r,θ two-dimensional calculation. This synthesis procedure was carried out for each operating cycle at South Texas Project Unit 2.

For the South Texas Project Unit 2 transport calculations, the r,θ models depicted in Figure 6-1 were utilized since, with the exception of the neutron pads, the reactor is octant symmetric. These r,θ models include the core, the reactor internals, the neutron pads -- including explicit representations of octants not containing surveillance capsules and octants with surveillance capsules at 29° and 31.5°, the pressure vessel cladding and vessel wall, the insulation external to the pressure vessel, and the primary biological shield wall. These models formed the basis for the calculated results and enabled making comparisons to the surveillance capsule dosimetry evaluations. In developing these analytical models, nominal design dimensions were employed for the various structural components. Likewise, water temperatures, and hence, coolant densities in the reactor core and downcomer regions of the reactor were taken to be representative of full power operating conditions. The coolant densities were treated on a fuel cycle specific basis. The reactor core itself was treated as a homogeneous mixture of fuel, cladding, water, and miscellaneous core structures such as fuel assembly grids, guide tubes, et cetera. The geometric mesh description of the r,θ reactor models consisted of 183 radial by 99 azimuthal intervals. Mesh sizes were

description of the r,θ reactor models consisted of 183 radial by 99 azimuthal intervals. Mesh sizes were chosen to assure that proper convergence of the inner iterations was achieved on a pointwise basis. The pointwise inner iteration flux convergence criterion utilized in the r,θ calculations was set at a value of 0.001.

The r,z models used for the South Texas Project Unit 2 calculations are shown in Figure 6-2 and extend radially from the centerline of the reactor core out to a location interior to the primary biological shield and over an axial span from an elevation 3-feet below the active fuel to approximately 5-feet above the active fuel. (Note that the only difference between these r,z models, and the corresponding r models, is the inclusion or exclusion of the neutron pads. R,Z / R synthesis factors with the neutron pad were used for the capsule locations and the 45° vessel location, whereas the corresponding synthesis factors without the neutron pad were used for the 0°, 15°, and 30° azimuthal locations of the pressure vessel.) As in the case of the r,θ models, nominal design dimensions and full power coolant densities were employed in the calculations. In this case, the homogenous core region was treated as an equivalent cylinder with a volume equal to that of the active core zone. The stainless steel former plates located between the core baffle and core barrel regions were also explicitly included in the model. The r,z geometric mesh description of these reactor models consisted of 137 radial by 191 axial intervals. As in the case of the r,θ calculations, mesh sizes were chosen to assure that proper convergence of the inner iterations was achieved on a pointwise basis. The pointwise inner iteration flux convergence criterion utilized in the r,z calculations was also set at a value of 0.001.

The one-dimensional radial models used in the synthesis procedure consisted of the same 137 radial mesh intervals included in the r,z models. Thus, radial synthesis factors could be determined on a meshwise basis throughout the entire geometry.

The core power distributions used in the plant specific transport analysis were taken from the appropriate South Texas Project Unit 2 fuel cycle design reports. The data extracted from the design reports represented cycle dependent fuel assembly enrichments, burnups, and axial power distributions. This information was used to develop spatial and energy dependent core source distributions averaged over each individual fuel cycle. Therefore, the results from the neutron transport calculations provided data in terms of fuel cycle averaged neutron flux, which when multiplied by the appropriate fuel cycle length, generated the incremental fast neutron exposure for each fuel cycle. In constructing these core source distributions, the energy distribution of the source was based on an appropriate fission split for uranium and plutonium isotopes based on the initial enrichment and burnup history of individual fuel assemblies. From these assembly dependent fission splits, composite values of energy release per fission, neutron yield per fission, and fission spectrum were determined.

All of the transport calculations supporting this analysis were carried out using the DORT discrete ordinates code Version 3.1[22] and the BUGLE-96 cross-section library.[23] The BUGLE-96 library provides a 67 group coupled neutron-gamma ray cross-section data set produced specifically for light water reactor (LWR) applications. In these analyses, anisotropic scattering was treated with a P_5 legendre expansion and angular discretization was modeled with an S_{16} order of angular quadrature. Energy and space dependent core power distributions, as well as system operating temperatures, were treated on a fuel cycle specific basis.

Selected results from the neutron transport analyses are provided in Tables 6-1 through 6-7. In Table 6-1, the calculated exposure rates and integrated exposures, expressed in terms of both neutron fluence (E > 1.0 MeV) and dpa, are given at the radial and azimuthal center of the octant symmetric surveillance capsule positions, i.e., for the 29° dual capsule, 31.5° dual capsule, and 31.5° single capsule. These results, representative of the axial midplane of the active core, establish the calculated exposure of the surveillance capsules withdrawn to date as well as projected into the future. Similar information is provided in Tables 6-2 and 6-3 for the reactor vessel inner radius. The vessel data given in Table 6-2 are representative of the axial location of the maximum neutron exposure at each of the four azimuthal locations. Maximum integrated neutron exposure results for key vessel plate and weld materials are subsequently given in Table 6-3 for the end of Cycle 9 and beyond. It is also important to note that the data for the vessel inner radius were taken at the clad/base metal interface, and thus, represent the maximum calculated exposure levels of the vessel plates and welds.

Both calculated fluence (E > 1.0 MeV) and dpa data are provided in Table 6-1 through Table 6-3. These data tabulations include both plant and fuel cycle specific calculated neutron exposures at the end of the ninth operating fuel cycle as well as projections for the current operating fuel cycle, i.e., Cycle 10, and future projections to 16, 32, 48, and 54 effective full power years (EFPY). The projections were based on the assumption that the core power distributions and associated plant operating characteristics from Cycle 10 were representative of future plant operation. The future projections are also based on the current reactor power level of 3853 MWt.

Radial gradient information applicable to fast (E > 1.0 MeV) neutron fluence and dpa are given in Tables 6-4 and 6-5, respectively. The data, based on the cumulative integrated exposures from Cycles 1 through 10, are presented on a relative basis for each exposure parameter at several azimuthal locations. Exposure distributions through the vessel wall may be obtained by multiplying the calculated exposure at the vessel inner radius by the gradient data listed in Tables 6-4 and 6-5.

The calculated fast neutron exposures for the three surveillance capsules withdrawn from the South Texas Project Unit 2 reactor are provided in Table 6-6. These assigned neutron exposure levels are based on the plant and fuel cycle specific neutron transport calculations performed for the South Texas Project Unit 2 reactor.

Updated lead factors for the South Texas Project Unit 2 surveillance capsules are provided in Table 6-7. The capsule lead factor is defined as the ratio of the calculated fluence (E > 1.0 MeV) at the geometric center of the surveillance capsule to the corresponding maximum calculated fluence at the pressure vessel clad/base metal interface. In Table 6-7, the lead factors for capsules that have been withdrawn from the reactor (V, Y, and U) were based on the calculated fluence values for the irradiation period corresponding to the time of withdrawal for the individual capsules. For the capsules remaining in the reactor (W, X, and Z), the lead factors correspond to the calculated fluence values at the end of Cycle 10, the current operating fuel cycle for South Texas Project Unit 2.

6.3 NEUTRON DOSIMETRY

The validity of the calculated neutron exposures previously reported in Section 6.2 is demonstrated by a direct comparison against the measured sensor reaction rates and via a least squares evaluation performed for each of the capsule dosimetry sets. However, since the neutron dosimetry measurement data merely serves to validate the calculated results, only the direct comparison of measured-to-calculated results for the most recent surveillance capsule removed from service is provided in this section of the report. For completeness, the assessment of all measured dosimetry removed to date, based on both direct and least squares evaluation comparisons, is documented in Appendix A.

The direct comparison of measured versus calculated fast neutron threshold reaction rates for the sensors from Capsule U, that was withdrawn from South Texas Project Unit 2 at the end of the ninth fuel cycle, is summarized below.

Reaction	Reaction Rates (rps/atom)		M/C
	Measured	Calculated	Ratio
$^{63}Cu(n,\alpha)^{60}Co$	4.32E-17	3.98E-17	1.09
$^{54}Fe(n,p)^{54}Mn$	4.30E-15	4.40E-15	0.98
$^{58}Ni(n,p)^{58}Co$	6.13E-15	6.17E-15	0.99
$^{238}U(n,p)^{137}Cs$ (Cd)	2.77E-14	2.36E-14	1.17
$^{237}Np(n,f)^{137}Cs$ (Cd)	2.49E-13	2.30E-13	1.08
		Average:	1.06
		% Standard Deviation:	7.5

The measured-to-calculated (M/C) reaction rate ratios for the Capsule U threshold reactions range from 0.98 to 1.17, and the average M/C ratio is 1.06 ± 7.5% (1σ). This direct comparison falls well within the ± 20% criterion specified in Regulatory Guide 1.190; furthermore, it is consistent with the full set of comparisons given in Appendix A for all measured dosimetry removed to date from the South Texas Project Unit 2 reactor. These comparisons validate the current analytical results described in Section 6.2; therefore, the calculations are deemed applicable for South Texas Project Unit 2.

6.4 CALCULATIONAL UNCERTAINTIES

The uncertainty associated with the calculated neutron exposure of the South Texas Project Unit 2 surveillance capsule and reactor pressure vessel is based on the recommended approach provided in Regulatory Guide 1.190. In particular, the qualification of the methodology was carried out in the following four stages:

1 - Comparison of calculations with benchmark measurements from the Pool Critical Assembly (PCA) simulator at the Oak Ridge National Laboratory (ORNL).

2 - Comparisons of calculations with surveillance capsule and reactor cavity measurements from the H. B. Robinson power reactor benchmark experiment.

3 - An analytical sensitivity study addressing the uncertainty components resulting from important input parameters applicable to the plant specific transport calculations used in the neutron exposure assessments.

4 - Comparisons of the plant specific calculations with all available dosimetry results from the South Texas Project Unit 2 surveillance program.

The first phase of the methods qualification (PCA comparisons) addressed the adequacy of basic transport calculation and dosimetry evaluation techniques and associated cross-sections. This phase, however, did not test the accuracy of commercial core neutron source calculations nor did it address uncertainties in operational or geometric variables that impact power reactor calculations. The second phase of the qualification (H. B. Robinson comparisons) addressed uncertainties in these additional areas that are primarily methods related and would tend to apply generically to all fast neutron exposure evaluations. The third phase of the qualification (analytical sensitivity study) identified the potential uncertainties introduced into the overall evaluation due to calculational methods approximations as well as to a lack of knowledge relative to various plant specific input parameters. The overall calculational uncertainty applicable to the South Texas Project Unit 2 analysis was established from results of these three phases of the methods qualification.

The fourth phase of the uncertainty assessment (comparisons with South Texas Project Unit 2 measurements) was used solely to demonstrate the validity of the transport calculations and to confirm the uncertainty estimates associated with the analytical results. The comparison was used only as a check and was not used in any way to modify the calculated surveillance capsule and pressure vessel neutron exposures previously described in Section 6.2. As such, the validation of the South Texas Project Unit 2 analytical model based on the measured plant dosimetry is completely described in Appendix A.

The following summarizes the uncertainties developed from the first three phases of the methodology qualification. Additional information pertinent to these evaluations is provided in Reference 21.

	Capsule	Vessel IR
PCA Comparisons	3%	3%
H. B. Robinson Comparisons	3%	3%
Analytical Sensitivity Studies	10%	11%
Additional Uncertainty for Factors not Explicitly Evaluated	5%	5%
Net Calculational Uncertainty	12%	13%

The net calculational uncertainty was determined by combining the individual components in quadrature. Therefore, the resultant uncertainty was treated as random and no systematic bias was applied to the analytical results.

The plant specific measurement comparisons described in Appendix A support these uncertainty assessments for South Texas Project Unit 2.

Figure 6-1

South Texas Project Unit 2 r,θ Reactor Geometry with a 12.5° Neutron Pad at the Core Midplane

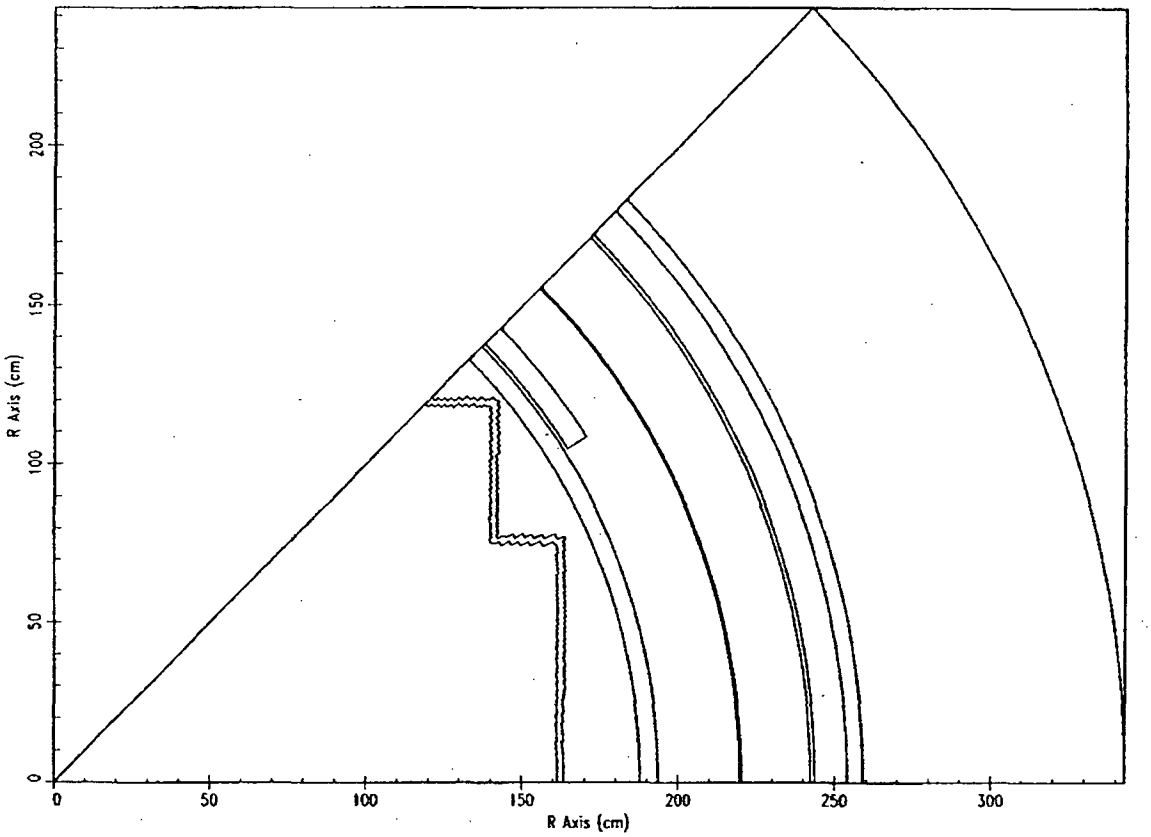

Figure 6-1 (continued)

South Texas Project Unit 2 r,θ Reactor Geometry with a 20.0° Neutron Pad at the Core Midplane

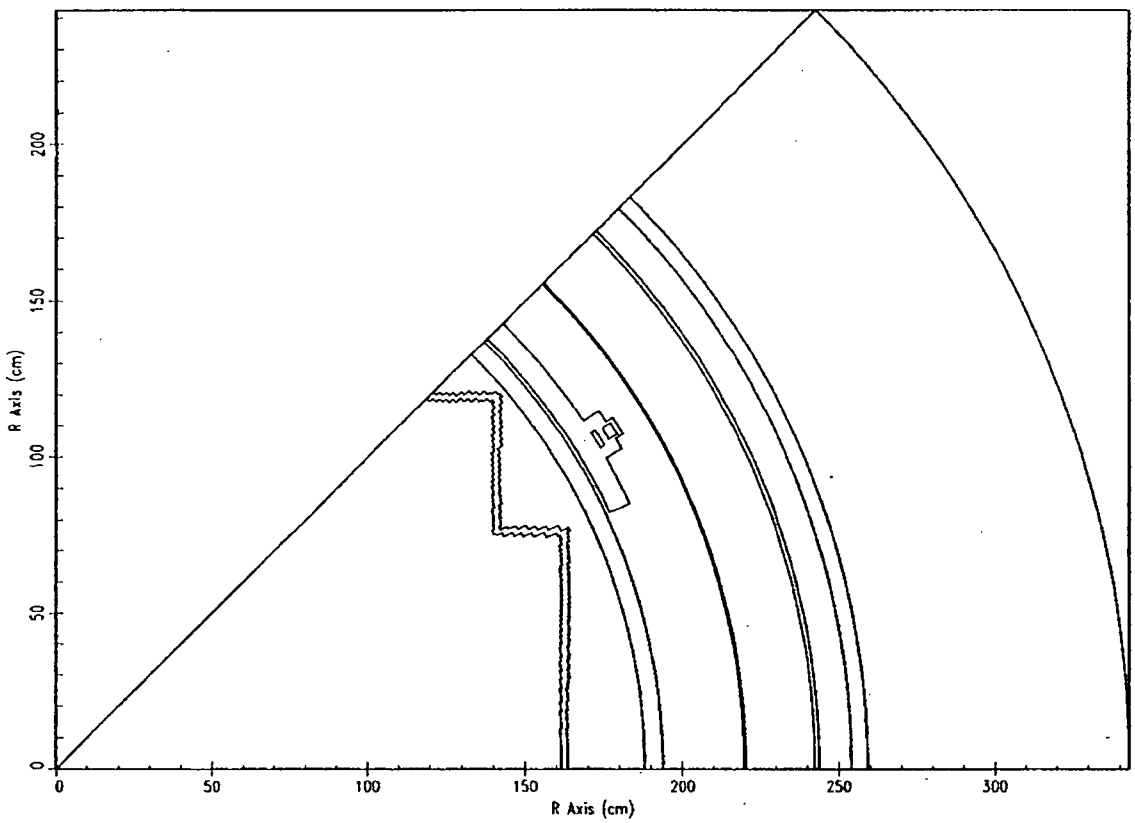

Figure 6-1 (continued)

South Texas Project Unit 2 r,θ Reactor Geometry with a 22.5° Neutron Pad at the Core Midplane

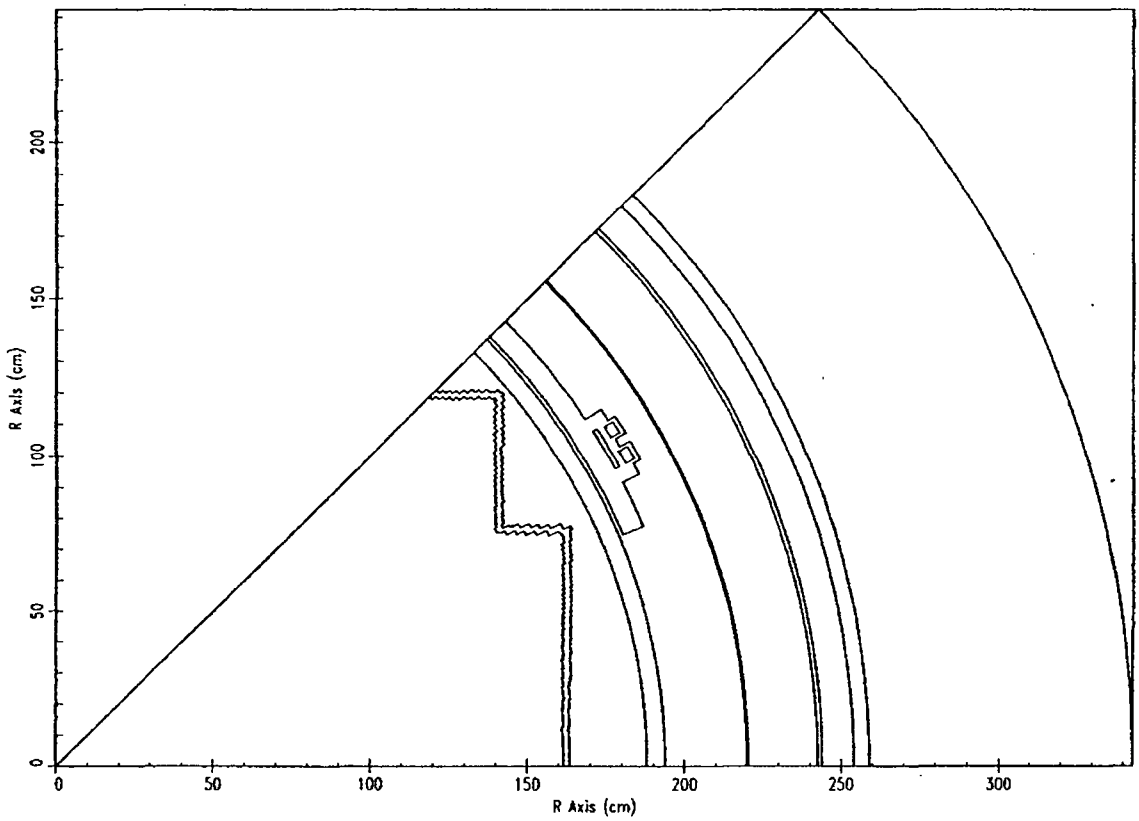

Figure 6-2

South Texas Project Unit 2 r,z Reactor Geometry with Neutron Pad

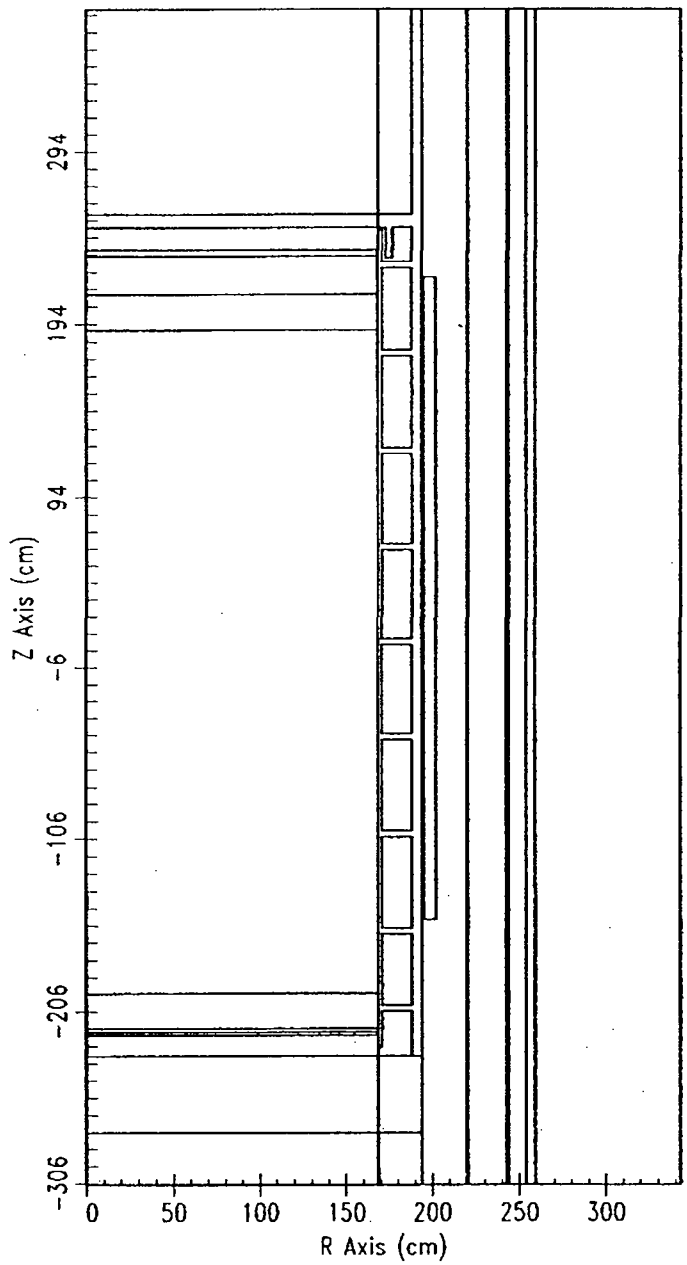

Note: This model was used in the assessment of the surveillance capsule neutron exposures and reactor vessel neutron exposures at the 45° azimuthal location only.

Figure 6-2 (continued)

South Texas Project Unit 2 r,z Reactor Geometry without Neutron Pad

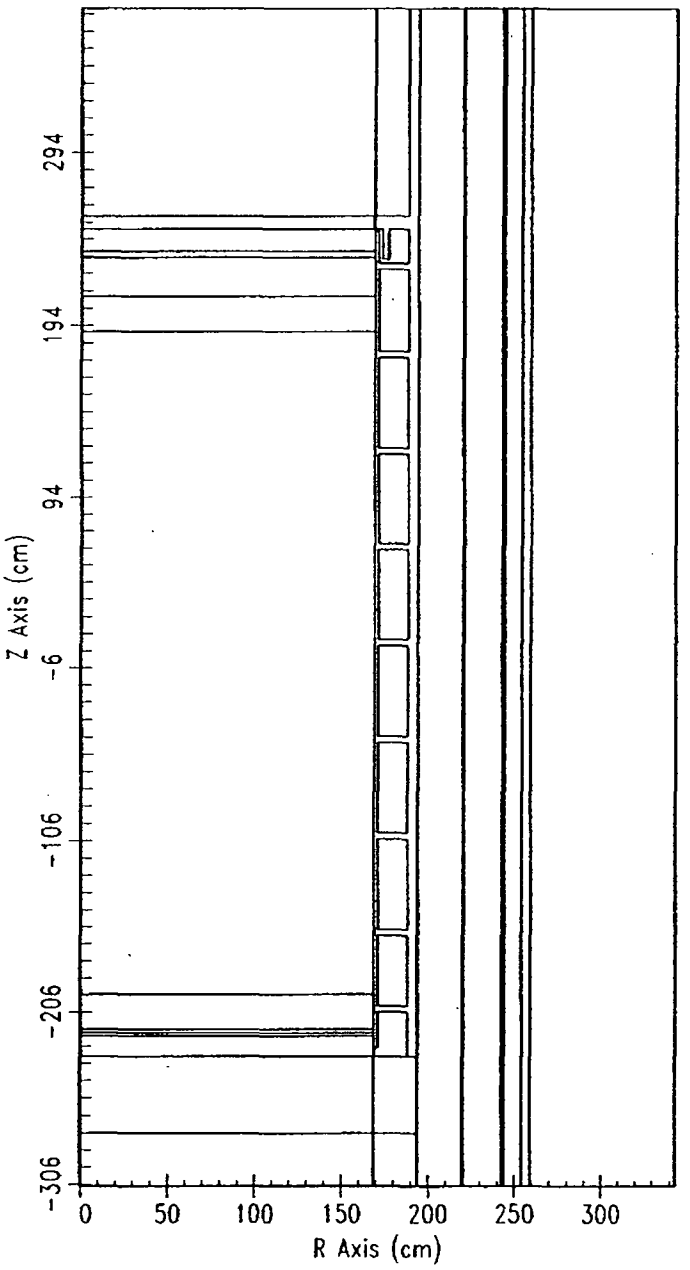

Note: This model was used in the assessment of the reactor vessel neutron exposures at the 0°, 15°, and 30° azimuthal locations only.

Table 6-1

Calculated Neutron Exposure Rates And Integrated Exposures
At The Surveillance Capsule Center

Neutrons (E > 1.0 MeV)

Cycle	Cycle Length [EFPS]	Cumulative Irradiation Time [EFPS]	Cumulative Irradiation Time [EFPY]	Neutron Flux (E > 1.0 MeV) [n/cm^2-s]		
				Dual 29°	Dual 31.5°	Single 31.5°
1	2.73E+07	2.73E+07	0.87	8.58E+10	9.30E+10	9.20E+10
2	2.25E+07	4.98E+07	1.58	6.49E+10	6.84E+10	6.76E+10
3	3.28E+07	8.26E+07	2.62	7.48E+10	7.93E+10	7.83E+10
4	4.13E+07	1.24E+08	3.92	7.91E+10	8.51E+10	8.42E+10
5	3.80E+07	1.62E+08	5.13	6.83E+10	7.35E+10	7.27E+10
6	4.89E+07	2.11E+08	6.68	5.35E+10	5.63E+10	5.56E+10
7	2.95E+07	2.40E+08	7.61	6.97E+10	8.18E+10	8.11E+10
8	3.96E+07	2.80E+08	8.87	6.56E+10	7.20E+10	7.13E+10
9	4.55E+07	3.25E+08	10.31	6.30E+10	6.71E+10	6.63E+10
10(Prj.)	4.19E+07	3.67E+08	11.64	6.79E+10	7.31E+10	7.23E+10
Future	1.38E+08	5.05E+08	16.00	6.79E+10	7.31E+10	7.23E+10
Future	5.05E+08	1.01E+09	32.00	6.79E+10	7.31E+10	7.23E+10
Future	5.05E+08	1.51E+09	48.00	6.79E+10	7.31E+10	7.23E+10
Future	1.89E+08	1.70E+09	54.00	6.79E+10	7.31E+10	7.23E+10

Note: Neutron exposure values reported for the surveillance capsules are centered at the core midplane.

Table 6-1 cont'd

Calculated Neutron Exposure Rates And Integrated Exposures
At The Surveillance Capsule Center

Neutrons (E > 1.0 MeV)

Cycle	Cycle Length [EFPS]	Cumulative Irradiation Time [EFPS]	Cumulative Irradiation Time [EFPY]	Neutron Fluence (E > 1.0 MeV) [n/cm^2]		
				Dual 29°	Dual 31.5°	Single 31.5°
1	2.73E+07	2.73E+07	0.87	2.34E+18	2.54E+18	2.51E+18
2	2.25E+07	4.98E+07	1.58	3.80E+18	4.08E+18	4.03E+18
3	3.28E+07	8.26E+07	2.62	6.25E+18	6.68E+18	6.60E+18
4	4.13E+07	1.24E+08	3.92	9.52E+18	1.02E+19	1.01E+19
5	3.80E+07	1.62E+08	5.13	1.21E+19	1.30E+19	1.28E+19
6	4.89E+07	2.11E+08	6.68	1.47E+19	1.57E+19	1.56E+19
7	2.95E+07	2.40E+08	7.61	1.68E+19	1.81E+19	1.79E+19
8	3.96E+07	2.80E+08	8.87	1.94E+19	2.10E+19	2.08E+19
9	4.55E+07	3.25E+08	10.31	2.23E+19	2.40E+19	2.38E+19
10(Prj.)	4.19E+07	3.67E+08	11.64	2.51E+19	2.71E+19	2.68E+19
Future	1.38E+08	5.05E+08	16.00	3.44E+19	3.72E+19	3.68E+19
Future	5.05E+08	1.01E+09	32.00	6.87E+19	7.41E+19	7.33E+19
Future	5.05E+08	1.51E+09	48.00	1.03E+20	1.11E+20	1.10E+20
Future	1.89E+08	1.70E+09	54.00	1.16E+20	1.25E+20	1.24E+20

Note: Neutron exposure values reported for the surveillance capsules are centered at the core midplane.

Table 6-1 cont'd

Calculated Neutron Exposure Rates And Integrated Exposures
At The Surveillance Capsule Center

Iron Atom Displacements

Cycle	Cycle Length [EFPS]	Cumulative Irradiation Time [EFPS]	Cumulative Irradiation Time [EFPY]	Displacement Rate [dpa/s]		
				Dual 29°	Dual 31.5°	Single 31.5°
1	2.73E+07	2.73E+07	0.87	1.67E-10	1.81E-10	1.79E-10
2	2.25E+07	4.98E+07	1.58	1.26E-10	1.33E-10	1.31E-10
3	3.28E+07	8.26E+07	2.62	1.45E-10	1.54E-10	1.51E-10
4	4.13E+07	1.24E+08	3.92	1.54E-10	1.65E-10	1.63E-10
5	3.80E+07	1.62E+08	5.13	1.32E-10	1.42E-10	1.41E-10
6	4.89E+07	2.11E+08	6.68	1.03E-10	1.09E-10	1.07E-10
7	2.95E+07	2.40E+08	7.61	1.35E-10	1.59E-10	1.57E-10
8	3.96E+07	2.80E+08	8.87	1.27E-10	1.39E-10	1.37E-10
9	4.55E+07	3.25E+08	10.31	1.22E-10	1.29E-10	1.28E-10
10(Prj.)	4.19E+07	3.67E+08	11.64	1.31E-10	1.41E-10	1.39E-10
Future	1.38E+08	5.05E+08	16.00	1.31E-10	1.41E-10	1.39E-10
Future	5.05E+08	1.01E+09	32.00	1.31E-10	1.41E-10	1.39E-10
Future	5.05E+08	1.51E+09	48.00	1.31E-10	1.41E-10	1.39E-10
Future	1.89E+08	1.70E+09	54.00	1.31E-10	1.41E-10	1.39E-10

Note: Neutron exposure values reported for the surveillance capsules are centered at the core midplane.

Table 6-1 cont'd

Calculated Neutron Exposure Rates And Integrated Exposures
At The Surveillance Capsule Center

Iron Atom Displacements

Cycle	Cycle Length [EFPS]	Cumulative Irradiation Time [EFPS]	Cumulative Irradiation Time [EFPY]	Displacements [dpa]		
				Dual 29°	Dual 31.5°	Single 31.5°
1	2.73E+07	2.73E+07	0.87	4.57E-03	4.95E-03	4.89E-03
2	2.25E+07	4.98E+07	1.58	7.41E-03	7.94E-03	7.83E-03
3	3.28E+07	8.26E+07	2.62	1.22E-02	1.30E-02	1.28E-02
4	4.13E+07	1.24E+08	3.92	1.85E-02	1.98E-02	1.95E-02
5	3.80E+07	1.62E+08	5.13	2.35E-02	2.52E-02	2.49E-02
6	4.89E+07	2.11E+08	6.68	2.86E-02	3.05E-02	3.01E-02
7	2.95E+07	2.40E+08	7.61	3.26E-02	3.52E-02	3.47E-02
8	3.96E+07	2.80E+08	8.87	3.76E-02	4.07E-02	4.02E-02
9	4.55E+07	3.25E+08	10.31	4.32E-02	4.66E-02	4.60E-02
10(Prj.)	4.19E+07	3.67E+08	11.64	4.87E-02	5.25E-02	5.18E-02
Future	1.38E+08	5.05E+08	16.00	6.68E-02	7.20E-02	7.10E-02
Future	5.05E+08	1.01E+09	32.00	1.33E-01	1.43E-01	1.41E-01
Future	5.05E+08	1.51E+09	48.00	1.99E-01	2.15E-01	2.12E-01
Future	1.89E+08	1.70E+09	54.00	2.24E-01	2.41E-01	2.38E-01

Note: Neutron exposure values reported for the surveillance capsules are centered at the core midplane.

Table 6-2

Calculated Azimuthal Variation Of Maximum Exposure Rates
And Integrated Exposures At The Reactor Vessel
Clad/Base Metal Interface

Cycle	Cycle Length [EFPS]	Cumulative Irradiation Time [EFPS]	Cumulative Irradiation Time [EFPY]	Neutron Flux (E > 1.0 MeV) [n/cm^2-s]			
				0°	15°	30°	45°
1	2.73E+07	2.73E+07	0.87	1.26E+10	1.87E+10	2.14E+10	2.77E+10
2	2.25E+07	4.98E+07	1.58	1.26E+10	1.75E+10	1.71E+10	2.17E+10
3	3.28E+07	8.26E+07	2.62	1.24E+10	1.81E+10	1.85E+10	2.21E+10
4	4.13E+07	1.24E+08	3.92	1.23E+10	1.79E+10	1.94E+10	2.62E+10
5	3.80E+07	1.62E+08	5.13	1.03E+10	1.50E+10	1.68E+10	2.24E+10
6	4.89E+07	2.11E+08	6.68	9.00E+09	1.28E+10	1.34E+10	1.85E+10
7	2.95E+07	2.40E+08	7.61	7.64E+09	1.16E+10	1.74E+10	3.02E+10
8	3.96E+07	2.80E+08	8.87	8.29E+09	1.26E+10	1.64E+10	2.36E+10
9	4.55E+07	3.25E+08	10.31	8.22E+09	1.24E+10	1.58E+10	1.95E+10
10(Prj.)	4.19E+07	3.67E+08	11.64	1.01E+10	1.50E+10	1.72E+10	2.16E+10
Future	1.38E+08	5.05E+08	16.00	1.01E+10	1.50E+10	1.72E+10	2.16E+10
Future	5.05E+08	1.01E+09	32.00	1.01E+10	1.50E+10	1.72E+10	2.16E+10
Future	5.05E+08	1.51E+09	48.00	1.01E+10	1.50E+10	1.72E+10	2.16E+10
Future	1.89E+08	1.70E+09	54.00	1.01E+10	1.50E+10	1.72E+10	2.16E+10

Table 6-2 cont'd

Calculated Azimuthal Variation Of Maximum Exposure Rates
And Integrated Exposures At The Reactor Vessel
Clad/Base Metal Interface

Cycle	Cycle Length [EFPS]	Cumulative Irradiation Time [EFPS]	Cumulative Irradiation Time [EFPY]	Neutron Fluence (E > 1.0 MeV) [n/cm^2]			
				0°	15°	30°	45°
1	2.73E+07	2.73E+07	0.87	3.43E+17	5.12E+17	5.85E+17	7.58E+17
2	2.25E+07	4.98E+07	1.58	6.04E+17	8.74E+17	9.39E+17	1.24E+18
3	3.28E+07	8.26E+07	2.62	1.01E+18	1.47E+18	1.54E+18	1.97E+18
4	4.13E+07	1.24E+08	3.92	1.52E+18	2.20E+18	2.34E+18	3.05E+18
5	3.80E+07	1.62E+08	5.13	1.91E+18	2.77E+18	2.98E+18	3.90E+18
6	4.89E+07	2.11E+08	6.68	2.34E+18	3.38E+18	3.62E+18	4.81E+18
7	2.95E+07	2.40E+08	7.61	2.56E+18	3.73E+18	4.13E+18	5.70E+18
8	3.96E+07	2.80E+08	8.87	2.89E+18	4.22E+18	4.78E+18	6.63E+18
9	4.55E+07	3.25E+08	10.31	3.26E+18	4.78E+18	5.49E+18	7.52E+18
10(Prj.)	4.19E+07	3.67E+08	11.64	3.68E+18	5.41E+18	6.21E+18	8.42E+18
Future	1.38E+08	5.05E+08	16.00	5.07E+18	7.48E+18	8.58E+18	1.14E+19
Future	5.05E+08	1.01E+09	32.00	1.02E+19	1.51E+19	1.73E+19	2.22E+19
Future	5.05E+08	1.51E+09	48.00	1.52E+19	2.26E+19	2.59E+19	3.31E+19
Future	1.89E+08	1.70E+09	54.00	1.71E+19	2.55E+19	2.92E+19	3.72E+19

Table 6-2 cont'd

Calculated Azimuthal Variation Of Fast Neutron Exposure Rates
And Iron Atom Displacement Rates At The Reactor Vessel
Clad/Base Metal Interface

Cycle	Cycle Length [EFPS]	Cumulative Irradiation Time [EFPS]	Cumulative Irradiation Time [EFPY]	Iron Atom Displacement Rate [dpa/s]			
				0°	15°	30°	45°
1	2.73E+07	2.73E+07	0.87	1.95E-11	2.88E-11	3.30E-11	4.27E-11
2	2.25E+07	4.98E+07	1.58	1.96E-11	2.69E-11	2.64E-11	3.33E-11
3	3.28E+07	8.26E+07	2.62	1.92E-11	2.78E-11	2.85E-11	3.40E-11
4	4.13E+07	1.24E+08	3.92	1.91E-11	2.76E-11	2.99E-11	4.04E-11
5	3.80E+07	1.62E+08	5.13	1.60E-11	2.30E-11	2.59E-11	3.45E-11
6	4.89E+07	2.11E+08	6.68	1.40E-11	1.97E-11	2.07E-11	2.85E-11
7	2.95E+07	2.40E+08	7.61	1.19E-11	1.79E-11	2.69E-11	4.64E-11
8	3.96E+07	2.80E+08	8.87	1.29E-11	1.94E-11	2.53E-11	3.63E-11
9	4.55E+07	3.25E+08	10.31	1.28E-11	1.91E-11	2.43E-11	3.01E-11
10(Prj.)	4.19E+07	3.67E+08	11.64	1.56E-11	2.31E-11	2.65E-11	3.32E-11
Future	1.38E+08	5.05E+08	16.00	1.56E-11	2.31E-11	2.65E-11	3.32E-11
Future	5.05E+08	1.01E+09	32.00	1.56E-11	2.31E-11	2.65E-11	3.32E-11
Future	5.05E+08	1.51E+09	48.00	1.56E-11	2.31E-11	2.65E-11	3.32E-11
Future	1.89E+08	1.70E+09	54.00	1.56E-11	2.31E-11	2.65E-11	3.32E-11

Table 6-2 cont'd

Calculated Azimuthal Variation Of Maximum Exposure Rates
And Integrated Exposures At The Reactor Vessel
Clad/Base Metal Interface

Cycle	Cycle Length [EFPS]	Cumulative Irradiation Time [EFPS]	Cumulative Irradiation Time [EFPY]	Iron Atom Displacements [dpa]			
				0°	15°	30°	45°
1	2.73E+07	2.73E+07	0.87	5.32E-04	7.86E-04	9.01E-04	1.17E-03
2	2.25E+07	4.98E+07	1.58	9.37E-04	1.34E-03	1.45E-03	1.91E-03
3	3.28E+07	8.26E+07	2.62	1.57E-03	2.25E-03	2.38E-03	3.03E-03
4	4.13E+07	1.24E+08	3.92	2.35E-03	3.38E-03	3.61E-03	4.69E-03
5	3.80E+07	1.62E+08	5.13	2.96E-03	4.25E-03	4.59E-03	6.00E-03
6	4.89E+07	2.11E+08	6.68	3.63E-03	5.20E-03	5.58E-03	7.39E-03
7	2.95E+07	2.40E+08	7.61	3.98E-03	5.73E-03	6.37E-03	8.76E-03
8	3.96E+07	2.80E+08	8.87	4.49E-03	6.49E-03	7.37E-03	1.02E-02
9	4.55E+07	3.25E+08	10.31	5.07E-03	7.35E-03	8.47E-03	1.16E-02
10(Prj.)	4.19E+07	3.67E+08	11.64	5.72E-03	8.32E-03	9.58E-03	1.30E-02
Future	1.38E+08	5.05E+08	16.00	7.87E-03	1.15E-02	1.32E-02	1.75E-02
Future	5.05E+08	1.01E+09	32.00	1.58E-02	2.32E-02	2.66E-02	3.43E-02
Future	5.05E+08	1.51E+09	48.00	2.37E-02	3.48E-02	4.00E-02	5.10E-02
Future	1.89E+08	1.70E+09	54.00	2.66E-02	3.92E-02	4.50E-02	5.73E-02

Table 6-3

Calculated Integrated Exposures for Key Vessel Plate and Weld Materials
At The Reactor Vessel Clad/Base Metal Interface

		Neutron Fluence (E > 1.0 MeV), n/cm^2					
Material	Location	10.31 EFPY	11.64 EFPY	16 EFPY	32 EFPY	48 EFPY	54 EFPY
Upper-to-Intermediate Shell Circumferential Weld	45°	8.03E+16	8.78E+16	1.13E+17	2.03E+17	2.94E+17	3.28E+17
Intermediate Shell Basemetal	45°	5.56E+18	6.27E+18	8.57E+18	1.70E+19	2.55E+19	2.86E+19
Intermediate Shell Longitudinal Weld 0° Azimuth	0°	3.20E+18	3.61E+18	4.97E+18	9.95E+18	1.49E+19	1.68E+19
Intermediate-to-Lower Shell Circumferential Weld	45°	5.54E+18	6.24E+18	8.52E+18	1.69E+19	2.52E+19	2.84E+19
Lower Shell Basemetal	45°	7.52E+18	8.42E+18	1.14E+19	2.22E+19	3.31E+19	3.72E+19
Lower Shell Longitudinal Weld 90° Azimuth	0°	3.26E+18	3.68E+18	5.07E+18	1.02E+19	1.52E+19	1.71E+19
Lower Shell Longitudinal Weld 210° and 330° Azimuth 12.5° Neutron Pad	30°	7.30E+18	8.21E+18	1.12E+19	2.22E+19	3.32E+19	3.73E+19
Lower Shell-to-Lower Head Circumferential Weld	45°	8.47E+16	9.26E+16	1.18E+17	2.13E+17	3.08E+17	3.43E+17

Notes:
(1) The Intermediate Shell Longitudinal Weld, 120° Azimuth, 20° Neutron Pad results at the 30° location are bounded by the Intermediate Shell Basemetal values at the 45° location.
(2) The Intermediate Shell Longitudinal Weld, 240° Azimuth, 22.5° Neutron Pad results at the 30° location are bounded by the Intermediate Shell Basemetal values at the 45° location.

Table 6-3 cont'd

Calculated Integrated Exposures for KeyVessel Plate and Weld Materials
At The Reactor Vessel Clad/Base Metal Interface

		Iron Atom Displacements, dpa					
Material	Location	10.31 EFPY	11.64 EFPY	16 EFPY	32 EFPY	48 EFPY	54 EFPY
Upper-to-Intermediate Shell Circumferential Weld	45°	1.39E-04	1.53E-04	1.96E-04	3.55E-04	5.14E-04	5.73E-04
Intermediate Shell Basemetal	45°	8.80E-03	9.91E-03	1.36E-02	2.69E-02	4.03E-02	4.53E-02
Intermediate Shell Longitudinal Weld 0° Azimuth	0°	4.96E-03	5.61E-03	7.72E-03	1.55E-02	2.32E-02	2.61E-02
Intermediate-to-Lower Shell Circumferential Weld	45°	8.78E-03	9.88E-03	1.35E-02	2.68E-02	4.00E-02	4.50E-02
Lower Shell Basemetal	45°	1.16E-02	1.30E-02	1.75E-02	3.43E-02	5.10E-02	5.73E-02
Lower Shell Longitudinal Weld 90° Azimuth	0°	5.07E-03	5.72E-03	7.87E-03	1.58E-02	2.37E-02	2.66E-02
Lower Shell Longitudinal Weld 210° and 330° Azimuth 12.5° Neutron Pad	30°	1.10E-02	1.23E-02	1.68E-02	3.34E-02	4.99E-02	5.61E-02
Lower Shell-to-Lower Head Circumferential Weld	45°	1.51E-04	1.65E-04	2.11E-04	3.82E-04	5.52E-04	6.16E-04

Notes:

(3) The Intermediate Shell Longitudinal Weld, 120° Azimuth, 20° Neutron Pad results at the 30° location are bounded by the Intermediate Shell Basemetal values at the 45° location.

(4) The Intermediate Shell Longitudinal Weld, 240° Azimuth, 22.5° Neutron Pad results at the 30° location are bounded by the Intermediate Shell Basemetal values at the 45° location.

Table 6-4

Relative Radial Distribution Of Neutron Fluence (E > 1.0 MeV)
Within The Reactor Vessel Wall

RADIUS	AZIMUTHAL ANGLE			
(cm)	0°	15°	30°	45°
220.350	1.000	1.000	1.000	1.000
225.868	0.563	0.559	0.553	0.550
231.385	0.277	0.272	0.268	0.264
236.903	0.131	0.127	0.125	0.122
242.420	0.063	0.058	0.057	0.055

Note:
Base Metal Inner Radius = 220.350 cm
Base Metal 1/4T = 225.868 cm
Base Metal 1/2T = 231.385 cm
Base Metal 3/4T = 236.903 cm
Base Metal Outer Radius = 242.420 cm

Table 6-5

Relative Radial Distribution Of Iron Atom Displacements (dpa)
Within The Reactor Vessel Wall

RADIUS	AZIMUTHAL ANGLE			
(cm)	0°	15°	30°	45°
220.350	1.000	1.000	1.000	1.000
225.868	0.638	0.633	0.632	0.642
231.385	0.388	0.380	0.381	0.392
236.903	0.236	0.226	0.229	0.236
242.420	0.142	0.129	0.130	0.134

Note:
Base Metal Inner Radius = 220.350 cm
Base Metal 1/4T = 225.868 cm
Base Metal 1/2T = 231.385 cm
Base Metal 3/4T = 236.903 cm
Base Metal Outer Radius = 242.420 cm

Table 6-6

Calculated Fast Neutron Exposure of Surveillance Capsules
Withdrawn from South Texas Project Unit 2

Capsule	Irradiation Time [EFPY]	Fluence (E > 1.0 MeV) [n/cm^2]	Iron Displacements [dpa]
V	0.87	2.34E+18	4.57E-03
Y	5.13	1.21E+19	2.35E-02
U	10.31	2.40E+19	4.66E-02

Table 6-7

Calculated Surveillance Capsule Lead Factors

Capsule ID And Location	Status	Lead Factor
V (29° dual)	Withdrawn EOC 1	3.09
Y (29° dual)	Withdrawn EOC 5	3.11
U (31.5° dual)	Withdrawn EOC 9	3.20
X (31.5° dual)	In Reactor	3.22
W (31.5° single)	In Reactor	3.19
Z (31.5° single)	In Reactor	3.19

Note: Lead factors for capsules remaining in the reactor are based on cycle specific exposure calculations through the current operating fuel reload, i.e., Cycle 10.

7 SURVEILLANCE CAPSULE REMOVAL SCHEDULE

The following surveillance capsule removal schedule meets the requirements of ASTM E185-82 and is recommended for future capsules to be removed from the South Texas Unit 2 reactor vessel. This recommended removal schedule is applicable to 32 EFPY of operation.

Table 7-1 Recommended Surveillance Capsule Withdrawal Schedule

Capsule	Capsule Location	Lead Factor [a]	Withdrawal EFPY [b]	Fluence (n/cm^2) [a]
V	61°	3.09	0.87	2.34×10^{18} (c)
Y	241°	3.11	5.13	1.21×10^{19} (c)
U	58.5°	3.20	10.31	2.40×10^{19} (c)
X	238.5°	3.22	Standby	(d)
W	121.5°	3.19	Standby	(d)
Z	301.5°	3.19	Standby	(d)

Notes:

(a) Updated in Capsule u dosimetry analysis.

(b) Effective Full Power Years (EFPY) from plant startup.

(c) Plant specific evaluation.

(d) Section X1.M31, "Reactor Vessel Surveillance," of NUREG-1801 states that any surveillance capsules that are left in the reactor vessel should provide meaningful metallurgical data. The NRC specifically states that anything beyond 60 years of exposure is not meaningful metallurgical data. Hence, it is recommended that Capsule "X" be removed and tested at 16 EFPY (3.65×10^{19} n/cm^2, E > 1.0 MeV, i.e., the peak 53 EFPY fluence). Capsules "W" and "Z" should be removed and placed in storage at 16 EFPY.

8 REFERENCES

1. Regulatory Guide 1.99, Revision 2, *Radiation Embrittlement of Reactor Vessel Materials*, U.S. Nuclear Regulatory Commission, May, 1988.

2. Code of Federal Regulations, 10CFR50, Appendix G, *Fracture Toughness Requirements*, and Appendix H, *Reactor Vessel Material Surveillance Program Requirements*, U.S. Nuclear Regulatory Commission, Washington, D.C.

3. WCAP-14978, *Analysis of Capsule Y from the Houston Lighting and Power Company South Texas Unit 2 Reactor Vessel Radiation Surveillance Program*, E. Terek, et. al., dated December 1997.

4. WCAP-9967, *Houston Lighting and Power Company South Texas Project Unit No. 2 Reactor Vessel Radiation Surveillance Program*, L.R. Singer, dated January 1982.

5. WCAP-13182, *Analysis of Capsule V from the Houston Lighting and Power Company South Texas Unit 2 Reactor Vessel Radiation Surveillance Program*, J.M. Chicots, et. al., dated February 1992.

6. ASTM E208, *Standard Test Method for Conducting Drop-Weight Test to Determine Nil-Ductility Transition Temperature of Ferritic Steels*, in ASTM Standards, Section 3, American Society for Testing and Materials, Philadelphia, PA.

7. Section XI of the ASME Boiler and Pressure Vessel Code, Appendix G, *Fracture Toughness Criteria for Protection Against Failure*

8. ASTM E185-82, *Standard Practice for Conducting Surveillance Tests for Light-Water Cooled Nuclear Power Reactor Vessels*, in ASTM Standards, Section 3, American Society for Testing and Materials, Philadelphia, PA.

9. Procedure RMF 8402, *Surveillance Capsule Testing Program*, Revision 2.

10. Procedure RMF 8102, *Tensile Testing*, Revision 1.

11. Procedure RMF 8103, *Charpy Impact Testing*, Revision 1.

12. ASTM E23-98, *Standard Test Method for Notched Bar Impact Testing of Metallic Materials*, in ASTM Standards, Section 3, American Society for Testing and Materials, Philadelphia, PA, 1998.

13. ASTM A370-97a, *Standard Test Methods and Definitions for Mechanical Testing of Steel Products*, in ASTM Standards, Section 3, American Society for Testing and Materials, Philadelphia, PA, 1997.

14. ASTM E8-99, *Standard Test Methods for Tension Testing of Metallic Materials*, in ASTM Standards, Section 3, American Society for Testing and Materials, Philadelphia, PA, 1999.

15. ASTM E21-92 (1998), *Standard Test Methods for Elevated Temperature Tension Tests of Metallic Materials*, in ASTM Standards, Section 3, American Society for Testing and Materials, Philadelphia, PA, 1998.

16. ASTM E83-93, *Standard Practice for Verification and Classification of Extensometers*, in ASTM Standards, Section 3, American Society for Testing and Materials, Philadelphia, PA, 1993.

17. ASTM E185-79, *Standard Practice for Conducting Surveillance Tests for Light-Water Cooled Nuclear Power Reactor Vessels*

18. WCAP-14370, *Use of the Hyperbolic Tangent Function for Fitting Transition Temperature Toughness Data*, T. R. Mager, et al, May 1995.

19. Regulatory Guide RG-1.190, *Calculational and Dosimetry Methods for Determining Pressure Vessel Neutron Fluence*, U. S. Nuclear Regulatory Commission, Office of Nuclear Regulatory Research, March 2001.

20. WCAP-14040-NP-A, Revision 2, *Methodology Used to Develop Cold Overpressure Mitigating System Setpoints and RCS Heatup and Cooldown Limit Curves*, January 1996.

21. WCAP-15557, Revision 0, *Qualification of the Westinghouse Pressure Vessel Neutron Fluence Evaluation Methodology*, August 2000.

22. RSICC Computer Code Collection CCC-650, *DOORS 3.1, One, Two- and Three-Dimensional Discrete Ordinates Neutron/Photon Transport Code System*, August 1996.

23. RSIC Data Library Collection DLC-185, "BUGLE-96, Coupled 47 Neutron, 20 Gamma-Ray Group Cross Section Library Derived from ENDF/B-VI for LWR Shielding and Pressure Vessel Dosimetry Applications," March 1996.

APPENDIX A

VALIDATION OF THE RADIATION TRANSPORT MODELS BASED ON NEUTRON DOSIMETRY MEASUREMENTS

A.1 Neutron Dosimetry

Comparisons of measured dosimetry results to both the calculated and least squares adjusted values for all surveillance capsules withdrawn from service to date at South Texas Project Unit 2 are described herein. The sensor sets from these capsules have been analyzed in accordance with the current dosimetry evaluation methodology described in Regulatory Guide 1.190, "Calculational and Dosimetry Methods for Determining Pressure Vessel Neutron Fluence."[A-1] One of the main purposes for presenting this material is to demonstrate that the overall measurements agree with the calculated and least squares adjusted values to within ± 20% as specified by Regulatory Guide 1.190, thus serving to validate the calculated neutron exposures previously reported in Section 6.2 of this report. This information may also be useful in the future, in particular, as least squares adjustment techniques become accepted in the regulatory environment.

A.1.1 Sensor Reaction Rate Determinations

In this section, the results of the evaluations of the three neutron sensor sets withdrawn to date as part of the South Texas Project Unit 2 Reactor Vessel Materials Surveillance Program are presented. The capsule designation, location within the reactor, and time of withdrawal of each of these dosimetry sets were as follows:

Capsule ID	Azimuthal Location	Withdrawal Time	Irradiation Time [EFPY]
V	29° dual	End of Cycle 1	0.87
Y	29° dual	End of Cycle 5	5.13
U	31.5° dual	End of Cycle 9	10.31

The azimuthal locations included in the above tabulation represent the first octant equivalent azimuthal angle of the geometric center of the respective surveillance capsules.

The passive neutron sensors included in the evaluations of Survillance Capsules V, Y, and U are summarized as follows:

Sensor Material	Reaction Of Interest	Capsule V	Capsule Y	Capsule U
Copper	$^{63}Cu(n,\alpha)^{60}Co$	X	X	X
Iron	$^{54}Fe(n,p)^{54}Mn$	X	X	X
Nickel	$^{58}Ni(n,p)^{58}Co$	X	X	X
Uranium-238	$^{238}U(n,f)^{137}Cs$	X	X	X
Neptunium-237	$^{237}Np(n,f)^{137}Cs$	X	X	X
Cobalt-Aluminum*	$^{59}Co(n,\gamma)^{60}Co$	X	X	X

* The cobalt-aluminum measurements for this plant include both bare wire and cadmium-covered sensors.

Since all of the dosimetry monitors were accommodated within the dosimeter block centered at the radial, azimuthal, and axial center of the material test specimen array, gradient corrections were not required for these reaction rates. Pertinent physical and nuclear characteristics of the passive neutron sensors are listed in Table A-1.

The use of passive monitors such as those listed above does not yield a direct measure of the energy dependent neutron flux at the point of interest. Rather, the activation or fission process is a measure of the integrated effect that the time and energy dependent neutron flux has on the target material over the course of the irradiation period. An accurate assessment of the average neutron flux level incident on the various monitors may be derived from the activation measurements only if the irradiation parameters are well known. In particular, the following variables are of interest:

- the measured specific activity of each monitor,
- the physical characteristics of each monitor,
- the operating history of the reactor,
- the energy response of each monitor, and
- the neutron energy spectrum at the monitor location.

The radiometric counting of the neutron sensors from Capsule V was carried out by the Westinghouse Analytical Services Laboratory at the Waltz Mill Site.[A-2] The radiometric counting of the sensors from Capsule Y were performed by the Antech Analytical Laboratory[A-3], and the sensors from Capsule U were counted by Pace Analytical Services, Inc., also located at the Waltz Mill Site. In all cases, the radiometric counting followed established ASTM procedures. Following sample preparation and weighing, the specific activity of each sensor was determined by means of a high-resolution gamma spectrometer. For the copper, iron, nickel, and cobalt-aluminum sensors, these analyses were performed by direct counting of each of the individual samples. In the case of the uranium and neptunium fission sensors, the analyses were carried out by direct counting preceded by dissolution and chemical separation of cesium from the sensor material.

The irradiation history of the reactor over the irradiation periods experienced by Capsules V, Y, and U was based on the reported monthly power generation of South Texas Project Unit 2 from initial reactor startup through the end of the dosimetry evaluation period. For the sensor sets utilized in the surveillance capsules, the half-lives of the product isotopes are long enough that a monthly histogram describing reactor operation has proven to be an adequate representation for use in radioactive decay corrections for the reactions of interest in the exposure evaluations. The irradiation history applicable to Capsules V, Y, and U is given in Table A-2.

Having the measured specific activities, the physical characteristics of the sensors, and the operating history of the reactor, reaction rates referenced to full-power operation were determined from the following equation:

$$R = \frac{A}{N_0 F Y \Sigma \frac{P_j}{P_{ref}} C_j [1-e^{-\lambda t_j}] [e^{-\lambda t_d}]}$$

where:

- R = Reaction rate averaged over the irradiation period and referenced to operation at a core power level of P_{ref} (rps/nucleus).
- A = Measured specific activity (dps/gm).
- N_0 = Number of target element atoms per gram of sensor.
- F = Weight fraction of the target isotope in the sensor material.
- Y = Number of product atoms produced per reaction.
- P_j = Average core power level during irradiation period j (MW).
- P_{ref} = Maximum or reference power level of the reactor (MW).
- C_j = Calculated ratio of $\phi(E > 1.0 \text{ MeV})$ during irradiation period j to the time weighted average $\phi(E > 1.0 \text{ MeV})$ over the entire irradiation period.
- λ = Decay constant of the product isotope (1/sec).
- t_j = Length of irradiation period j (sec).
- t_d = Decay time following irradiation period j (sec).

and the summation is carried out over the total number of monthly intervals comprising the irradiation period.

In the equation describing the reaction rate calculation, the ratio $[P_j]/[P_{ref}]$ accounts for month-by-month variation of reactor core power level within any given fuel cycle as well as over multiple fuel cycles. The ratio C_j, which was calculated for each fuel cycle using the transport methodology discussed in Section 6.2, accounts for the change in sensor reaction rates caused by variations in flux level induced by changes in core spatial power distributions from fuel cycle to fuel cycle. For a single-cycle irradiation, C_j is normally taken to be 1.0. However, for multiple-cycle irradiations, particularly those employing low leakage fuel management, the additional C_j term should be employed. The impact of changing flux levels for constant power operation can be quite significant for sensor sets that have been irradiated for many cycles in a reactor that has transitioned from non-low leakage to low leakage fuel management or for sensor sets contained in surveillance capsules that have been moved from one capsule location to another. The fuel cycle specific neutron flux values along with the computed values for C_j are listed in Table A-3. These flux values represent the cycle dependent results at the radial and azimuthal center of the respective capsules at the axial elevation of the active fuel midplane.

Prior to using the measured reaction rates in the least-squares evaluations of the dosimetry sensor sets, additional corrections were made to the ^{238}U measurements to account for the presence of ^{235}U impurities in the sensors as well as to adjust for the build-in of plutonium isotopes over the course of the irradiation. Corrections were also made to the ^{238}U and ^{237}Np sensor reaction rates to account for gamma ray induced fission reactions that occurred over the course of the capsule irradiations. The correction factors applied to the South Texas Project Unit 2 fission sensor reaction rates are summarized as follows:

Correction	Capsule V	Capsule Y	Capsule U
^{235}U Impurity/Pu Build-in	0.873	0.837	0.796
$^{238}U(\gamma,f)$	0.969	0.969	0.969
Net ^{238}U Correction	0.846	0.811	0.771
$^{237}Np(\gamma,f)$	0.991	0.991	0.991

These factors were applied in a multiplicative fashion to the decay corrected uranium and neptunium fission sensor reaction rates.

Results of the sensor reaction rate determinations for Capsules V, Y, and U are given in Table A-4. In Table A-4, the measured specific activities, decay corrected saturated specific activities, and computed reaction rates for each sensor indexed to the radial center of the capsule are listed. The fission sensor reaction rates are listed both with and without the applied corrections for ^{238}U impurities, plutonium build-in, and gamma ray induced fission effects.

A.1.2 Least Squares Evaluation of Sensor Sets

Least squares adjustment methods provide the capability of combining the measurement data with the corresponding neutron transport calculations resulting in a Best Estimate neutron energy spectrum with associated uncertainties. Best Estimates for key exposure parameters such as $\phi(E > 1.0\ MeV)$ or dpa/s along with their uncertainties are then easily obtained from the adjusted spectrum. In general, the least squares methods, as applied to surveillance capsule dosimetry evaluations, act to reconcile the measured sensor reaction rate data, dosimetry reaction cross-sections, and the calculated neutron energy spectrum within their respective uncertainties. For example,

$$R_i \pm \delta_{R_i} = \sum_g (\sigma_{ig} \pm \delta_{\sigma_{ig}})(\phi_g \pm \delta_{\phi_g})$$

relates a set of measured reaction rates, R_i, to a single neutron spectrum, ϕ_g, through the multigroup dosimeter reaction cross-section, σ_{ig}, each with an uncertainty δ. The primary objective of the least squares evaluation is to produce unbiased estimates of the neutron exposure parameters at the location of the measurement.

For the least squares evaluation of the South Texas Project Unit 2 surveillance capsule dosimetry, the FERRET code[A-4] was employed to combine the results of the plant specific neutron transport calculations and sensor set reaction rate measurements to determine best-estimate values of exposure parameters ($\phi(E > 1.0\ MeV)$ and dpa) along with associated uncertainties for the three in-vessel capsules withdrawn to date.

The application of the least squares methodology requires the following input:

1 - The calculated neutron energy spectrum and associated uncertainties at the measurement location.

2 - The measured reaction rates and associated uncertainty for each sensor contained in the multiple foil set.

3 - The energy dependent dosimetry reaction cross-sections and associated uncertainties for each sensor contained in the multiple foil sensor set.

For the South Texas Project Unit 2 application, the calculated neutron spectrum was obtained from the results of plant specific neutron transport calculations described in Section 6.2 of this report. The sensor reaction rates were derived from the measured specific activities using the procedures described in Section A.1.1. The dosimetry reaction cross-sections and uncertainties were obtained from the SNLRML dosimetry cross-section library[A-5]. The SNLRML library is an evaluated dosimetry reaction cross-section compilation recommended for use in LWR evaluations by ASTM Standard E1018, "Application of ASTM Evaluated Cross-Section Data File, Matrix E 706 (IIB)".

The uncertainties associated with the measured reaction rates, dosimetry cross-sections, and calculated neutron spectrum were input to the least squares procedure in the form of variances and covariances. The assignment of the input uncertainties followed the guidance provided in ASTM Standard E 944, "Application of Neutron Spectrum Adjustment Methods in Reactor Surveillance."

The following provides a summary of the uncertainties associated with the least squares evaluation of the South Texas Project Unit 2 surveillance capsule sensor sets.

Reaction Rate Uncertainties

The overall uncertainty associated with the measured reaction rates includes components due to the basic measurement process, irradiation history corrections, and corrections for competing reactions. A high level of accuracy in the reaction rate determinations is assured by utilizing laboratory procedures that conform to the ASTM National Consensus Standards for reaction rate determinations for each sensor type.

After combining all of these uncertainty components, the sensor reaction rates derived from the counting and data evaluation procedures were assigned the following net uncertainties for input to the least squares evaluation:

Reaction	Uncertainty
$^{63}Cu(n,\alpha)^{60}Co$	5%
$^{54}Fe(n,p)^{54}Mn$	5%
$^{58}Ni(n,p)^{58}Co$	5%
$^{238}U(n,f)^{137}Cs$	10%
$^{237}Np(n,f)^{137}Cs$	10%
$^{59}Co(n,\gamma)^{60}Co$	5%

These uncertainties are given at the 1σ level.

Dosimetry Cross-Section Uncertainties

The reaction rate cross-sections used in the least squares evaluations were taken from the SNLRML library. This data library provides reaction cross-sections and associated uncertainties, including covariances, for 66 dosimetry sensors in common use. Both cross-sections and uncertainties are provided in a fine multigroup structure for use in least squares adjustment applications. These cross-sections were compiled from the most recent cross-section evaluations and they have been tested with respect to their accuracy and consistency for least squares evaluations. Further, the library has been empirically tested for use in fission spectra determination as well as in the fluence and energy characterization of 14 MeV neutron sources.

For sensors included in the South Texas Project Unit 2 surveillance program, the following uncertainties in the fission spectrum averaged cross-sections are provided in the SNLRML documentation package.

Reaction	Uncertainty
$^{63}Cu(n,\alpha)^{60}Co$	4.08-4.16%
$^{54}Fe(n,p)^{54}Mn$	3.05-3.11%
$^{58}Ni(n,p)^{58}Co$	4.49-4.56%
$^{238}U(n,f)^{137}Cs$	0.54-0.64%
$^{237}Np(n,f)^{137}Cs$	10.32-10.97%
$^{59}Co(n,\gamma)^{60}Co$	0.79-3.59%

These tabulated ranges provide an indication of the dosimetry cross-section uncertainties associated with the sensor sets used in LWR irradiations.

Calculated Neutron Spectrum

The neutron spectra input to the least squares adjustment procedure were obtained directly from the results of plant specific transport calculations for each surveillance capsule irradiation period and location. The spectrum for each capsule was input in an absolute sense (rather than as simply a relative spectral shape). Therefore, within the constraints of the assigned uncertainties, the calculated data were treated equally with the measurements.

While the uncertainties associated with the reaction rates were obtained from the measurement procedures and counting benchmarks and the dosimetry cross-section uncertainties were supplied directly with the SNLRML library, the uncertainty matrix for the calculated spectrum was constructed from the following relationship:

$$M_{gg'} = R_n^2 + R_g * R_{g'} * P_{gg'}$$

where R_n specifies an overall fractional normalization uncertainty and the fractional uncertainties R_g and $R_{g'}$ specify additional random groupwise uncertainties that are correlated with a correlation matrix given by:

$$P_{gg'} = [1-\theta]\delta_{gg'} + \theta e^{-H}$$

where

$$H = \frac{(g-g')^2}{2\gamma^2}$$

The first term in the correlation matrix equation specifies purely random uncertainties, while the second term describes the short-range correlations over a group range γ (θ specifies the strength of the latter term). The value of δ is 1.0 when g = g', and is 0.0 otherwise.

The set of parameters defining the input covariance matrix for the South Texas Project Unit 2 calculated spectra was as follows:

Flux Normalization Uncertainty (R_n) 15%

Flux Group Uncertainties (R_g, $R_{g'}$)

(E > 0.0055 MeV)	15%
(0.68 eV < E < 0.0055 MeV)	29%
(E < 0.68 eV)	52%

Short Range Correlation (θ)

(E > 0.0055 MeV)	0.9
(0.68 eV < E < 0.0055 MeV)	0.5
(E < 0.68 eV)	0.5

Flux Group Correlation Range (γ)

(E > 0.0055 MeV)	6
(0.68 eV < E < 0.0055 MeV)	3
(E < 0.68 eV)	2

A.1.3 Comparisons of Measurements and Calculations

Results of the least squares evaluations of the dosimetry from the South Texas Project Unit 2 surveillance capsules withdrawn to date are provided in Tables A-5 and A-6. In Table A-5, measured, calculated, and best-estimate values for sensor reaction rates are given for each capsule. Also provided in this tabulation are ratios of the measured reaction rates to both the calculated and least squares adjusted reaction rates. These ratios of M/C and M/BE illustrate the consistency of the fit of the calculated neutron energy spectra to the measured reaction rates both before and after adjustment. In Table A-6, comparison of the calculated and best estimate values of neutron flux (E > 1.0 MeV) and iron atom displacement rate are tabulated along with the BE/C ratios observed for each of the capsules.

The data comparisons provided in Tables A-5 and A-6 show that the adjustments to the calculated spectra are relatively small and well within the assigned uncertainties for the calculated spectra, measured sensor reaction rates, and dosimetry reaction cross-sections. Further, these results indicate that the use of the least squares evaluation results in a reduction in the uncertainties associated with the exposure of the surveillance capsules. From Section 6.4 of this report, it may be noted that the uncertainty associated with the unadjusted calculation of neutron fluence (E > 1.0 MeV) and iron atom displacements at the surveillance capsule locations is specified as 12% at the 1σ level. From Table A-6, it is noted that the corresponding uncertainties associated with the least squares adjusted exposure parameters have been reduced to 6% for neutron flux (E > 1.0 MeV) and 8% for iron atom displacement rate. Again, the uncertainties from the least squares evaluation are at the 1σ level.

Further comparisons of the measurement results with calculations are given in Tables A-7 and A-8. These comparisons are given on two levels. In Table A-7, calculations of individual threshold sensor reaction rates are compared directly with the corresponding measurements. These threshold reaction rate comparisons provide a good evaluation of the accuracy of the fast neutron portion of the calculated energy spectra. In Table A-8, calculations of fast neutron exposure rates in terms of ϕ(E > 1.0 MeV) and dpa/s are compared with the best estimate results obtained from the least squares evaluation of the capsule dosimetry results. These two levels of comparison yield consistent and similar results with all measurement-to-calculation comparisons falling well within the 20% limits specified as the acceptance criteria in Regulatory Guide 1.190.

In the case of the direct comparison of measured and calculated sensor reaction rates, the M/C comparisons for fast neutron reactions range from 0.90–1.21 for the 15 samples included in the data set. The overall average M/C ratio for the entire set of South Texas Project Unit 2 data is 1.04 with an associated standard deviation of 10.5%.

In the comparisons of best estimate and calculated fast neutron exposure parameters, the corresponding BE/C comparisons for the capsule data sets range from 0.95–1.06 for neutron flux (E > 1.0 MeV) and from 0.95 to 1.07 for iron atom displacement rate. The overall average BE/C ratios for neutron flux (E > 1.0 MeV) and iron atom displacement rate are 1.02 with a standard deviation of 5.6% and 1.02 with a standard deviation of 6.3%, respectively.

Based on these comparisons, it is concluded that the calculated fast neutron exposures provided in Section 6.2 of this report are validated for use in the assessment of the condition of the materials comprising the beltline region of the South Texas Project Unit 2 reactor pressure vessel.

Table A-1

Nuclear Parameters Used In The Evaluation Of Neutron Sensors

Monitor Material	Reaction of Interest	Target Atom Fraction	90% Response Range (MeV)	Product Half-life	Fission Yield (%)
Copper	^{63}Cu (n,α)	0.6917	4.9 – 11.9	5.271 y	
Iron	^{54}Fe (n,p)	0.0585	2.1 – 8.4	312.3 d	
Nickel	^{58}Ni (n,p)	0.6808	1.5 – 8.3	70.82 d	
Uranium-238	^{238}U (n,f)	1.0000	1.3 – 6.9	30.07 y	6.02
Neptunium-237	^{237}Np (n,f)	1.0000	0.3 – 3.8	30.07 y	6.17
Cobalt-Aluminum	^{59}Co (n,γ)	0.0015	non-threshold	5.271 y	

Note: The 90% response range is defined such that, in the neutron spectrum characteristic of the South Texas Project Unit 2 surveillance capsules, approximately 90% of the sensor response is due to neutrons in the energy range specified with approximately 5% of the total response due to neutrons with energies below the lower limit and 5% of the total response due to neutrons with energies above the upper limit.

Table A-2

Monthly Thermal Generation During The First Nine Fuel Cycles
Of The South Texas Project Unit 2 Reactor
(Reactor Power of 3800 MWt through the end of Cycle 9)

Year	Month	Thermal Generation (MWt-hr)	Year	Month	Thermal Generation (MWt-hr)	Year	Month	Thermal Generation (MWt-hr)
89	3	0	92	3	2663411	95	3	2515372
89	4	76126	92	4	2374113	95	4	2736514
89	5	656280	92	5	2826840	95	5	2839848
89	6	1094991	92	6	2746316	95	6	2747965
89	7	1902515	92	7	2830229	95	7	2839756
89	8	1794876	92	8	2828031	95	8	2839848
89	9	1886300	92	9	2744301	95	9	2748240
89	10	2579773	92	10	2842963	95	10	538289
89	11	263923	92	11	2648845	95	11	2174143
89	12	0	92	12	2601026	95	12	2792787
90	1	1191912	93	1	1988535	96	1	1428146
90	2	2252641	93	2	242486	96	2	2391887
90	3	2297162	93	3	0	96	3	2804951
90	4	1397572	93	4	0	96	4	2735628
90	5	1523075	93	5	0	96	5	2826664
90	6	2644265	93	6	0	96	6	2735536
90	7	2077578	93	7	0	96	7	2826866
90	8	2828214	93	8	0	96	8	2826725
90	9	2361563	93	9	0	96	9	2735681
90	10	0	93	10	0	96	10	2826463
90	11	0	93	11	0	96	11	2735320
90	12	1608911	93	12	0	96	12	2823541
91	1	2607255	94	1	0	97	1	2816803
91	2	2427337	94	2	0	97	2	586009
91	3	2372189	94	3	0	97	3	2589484
91	4	2578032	94	4	0	97	4	2722685
91	5	2550275	94	5	89867	97	5	2521680
91	6	2746866	94	6	1616148	97	6	2735544
91	7	2837924	94	7	2744301	97	7	2826926
91	8	2837741	94	8	2838840	97	8	2827018
91	9	1177346	94	9	2746957	97	9	2736000
91	10	0	94	10	2843329	97	10	2830666
91	11	0	94	11	2748148	97	11	2568374
91	12	553038	94	12	2719383	97	12	2629752
92	1	2191813	95	1	2833527	98	1	2647080
92	2	2511067	95	2	2565024	98	2	2553509

Table A-2 cont'd

Monthly Thermal Generation During The First Nine Fuel Cycles
Of The South Texas Project Unit 2 Reactor
(Reactor Power of 3800 MWt through the end of Cycle 9)

Year	Month	Thermal Generation (MWt-hr)	Year	Month	Thermal Generation (MWt-hr)	Year	Month	Thermal Generation (MWt-hr)
98	3	2826653	99	10	982406	2001	5	2464498
98	4	2732170	99	11	1765723	2001	6	2723050
98	5	2827200	99	12	2783242	2001	7	2825650
98	6	2735818	2000	1	2614339	2001	8	2817989
98	7	2656018	2000	2	2114928	2001	9	2735635
98	8	2826562	2000	3	2826014	2001	10	2210962
98	9	2569469	2000	4	2731166	2001	11	2735909
98	10	273600	2000	5	2826379	2001	12	2826835
98	11	3057298	2000	6	2144477	2002	1	2826197
98	12	2715389	2000	7	2826014	2002	2	2552050
99	1	2694504	2000	8	2826562	2002	3	2827200
99	2	2553418	2000	9	2735818	2002	4	2731622
99	3	2827109	2000	10	2830210	2002	5	2821637
99	4	2732078	2000	11	2735453	2002	6	2294318
99	5	2791085	2000	12	2826379	2002	7	2653555
99	6	2729069	2001	1	2826470	2002	8	2827200
99	7	2713930	2001	2	2066683	2002	9	2735818
99	8	2606405	2001	3	292752	2002	10	79253
99	9	2727336	2001	4	2383238			

Table A-3

Calculated C_j Factors at the Surveillance Capsule Center
Core Midplane Elevation

Fuel Cycle	ϕ(E > 1.0 MeV) [n/cm^2-s]			C_j		
	Capsule V	Capsule Y	Capsule U	V	Y	U
1	8.58E+10	8.58E+10	9.30E+10	1.000	1.146	1.258
2		6.49E+10	6.84E+10		0.867	0.925
3		7.48E+10	7.93E+10		0.999	1.073
4		7.91E+10	8.51E+10		1.057	1.151
5		6.83E+10	7.35E+10		0.912	0.994
6			5.63E+10			0.761
7			8.18E+10			1.106
8			7.20E+10			0.975
9			6.71E+10			0.908
Average	8.58E+10	7.49E+10	7.39E+10	1.000	1.000	1.000

Table A-4
Measured Sensor Activities And Reaction Rates
Surveillance Capsule V

Reaction	Location	Measured Activity (dps/g)	Saturated Activity (dps/g)	Radially Adjusted Saturated Activity (dps/g)	Radially Adjusted Reaction Rate (rps/atom)
^{63}Cu (n,α) ^{60}Co	Top	3.50E+04	3.54E+05	3.54E+05	5.39E-17
	Middle	3.38E+04	3.42E+05	3.42E+05	5.21E-17
	Bottom	3.33E+04	3.36E+05	3.36E+05	5.13E-17
	Average				**5.25E-17**
^{54}Fe (n,p) ^{54}Mn	Top	9.97E+05	3.21E+06	3.21E+06	5.08E-15
	Middle	9.73E+05	3.13E+06	3.13E+06	4.96E-15
	Bottom	9.43E+05	3.03E+06	3.03E+06	4.81E-15
	Average				**4.95E-15**
^{58}Ni (n,p) ^{58}Co	Top	7.13E+06	4.60E+07	4.60E+07	6.59E-15
	Middle	6.89E+06	4.45E+07	4.45E+07	6.37E-15
	Bottom	6.60E+06	4.26E+07	4.26E+07	6.10E-15
	Average				**6.35E-15**
^{238}U (n,f) ^{137}Cs (Cd)	Middle	1.15E+05	5.91E+06	5.91E+06	3.88E-14
^{238}U (n,f) ^{137}Cs (Cd)		Including ^{235}U, ^{239}Pu, and γ,fission corrections:			**3.28E-14**
^{237}Np (n,f) ^{137}Cs (Cd)	Middle	9.86E+05	5.07E+07	5.07E+07	3.23E-13
^{237}Np (n,f) ^{137}Cs (Cd)			Including γ,fission correction:		**3.20E-13**
^{59}Co (n,γ) ^{60}Co	Top	7.25E+06	7.32E+07	7.32E+07	4.78E-12
	Middle	7.47E+06	7.55E+07	7.55E+07	4.92E-12
	Bottom	7.80E+06	7.88E+07	7.88E+07	5.14E-12
	Average				**4.95E-12**
^{59}Co (n,γ) ^{60}Co (Cd)	Middle	4.09E+06	4.13E+07	4.13E+07	2.70E-12
	Bottom	4.24E+06	4.28E+07	4.28E+07	2.80E-12
	Average				**2.75E-12**

Notes: 1) Measured specific activities are indexed to a counting date of March 15, 1991.
2) The average ^{238}U (n,f) reaction rate of 3.28E-14 includes a correction factor of 0.873 to account for plutonium build-in and an additional factor of 0.969 to account for photo-fission effects in the sensor.
3) The average ^{237}Np (n,f) reaction rate of 3.20E-13 includes a correction factor of 0.991 to account for photo-fission effects in the sensor.

Table A-4 cont'd
Measured Sensor Activities And Reaction Rates
Surveillance Capsule Y

Reaction	Location	Measured Activity (dps/g)	Saturated Activity (dps/g)	Radially Adjusted Saturated Activity (dps/g)	Radially Adjusted Reaction Rate (rps/atom)
^{63}Cu (n,α) ^{60}Co	Top	1.19E+05	2.85E+05	2.85E+05	4.34E-17
	Middle	1.16E+05	2.78E+05	2.78E+05	4.23E-17
	Bottom	1.14E+05	2.73E+05	2.73E+05	4.16E-17
	Average				**4.25E-17**
^{54}Fe (n,p) ^{54}Mn	Top	1.63E+06	2.64E+06	2.64E+06	4.19E-15
	Middle	1.59E+06	2.58E+06	2.58E+06	4.09E-15
	Bottom	1.55E+06	2.51E+06	2.51E+06	3.99E-15
	Average				**4.09E-15**
^{58}Ni (n,p) ^{58}Co	Top	1.03E+07	4.16E+07	4.16E+07	5.96E-15
	Middle	1.01E+07	4.08E+07	4.08E+07	5.84E-15
	Bottom	9.70E+06	3.92E+07	3.92E+07	5.61E-15
	Average				**5.80E-15**
^{238}U (n,f) ^{137}Cs (Cd)	Middle	5.06E+05	4.69E+06	4.69E+06	3.08E-14
^{238}U (n,f) ^{137}Cs (Cd)	Including ^{235}U, ^{239}Pu, and γ,fission corrections:				**2.50E-14**
^{237}Np (n,f) ^{137}Cs (Cd)	Middle	3.56E+06	3.30E+07	3.30E+07	2.11E-13
^{237}Np (n,f) ^{137}Cs (Cd)	Including γ,fission correction:				**2.09E-13**
^{59}Co (n,γ) ^{60}Co	Top	2.33E+07	5.58E+07	5.58E+07	3.64E-12
	Middle	2.41E+07	5.77E+07	5.77E+07	3.76E-12
	Bottom	2.45E+07	5.86E+07	5.86E+07	3.82E-12
	Average				**3.74E-12**
^{59}Co (n,γ) ^{60}Co (Cd)	Top	1.26E+07	3.02E+07	3.02E+07	1.97E-12
	Middle	1.29E+07	3.09E+07	3.09E+07	2.01E-12
	Bottom	1.32E+07	3.16E+07	3.16E+07	2.06E-12
	Average				**2.01E-12**

Notes: 1) Measured specific activities are indexed to a counting date of June 19, 1997.
2) The average ^{238}U (n,f) reaction rate of 2.50E-14 includes a correction factor of 0.837 to account for plutonium build-in and an additional factor of 0.969 to account for photo-fission effects in the sensor.
3) The average ^{237}Np (n,f) reaction rate of 2.09E-13 includes a correction factor of 0.991 to account for photo-fission effects in the sensor.

Table A-4 cont'd
Measured Sensor Activities And Reaction Rates
Surveillance Capsule U

Reaction	Location	Measured Activity (dps/g)	Saturated Activity (dps/g)	Radially Adjusted Saturated Activity (dps/g)	Radially Adjusted Reaction Rate (rps/atom)
^{63}Cu (n,α) ^{60}Co	Top	1.88E+05	2.92E+05	2.92E+05	4.46E-17
	Middle	1.80E+05	2.80E+05	2.80E+05	4.27E-17
	Bottom	1.78E+05	2.77E+05	2.77E+05	4.22E-17
	Average				**4.32E-17**
^{54}Fe (n,p) ^{54}Mn	Top	1.86E+06	2.81E+06	2.81E+06	4.46E-15
	Middle	1.78E+06	2.69E+06	2.69E+06	4.27E-15
	Bottom	1.74E+06	2.63E+06	2.63E+06	4.17E-15
	Average				**4.30E-15**
^{58}Ni (n,p) ^{58}Co	Top	1.17E+07	4.43E+07	4.43E+07	6.34E-15
	Middle	1.13E+07	4.28E+07	4.28E+07	6.13E-15
	Bottom	1.09E+07	4.13E+07	4.13E+07	5.91E-15
	Average				**6.13E-15**
^{238}U (n,f) ^{137}Cs (Cd)	Middle	1.12E+06	5.47E+06	5.47E+06	3.59E-14
^{238}U (n,f) ^{137}Cs (Cd)	Including ^{235}U, ^{239}Pu, and γ,fission corrections:				**2.77E-14**
^{237}Np (n,f) ^{137}Cs (Cd)	Middle	8.07E+06	3.94E+07	3.94E+07	2.51E-13
^{237}Np (n,f) ^{137}Cs (Cd)	Including γ,fission correction:				**2.49E-13**
^{59}Co (n,γ) ^{60}Co	Top	3.61E+07	5.61E+07	5.61E+07	3.66E-12
	Middle	3.76E+07	5.85E+07	5.85E+07	3.82E-12
	Bottom	3.79E+07	5.89E+07	5.89E+07	3.85E-12
	Average				**3.77E-12**
^{59}Co (n,γ) ^{60}Co (Cd)	Top	1.94E+07	3.02E+07	3.02E+07	1.97E-12
	Middle	1.99E+07	3.10E+07	3.10E+07	2.02E-12
	Bottom	2.05E+07	3.19E+07	3.19E+07	2.08E-12
	Average				**2.02E-12**

Notes: 1) Measured specific activities are indexed to a counting date of February 1, 2003.
2) The average ^{238}U (n,f) reaction rate of 2.77E-14 includes a correction factor of 0.796 to account for plutonium build-in and an additional factor of 0.969 to account for photo-fission effects in the sensor.
3) The average ^{237}Np (n,f) reaction rate of 2.49E-13 includes a correction factor of 0.991 to account for photo-fission effects in the sensor.

Table A-5
Comparison of Measured, Calculated, and Best Estimate
Reaction Rates At The Surveillance Capsule Center

Capsule V

Reaction	Reaction Rate [rps/atom]				
	Measured	Calculated	Best Estimate	M/C	M/BE
$^{63}Cu(n,\alpha)^{60}Co$	5.25E-17	4.41E-17	4.94E-17	1.19	1.06
$^{54}Fe(n,p)^{54}Mn$	4.95E-15	4.99E-15	5.09E-15	0.99	0.97
$^{58}Ni(n,p)^{58}Co$	6.35E-15	7.02E-15	6.97E-15	0.90	0.91
$^{238}U(n,f)^{137}Cs$ (Cd)	3.28E-14	2.72E-14	2.80E-14	1.21	1.17
$^{237}Np(n,f)^{137}Cs$ (Cd)	3.20E-13	2.68E-13	3.01E-13	1.19	1.06
$^{59}Co(n,\gamma)^{60}Co$	4.95E-12	3.70E-12	4.85E-12	1.34	1.02
$^{59}Co(n,\gamma)^{60}Co$ (Cd)	2.75E-12	2.62E-12	2.79E-12	1.05	0.99

Capsule Y

Reaction	Reaction Rate [rps/atom]				
	Measured	Calculated	Best Estimate	M/C	M/BE
$^{63}Cu(n,\alpha)^{60}Co$	4.25E-17	3.99E-17	4.11E-17	1.07	1.03
$^{54}Fe(n,p)^{54}Mn$	4.09E-15	4.42E-15	4.24E-15	0.93	0.96
$^{58}Ni(n,p)^{58}Co$	5.80E-15	6.21E-15	5.93E-15	0.93	0.98
$^{238}U(n,f)^{137}Cs$ (Cd)	2.50E-14	2.39E-14	2.27E-14	1.05	1.10
$^{237}Np(n,f)^{137}Cs$ (Cd)	2.09E-13	2.33E-13	2.15E-13	0.90	0.97
$^{59}Co(n,\gamma)^{60}Co$	3.74E-12	3.19E-12	3.67E-12	1.17	1.02
$^{59}Co(n,\gamma)^{60}Co$ (Cd)	2.01E-12	2.25E-12	2.04E-12	0.89	0.99

Capsule U

Reaction	Reaction Rate [rps/atom]				
	Measured	Calculated	Best Estimate	M/C	M/BE
$^{63}Cu(n,\alpha)^{60}Co$	4.32E-17	3.98E-17	4.20E-17	1.09	1.03
$^{54}Fe(n,p)^{54}Mn$	4.30E-15	4.40E-15	4.47E-15	0.98	0.96
$^{58}Ni(n,p)^{58}Co$	6.13E-15	6.17E-15	6.28E-15	0.99	0.98
$^{238}U(n,f)^{137}Cs$ (Cd)	2.77E-14	2.36E-14	2.45E-14	1.17	1.13
$^{237}Np(n,f)^{137}Cs$ (Cd)	2.49E-13	2.30E-13	2.45E-13	1.08	1.02
$^{59}Co(n,\gamma)^{60}Co$	3.77E-12	3.17E-12	3.70E-12	1.19	1.02
$^{59}Co(n,\gamma)^{60}Co$ (Cd)	2.02E-12	2.23E-12	2.05E-12	0.91	0.99

Table A-6

Comparison of Calculated and Best Estimate Exposure Rates
At The Surveillance Capsule Center

Capsule ID	ϕ(E > 1.0 MeV) [n/cm^2-s]			
	Calculated	Best Estimate	Uncertainty (1σ)	BE/C
V	8.58E+10	8.99E+10	6%	1.05
Y	7.49E+10	7.14E+10	6%	0.95
U	7.39E+10	7.80E+10	6%	1.06

Note: Calculated results are based on the synthesized transport calculations taken at the core midplane following the completion of each respective capsules irradiation period.

Capsule ID	Iron Atom Displacement Rate [dpa/s]			
	Calculated	Best Estimate	Uncertainty (1σ)	BE/C
V	1.67E-10	1.79E-10	8%	1.07
Y	1.46E-10	1.38E-10	8%	0.95
U	1.43E-10	1.51E-10	8%	1.05

Note: Calculated results are based on the synthesized transport calculations taken at the core midplane following the completion of each respective capsules irradiation period.

Table A-7

Comparison of Measured/Calculated (M/C) Sensor Reaction Rate Ratios Including all Fast Neutron Threshold Reactions

Reaction	M/C Ratio		
	Capsule V	Capsule Y	Capsule U
$^{63}Cu(n,\alpha)^{60}Co$	1.19	1.07	1.09
$^{54}Fe(n,p)^{54}Mn$	0.99	0.93	0.98
$^{58}Ni(n,p)^{58}Co$	0.90	0.93	0.99
$^{238}U(n,p)^{137}Cs$ (Cd)	1.21	1.05	1.17
$^{237}Np(n,f)^{137}Cs$ (Cd)	1.19	0.90	1.08
Average	1.10	0.97	1.06
% Standard Deviation	12.7	7.9	7.5

Note: The overall average M/C ratio for the set of 15 sensor measurements is 1.04 with an associated standard deviation of 10.5%.

Table A-8

Comparison of Best Estimate/Calculated (BE/C) Exposure Rate Ratios

Capsule ID	BE/C Ratio	
	$\phi(E > 1.0\ MeV)$	dpa/s
V	1.05	1.07
Y	0.95	0.95
U	1.06	1.05
Average	1.02	1.02
% Standard Deviation	5.6	6.3

Appendix A References

A-1. Regulatory Guide RG-1.190, "Calculational and Dosimetry Methods for Determining Pressure Vessel Neutron Fluence," U. S. Nuclear Regulatory Commission, Office of Nuclear Regulatory Research, March 2001.

A-2. WCAP-13182, Revision 0, "Analysis of Capsule V from the Houston Lighting and Power Company South Texas Unit 2 Reactor Vessel Radiation Surveillance Program," February 1992.

A-3. WCAP-14978, Revision 0, "Analysis of Capsule Y from the Houston Lighting and Power Company South Texas Unit 2 Reactor Vessel Radiation Surveillance Program," December 1997.

A-4. A. Schmittroth, *FERRET Data Analysis Core*, HEDL-TME 79-40, Hanford Engineering Development Laboratory, Richland, WA, September 1979.

A-5. RSIC Data Library Collection DLC-178, "SNLRML Recommended Dosimetry Cross-Section Compendium", July 1994.

APPENDIX B

LOAD-TIME RECORDS FOR CHARPY SPECIMEN TESTS

- Specimen prefix "HL" denotes Lower Plate, Longitudinal Orientation
- Specimen prefix "HT" denotes Lower Plate, Transverse Orientation
- Specimen prefix "HW" denotes Weld Material
- Specimen prefix "HH" denotes Heat-Affected Zone material
- Load (1) is in units of lbs
- Time (1) is in units of milli seconds

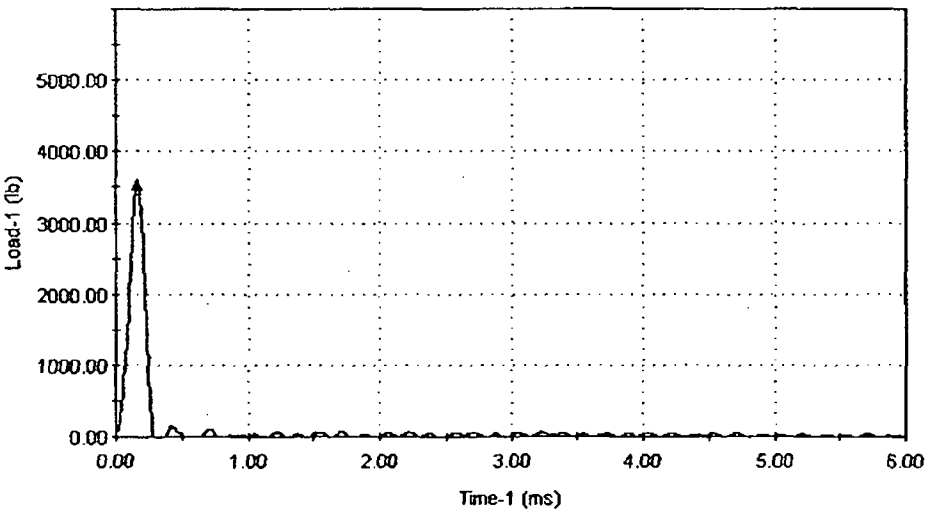

HL14, -50°F

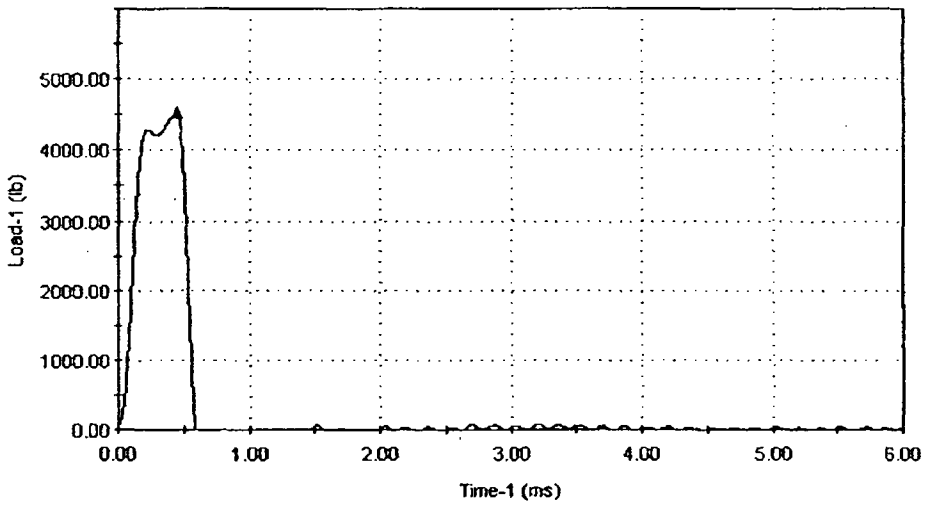

HL7, -25°F

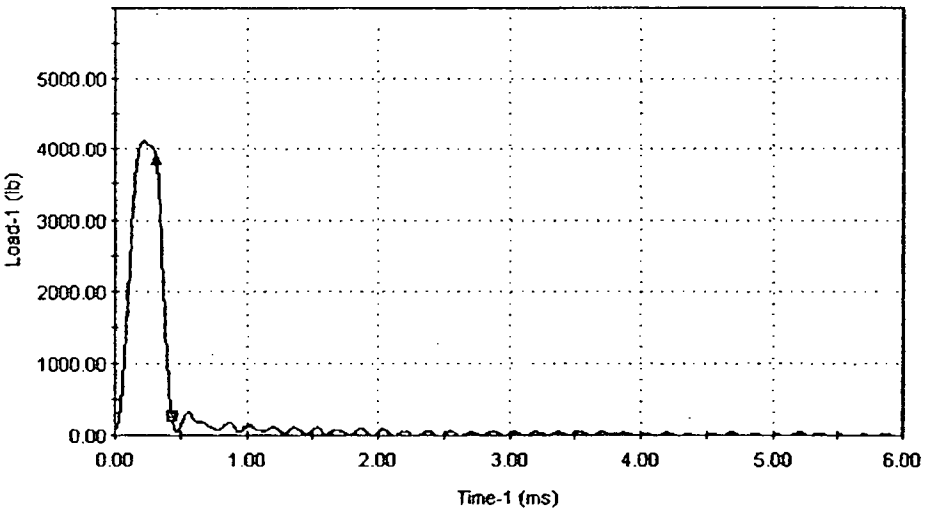

HL6, 0°F

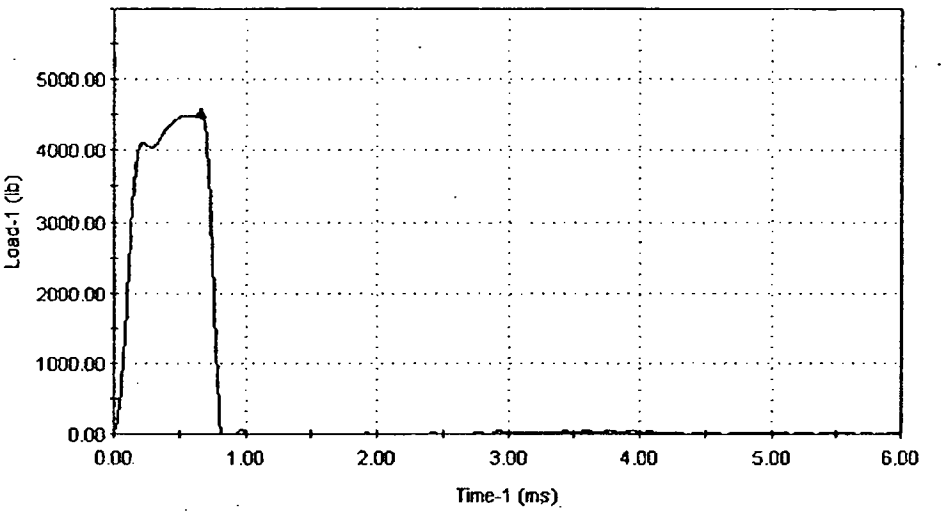

HL1, 10°F

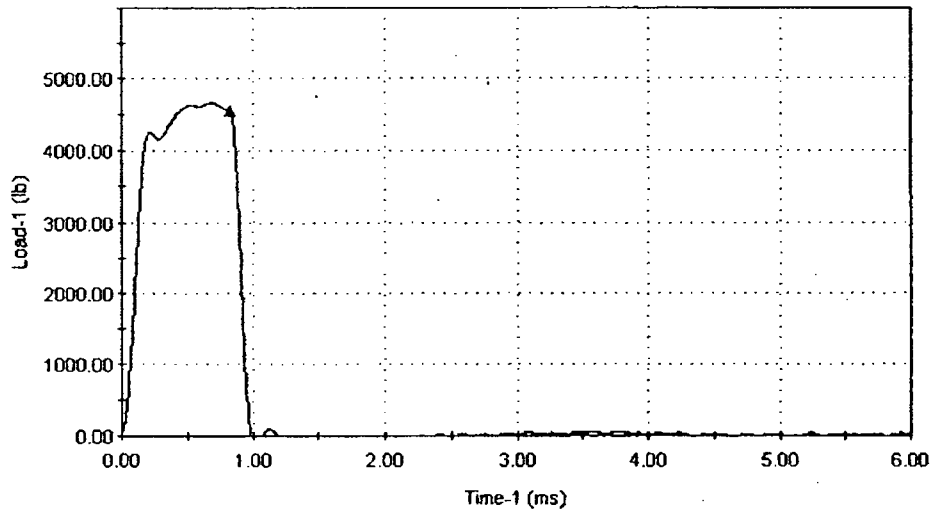

HL8, 20°F

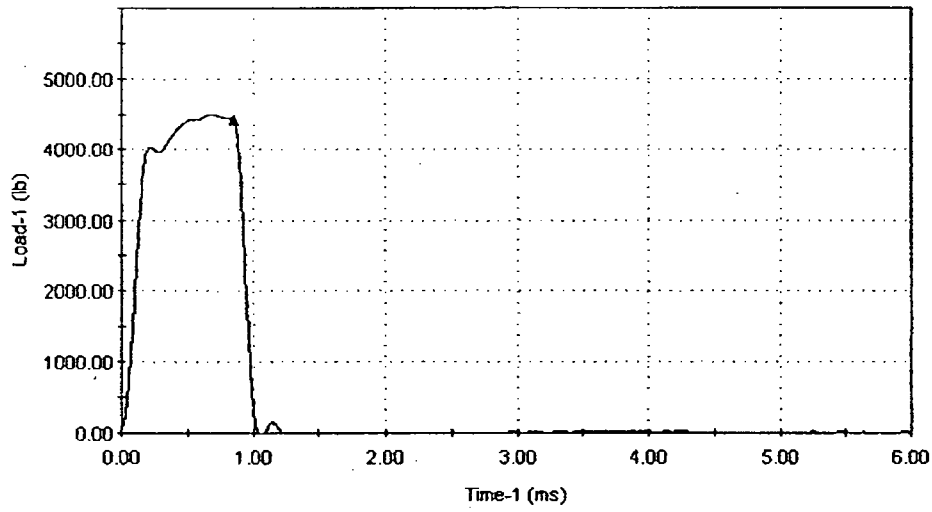

HL9, 40°F

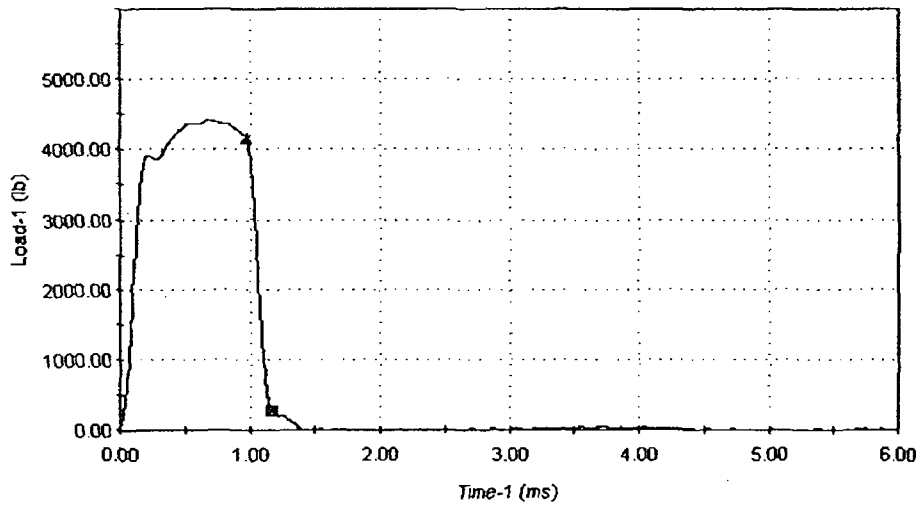

HL12, 50°F

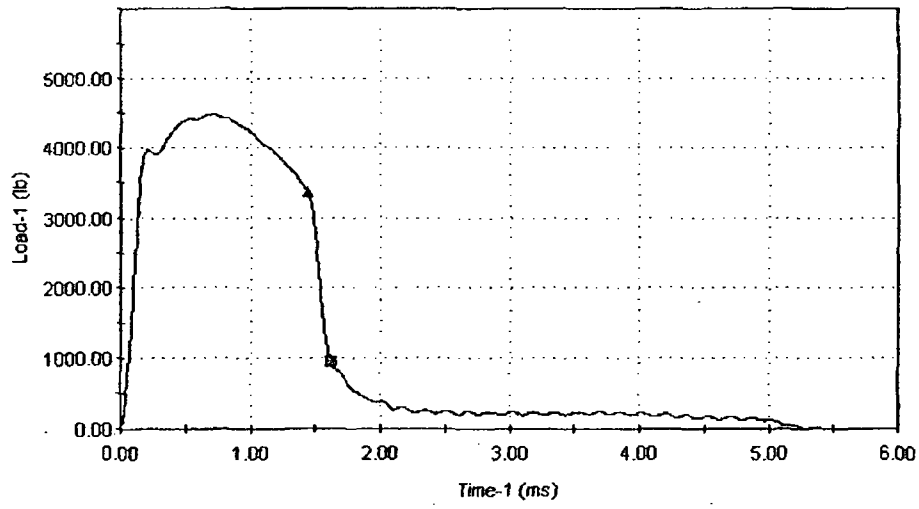

HL15, 75°F

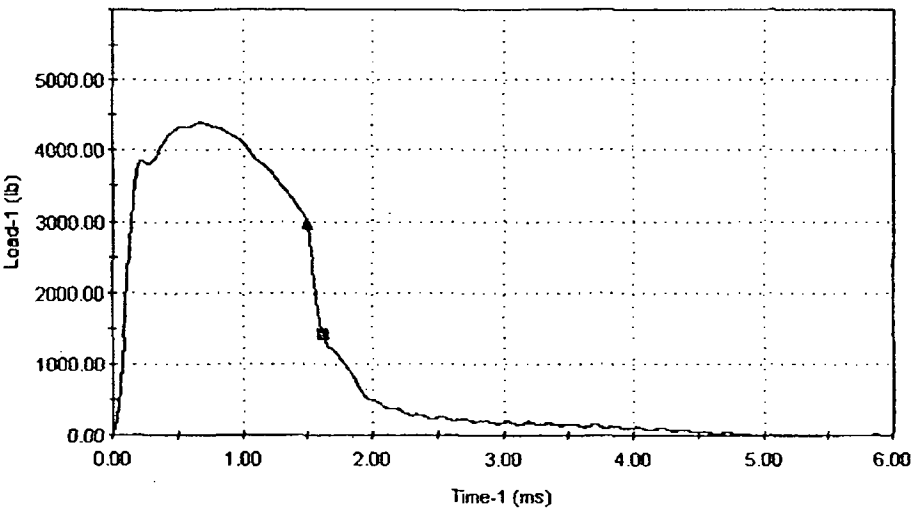

HL13, 100°F

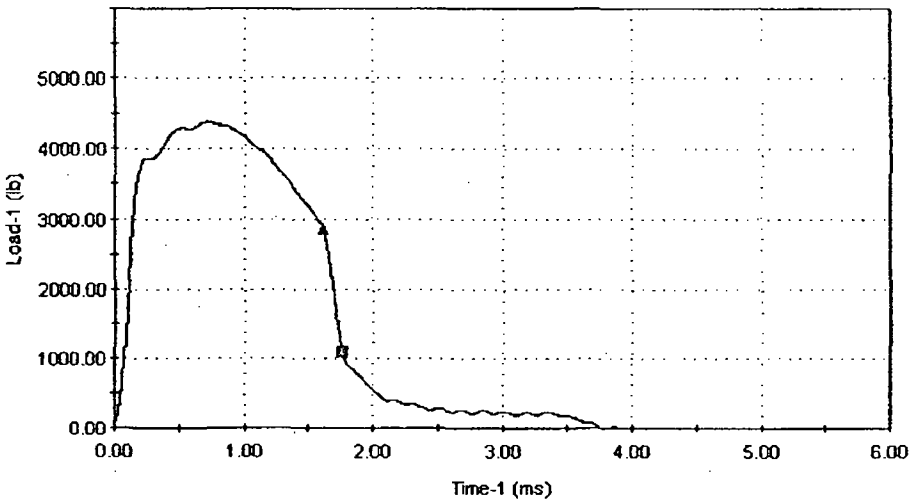

HL3, 125°F

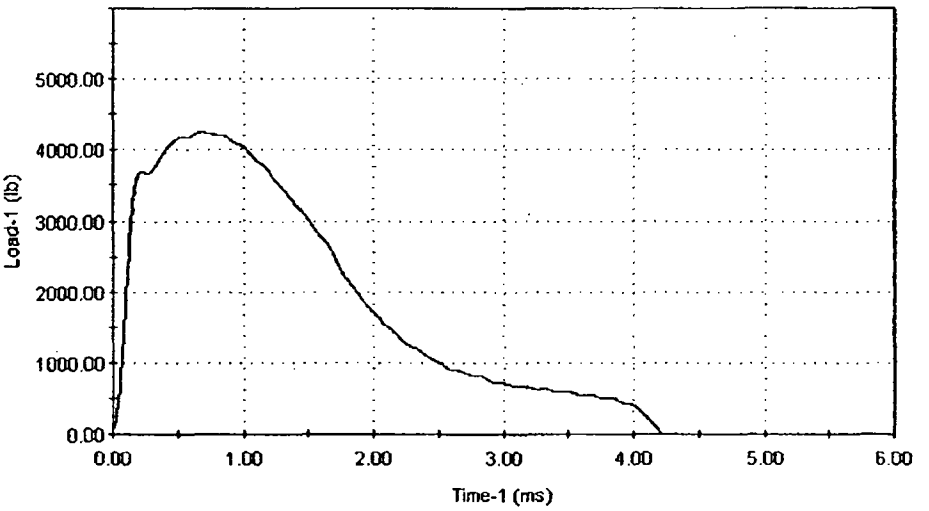

HL10, 150°F

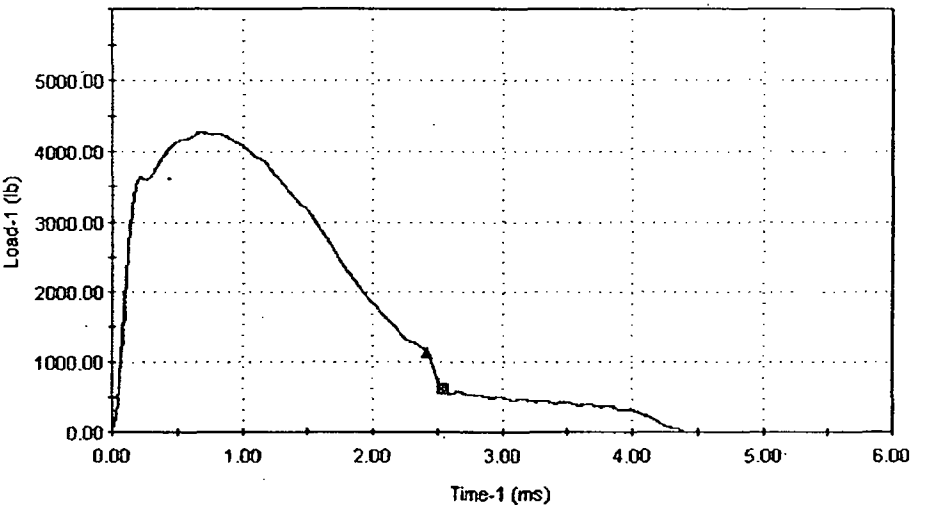

HL11, 175°F

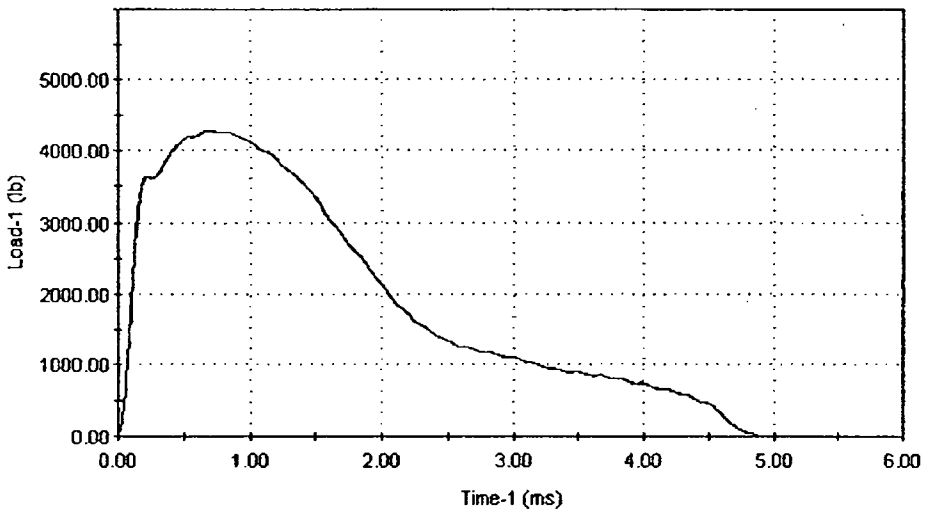

HL5, 200°F

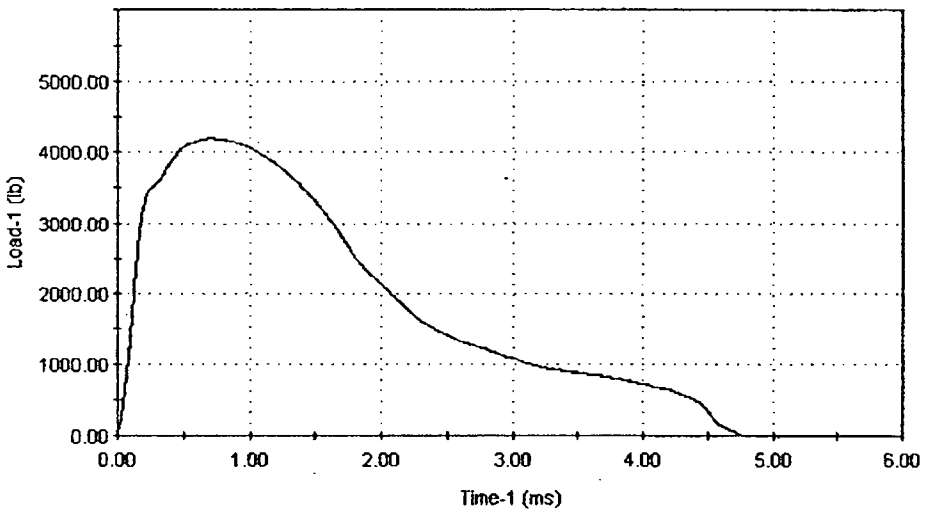

HL4, 225°F

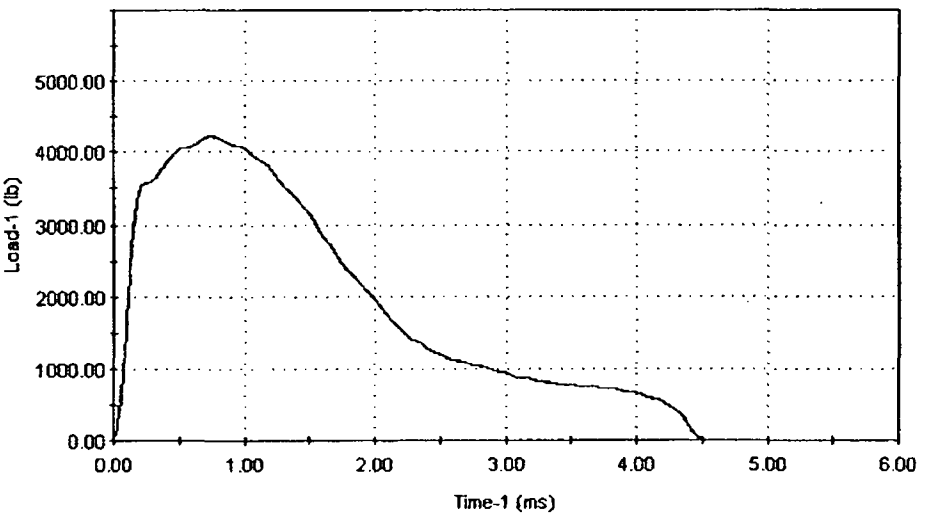

HL2, 250°F

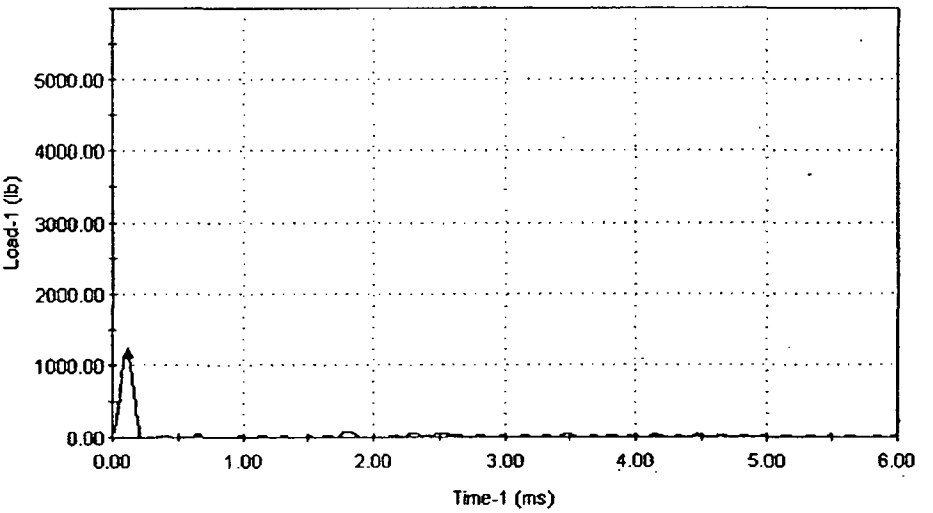

HT11, -75°F

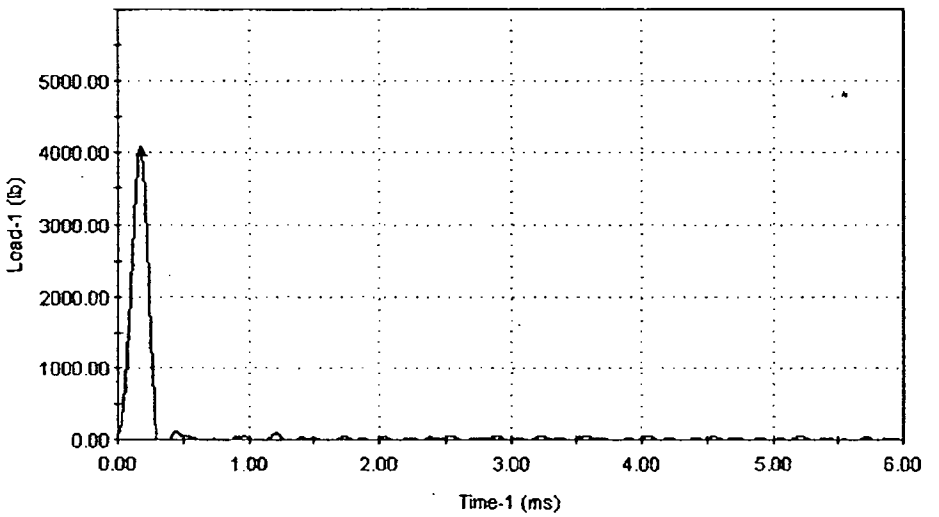

HT3, -50°F

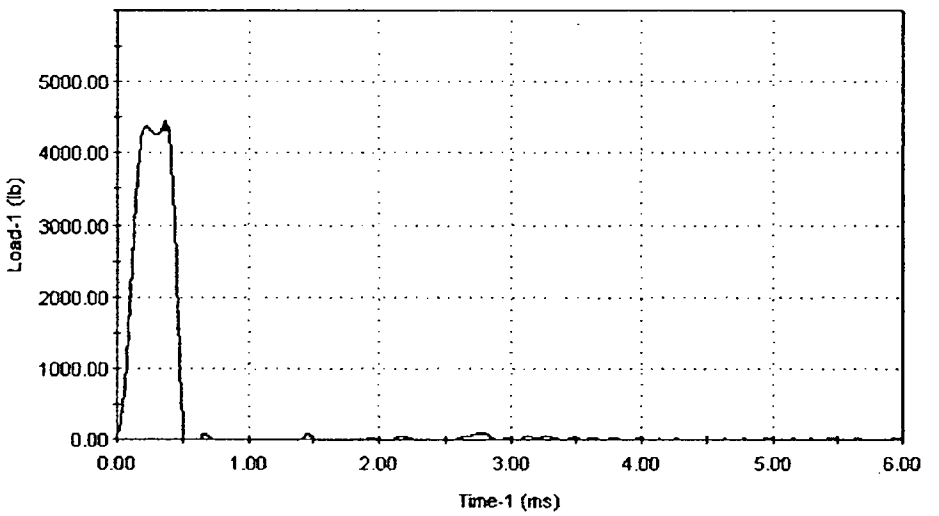

HT4, -25°F

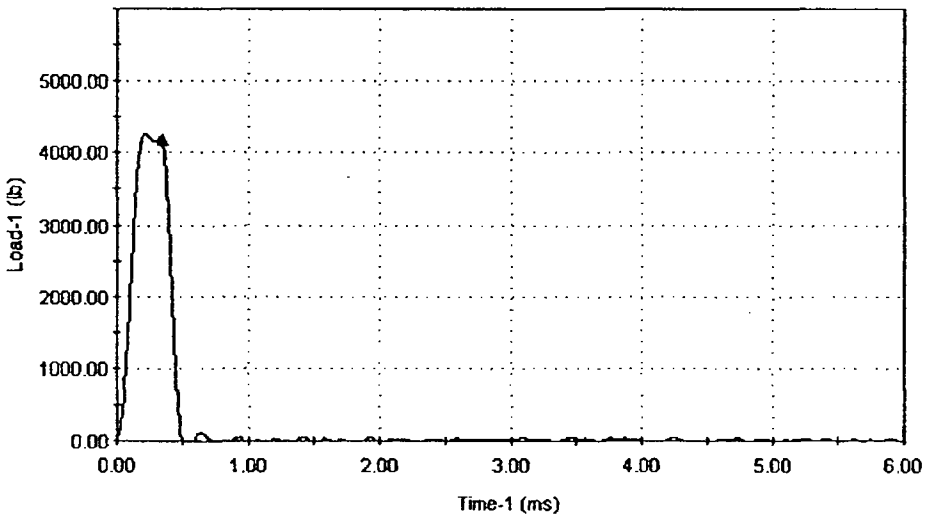

HT6, 0°F

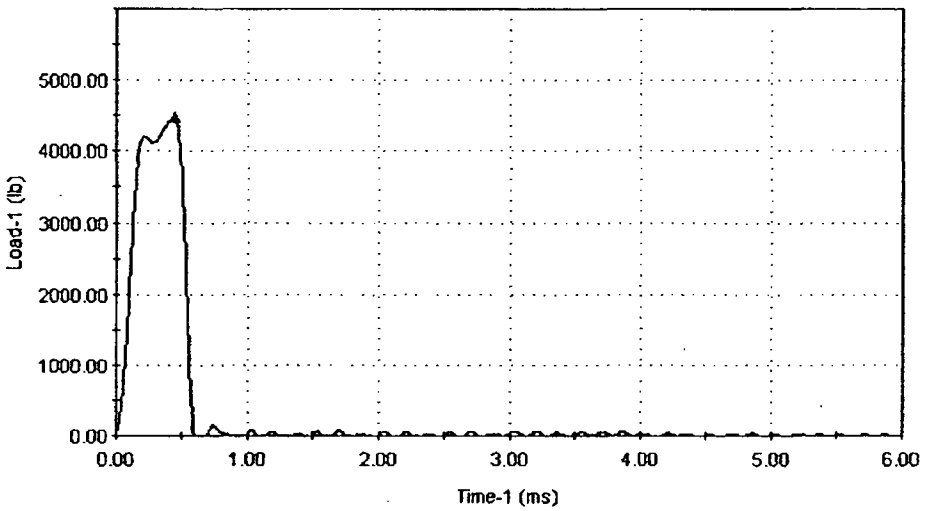

HT7, 25°F

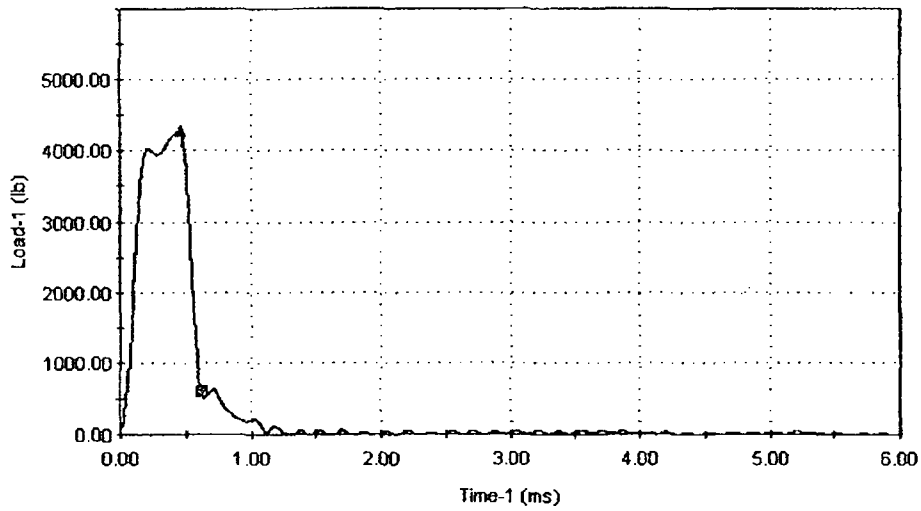

HT8, 50°F

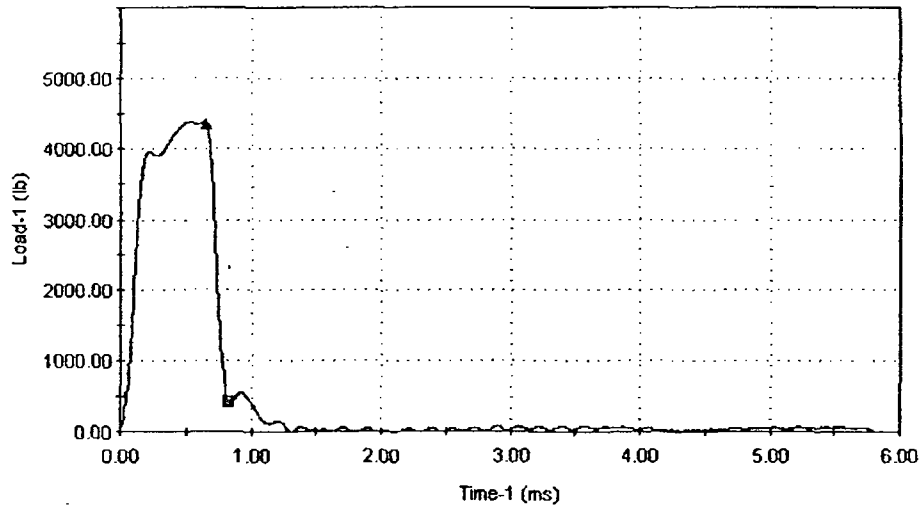

HT10, 60°F

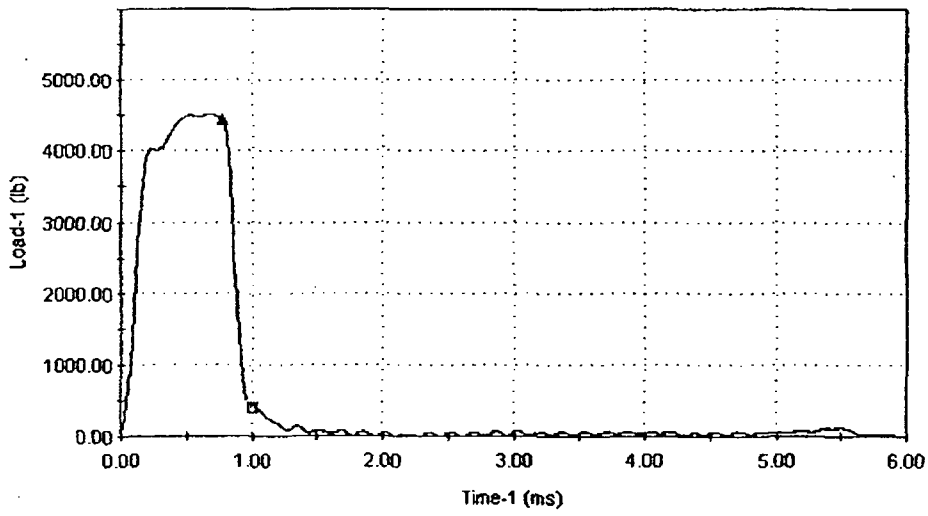

HT12, 75°F

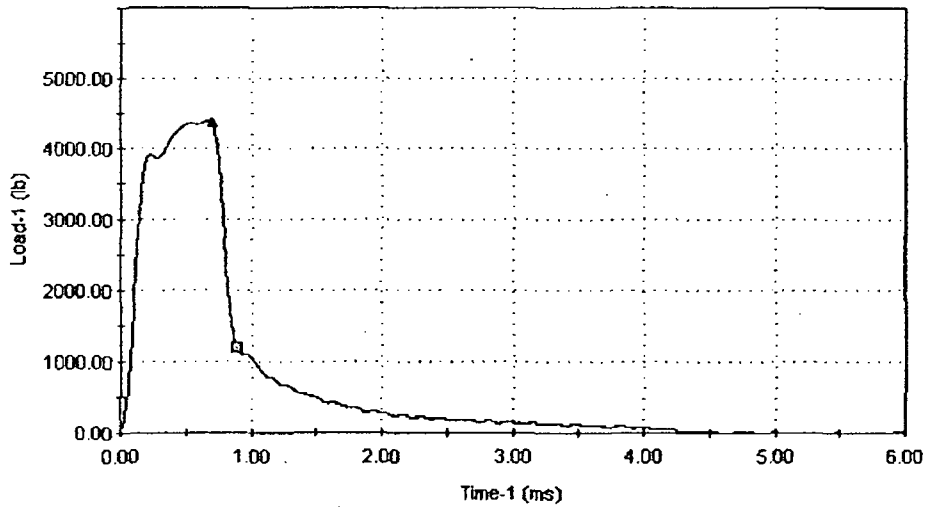

HT9, 100°F

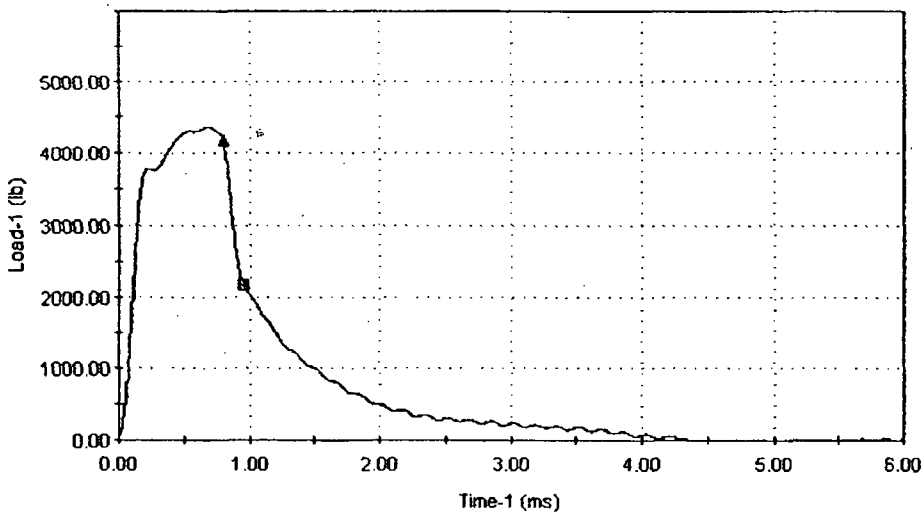

HT2, 125°F

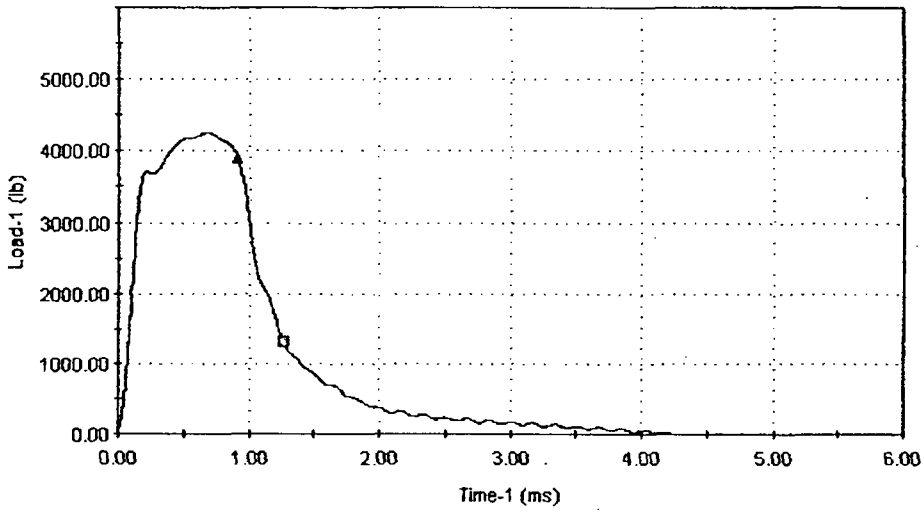

HT14, 150°F

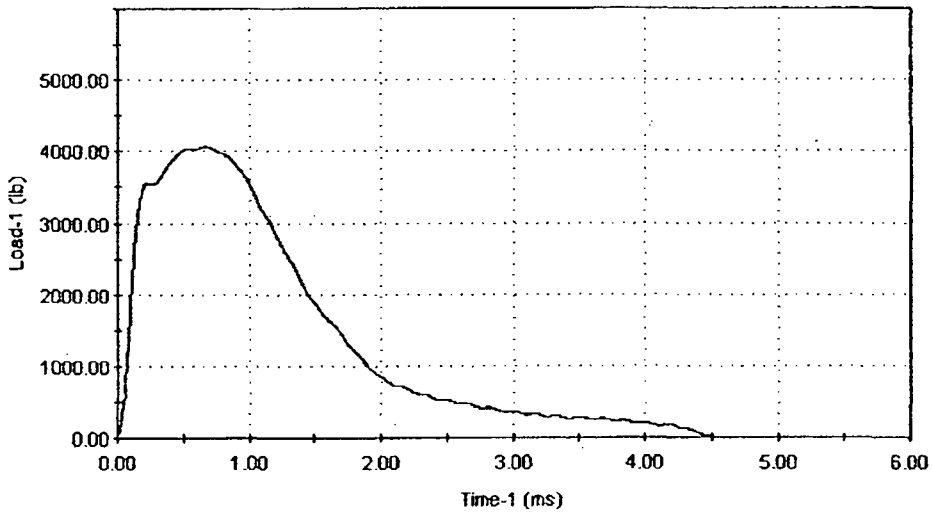

HT1, 190°F

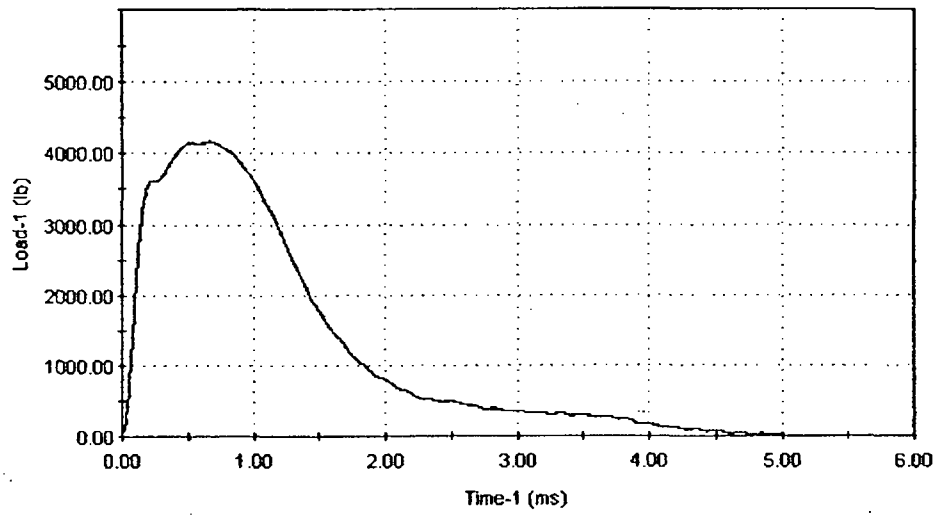

HT13, 225°F

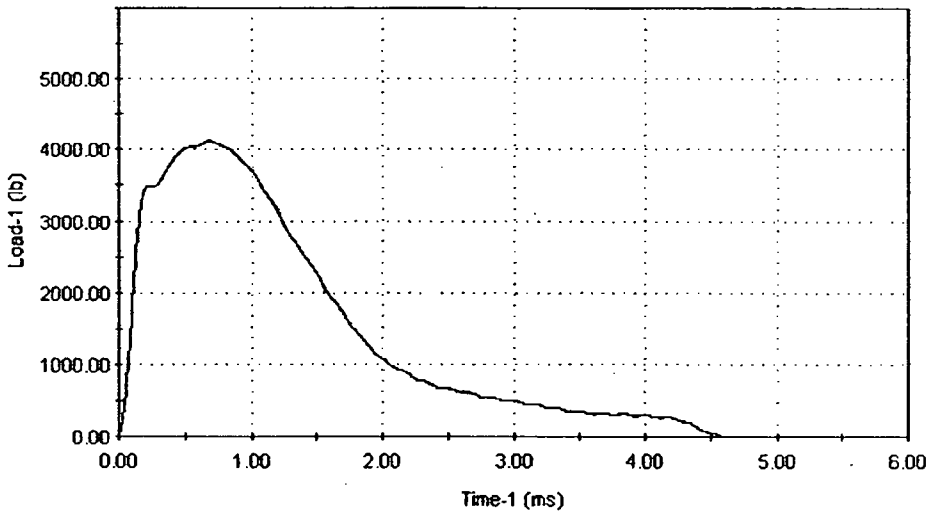

HT15, 250°F

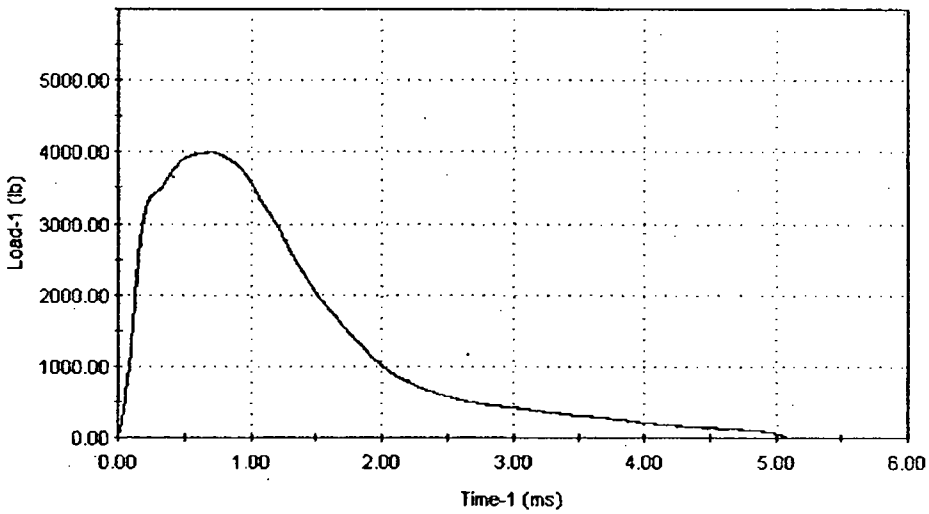

HT5, 275°F

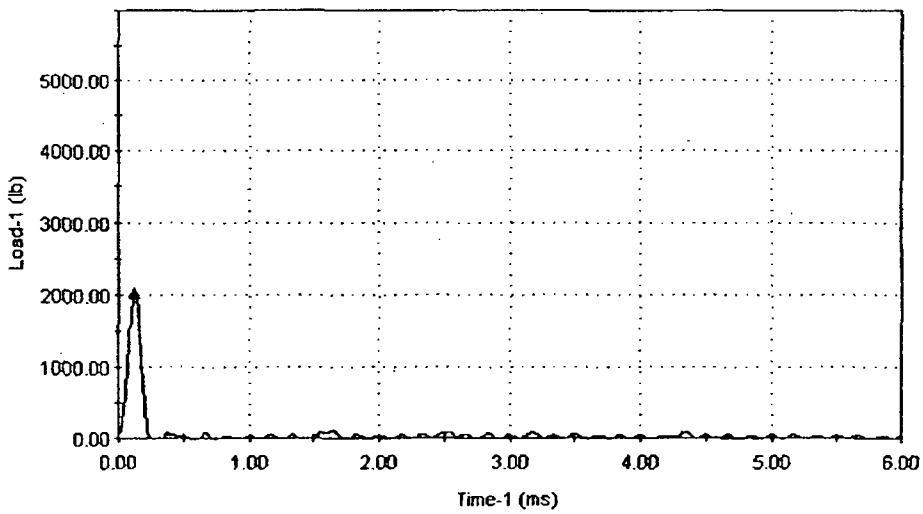

HW6, -75°F

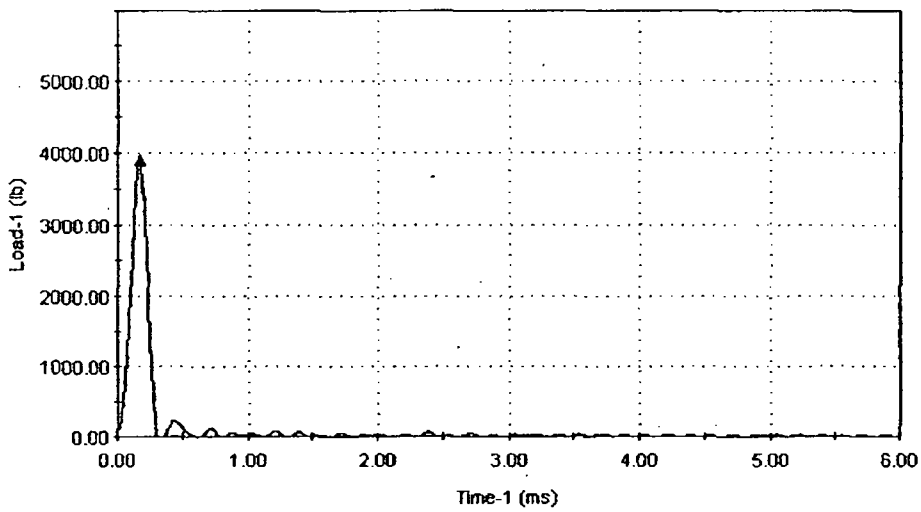

HW15, -50°F

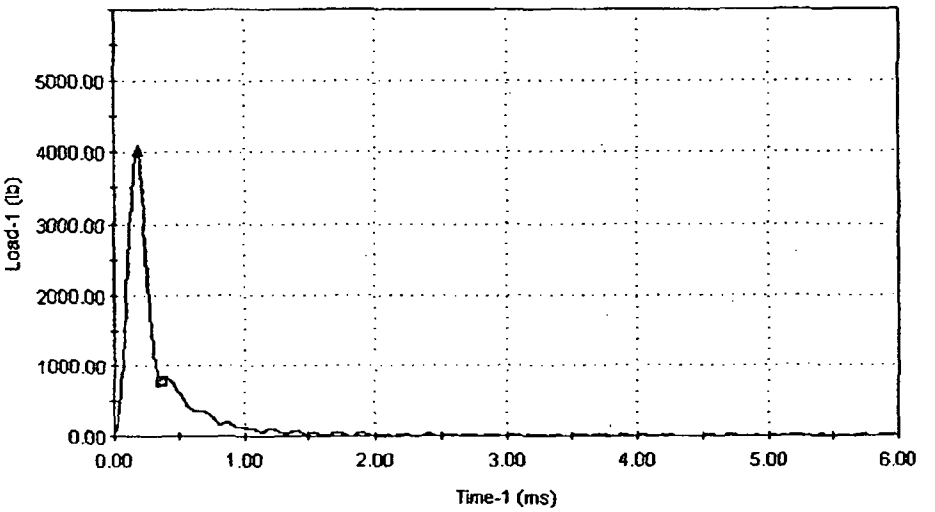

HW9, -25°F

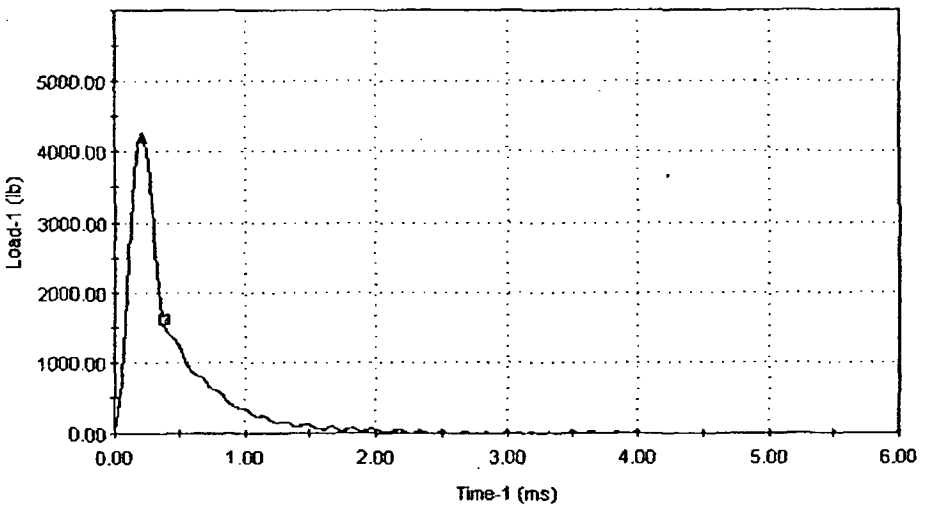

HW10, 0°F

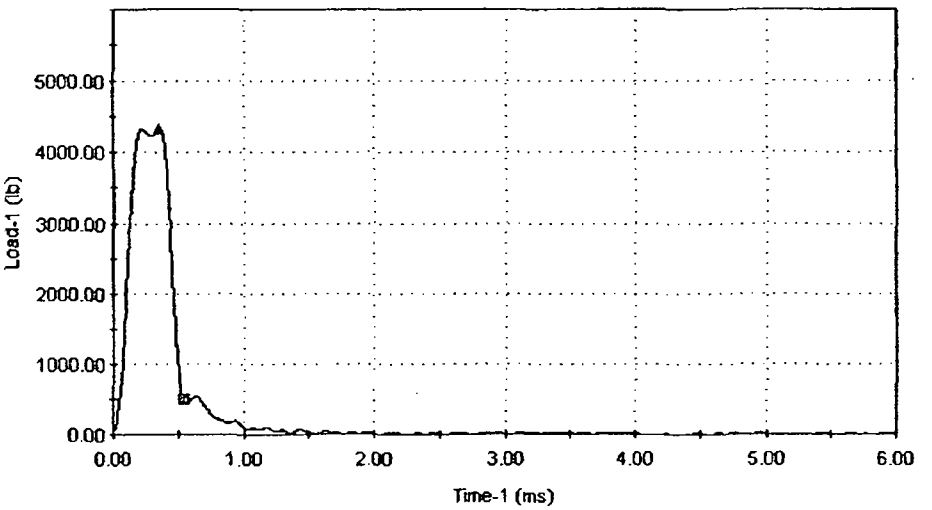

HW12, 10°F

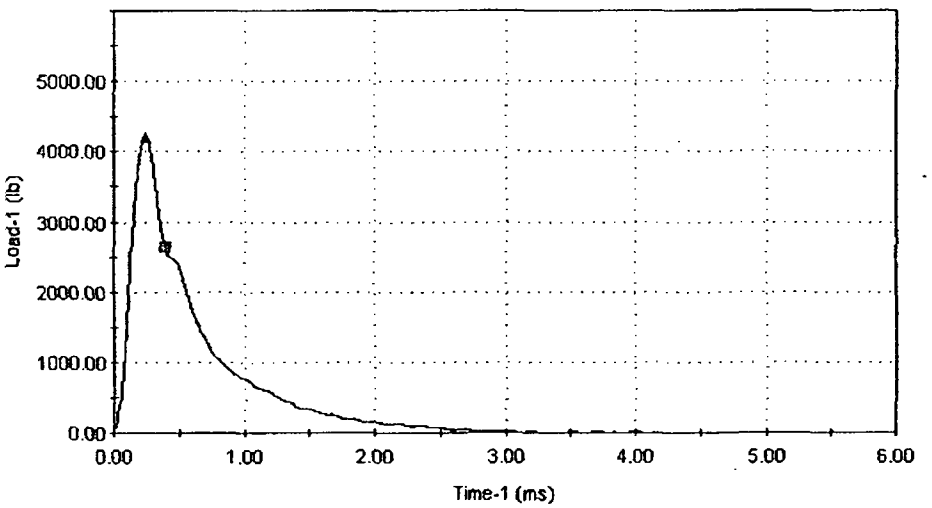

HW8, 30°F

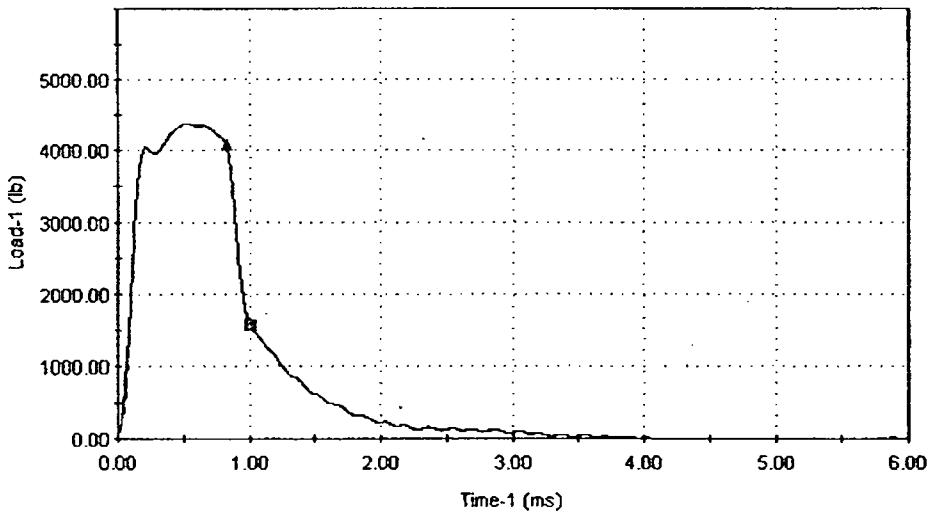

HW3, 50°F

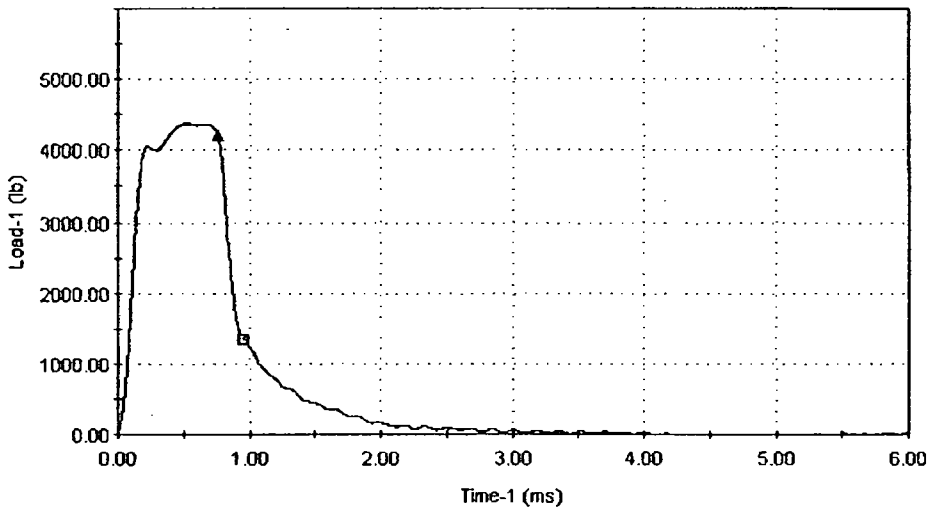

HW4, 50°F

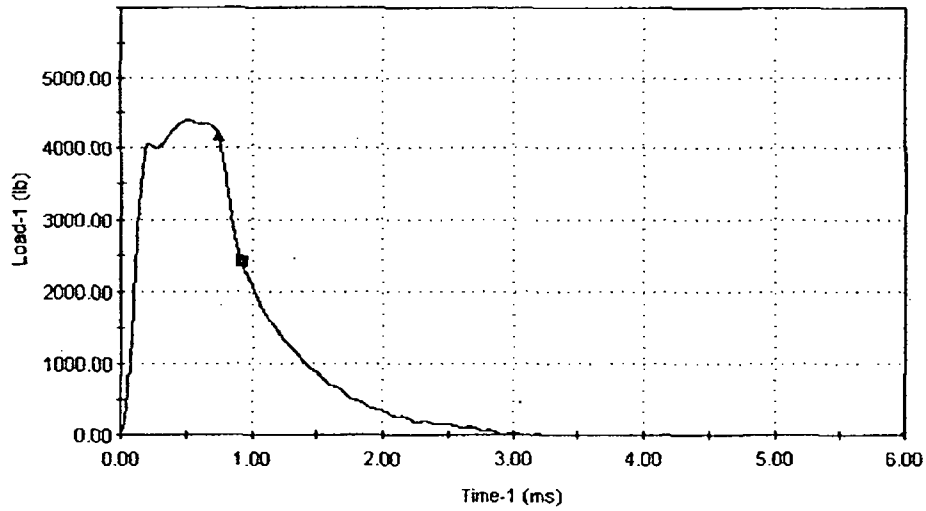

HW14, 75°F

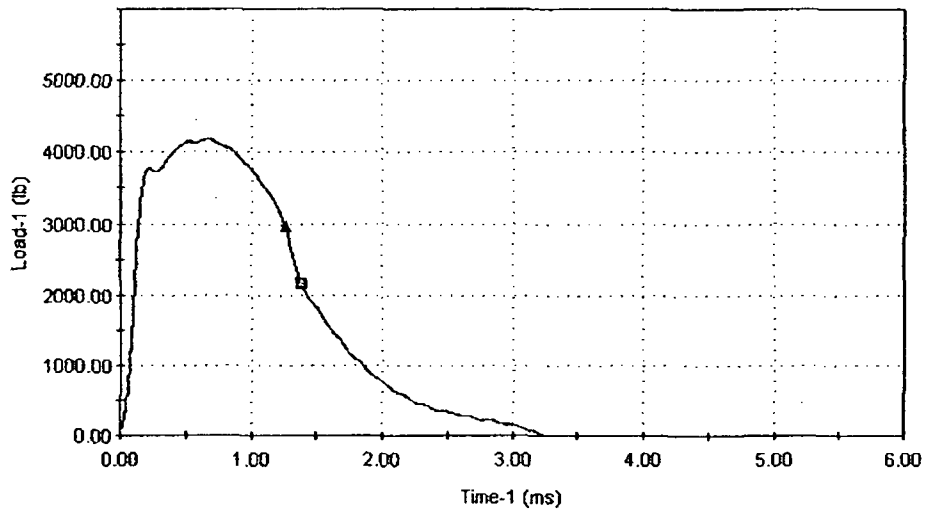

HW2, 125°F

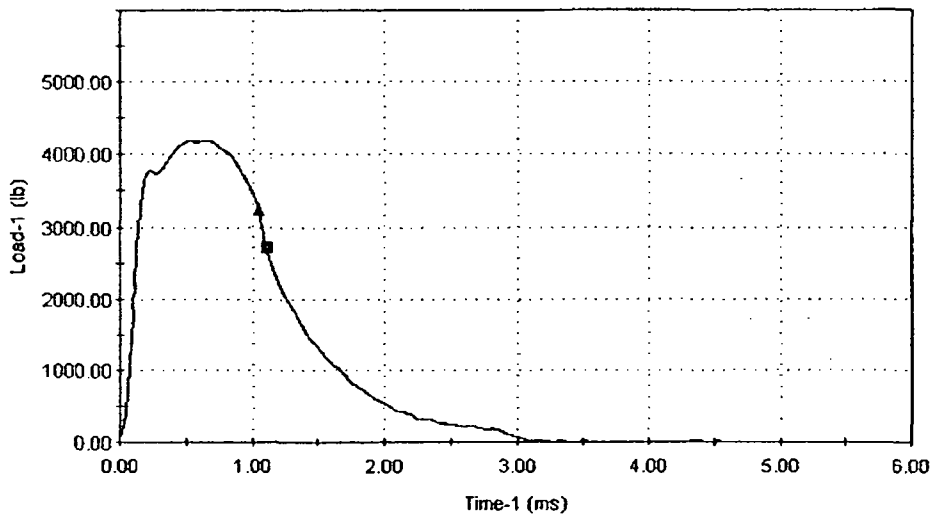

HW5, 150°F

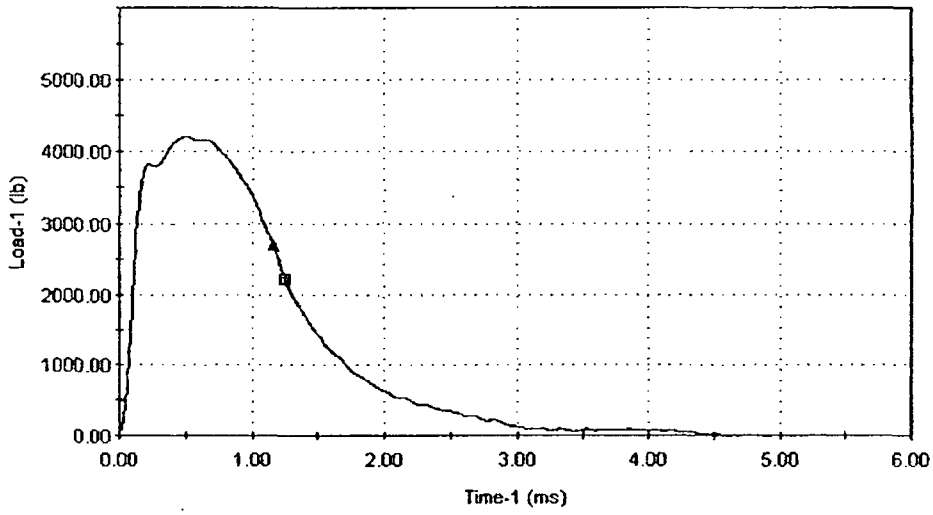

HW7, 200°F

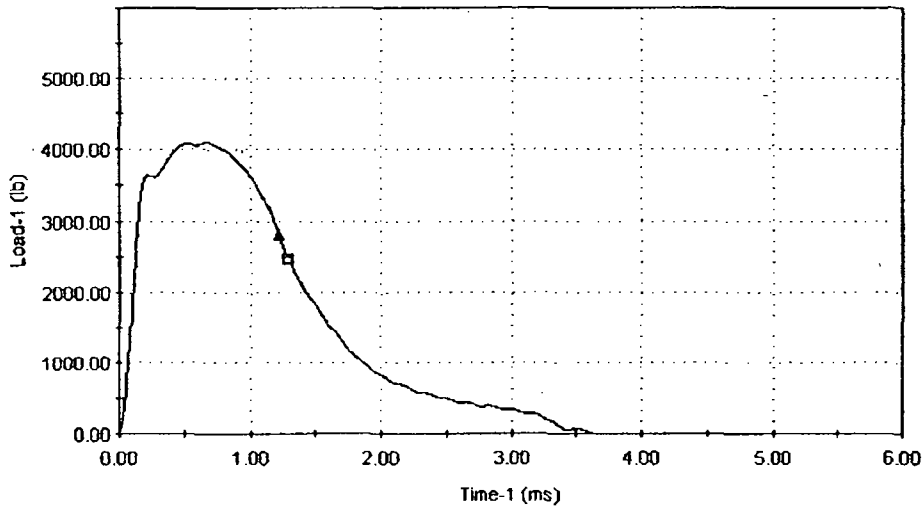

HW13, 225°F

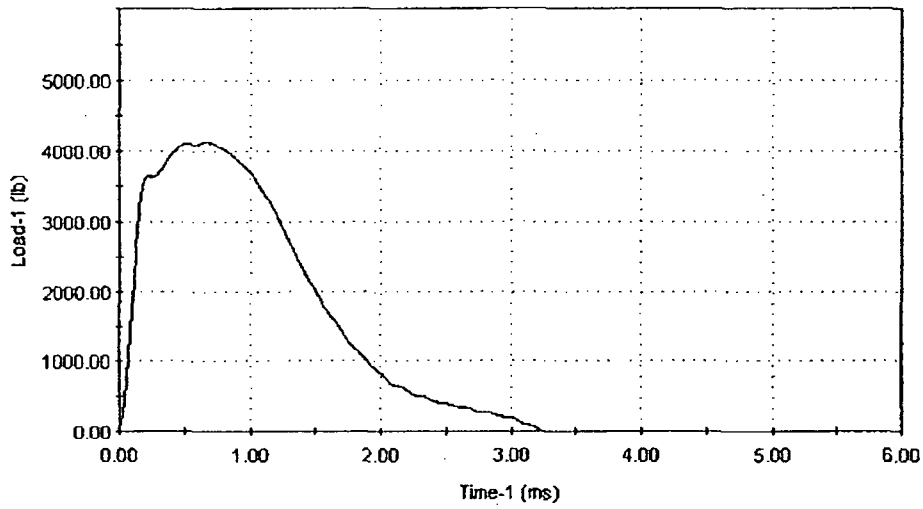

HW11, 250°F

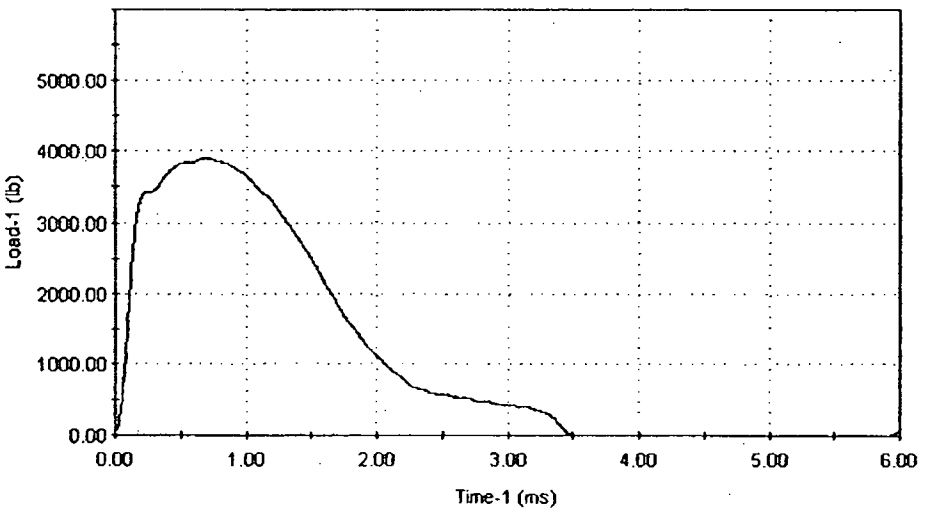

HW1, 275°F

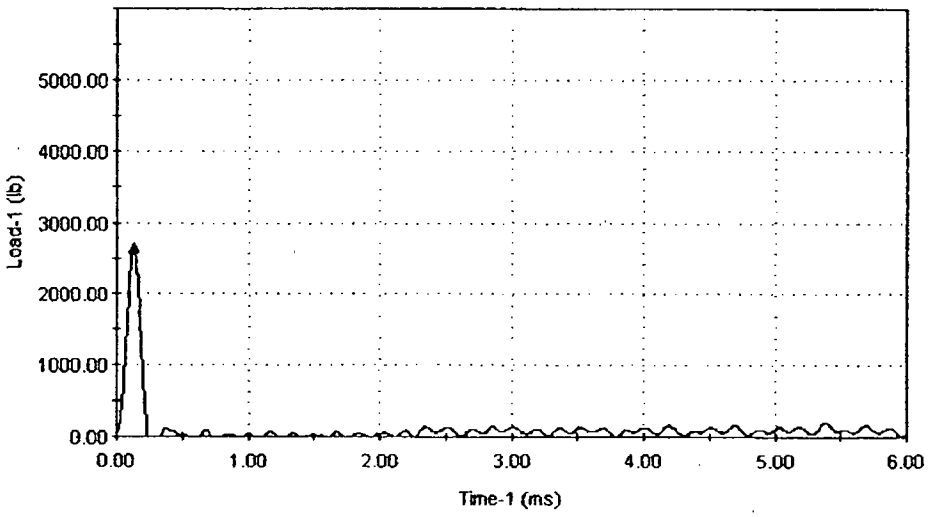

HH3, -200°F

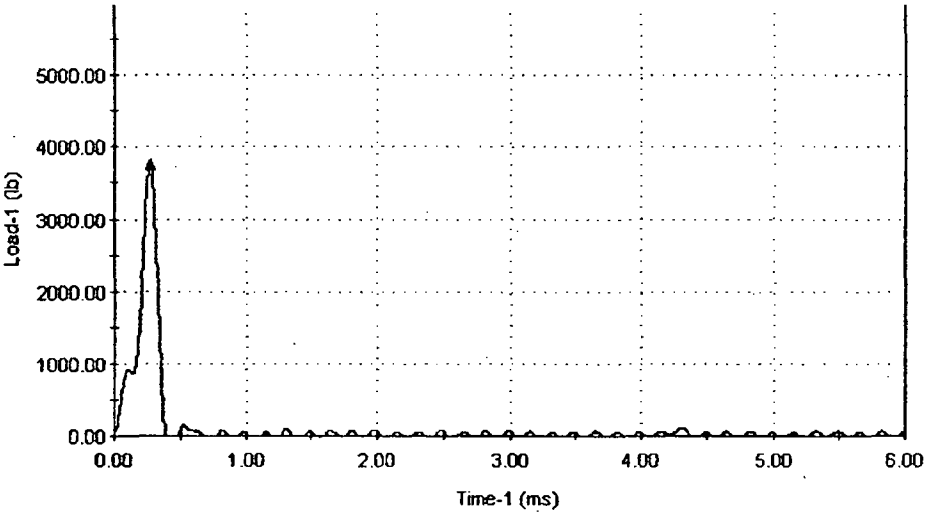

HH2, -150°F

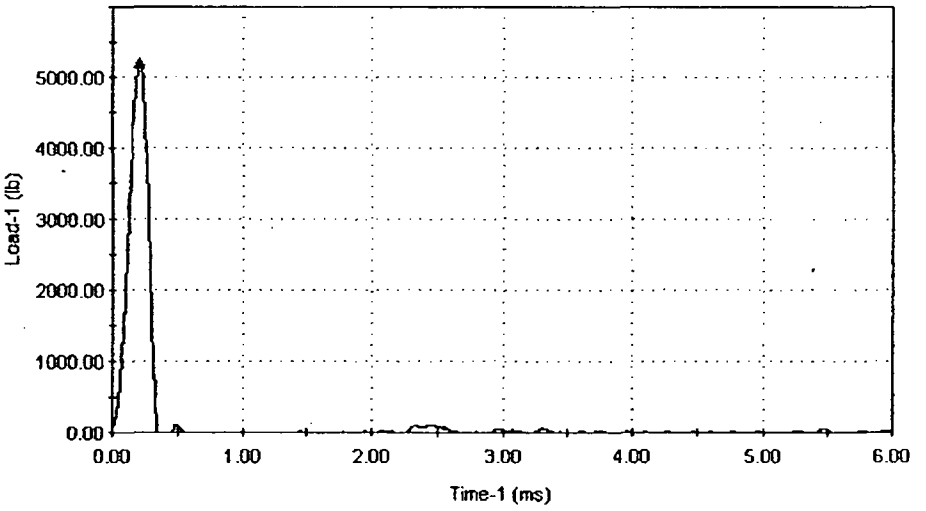

HH4, -125°F

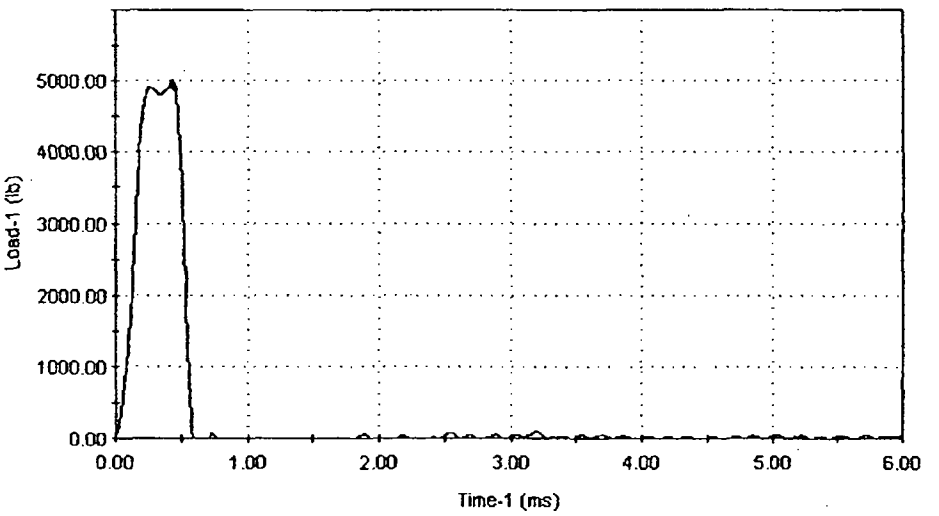

HH7, -108°F

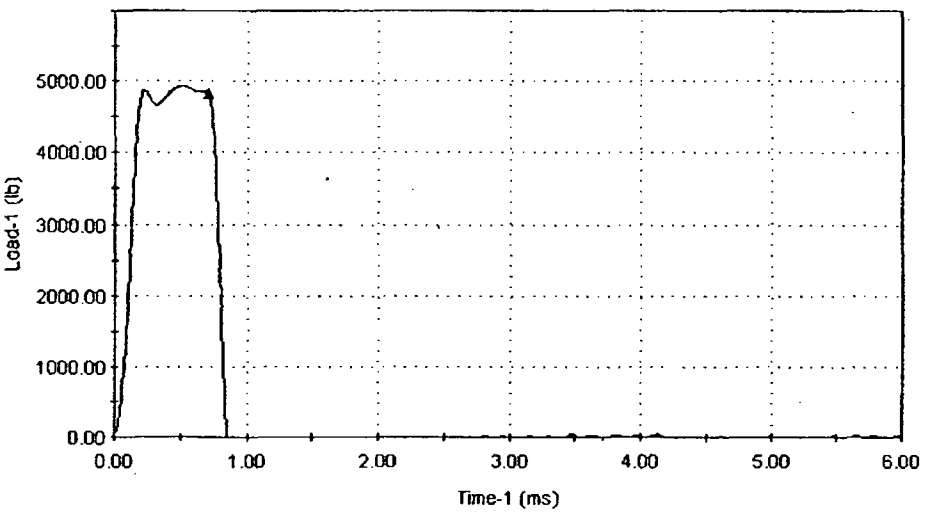

HH14, -75°F

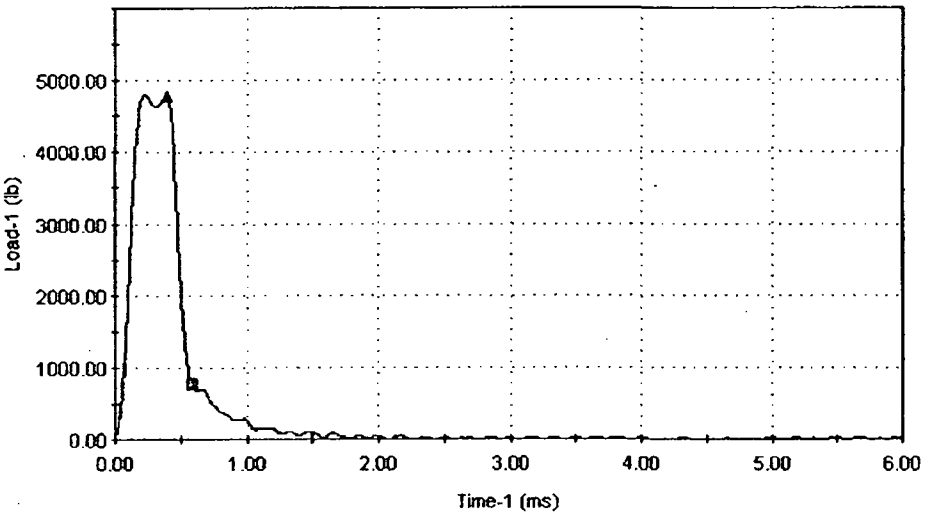

HH5, -50°F

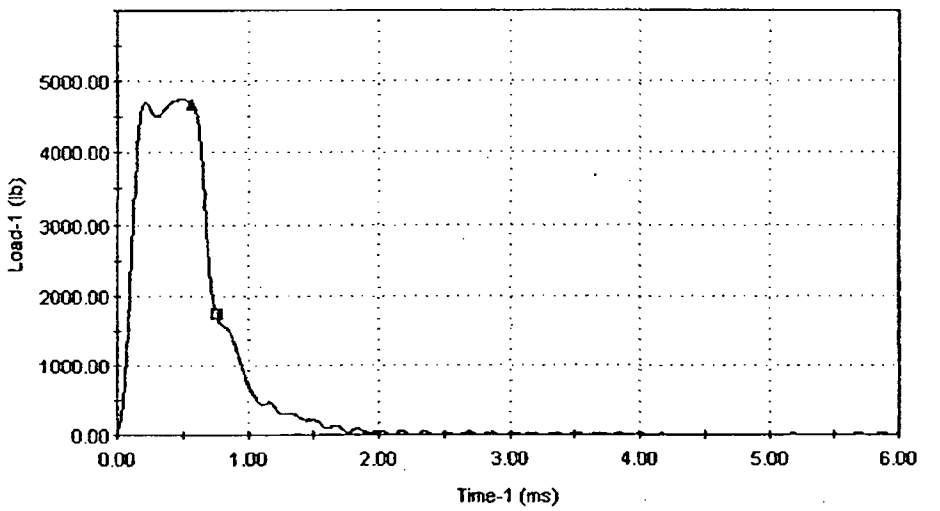

HH11, -25°F

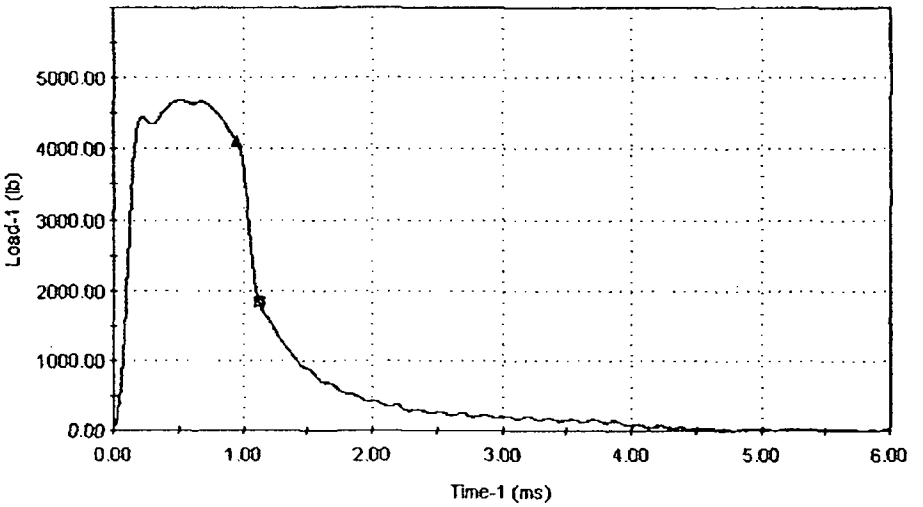

HH10, 0°F

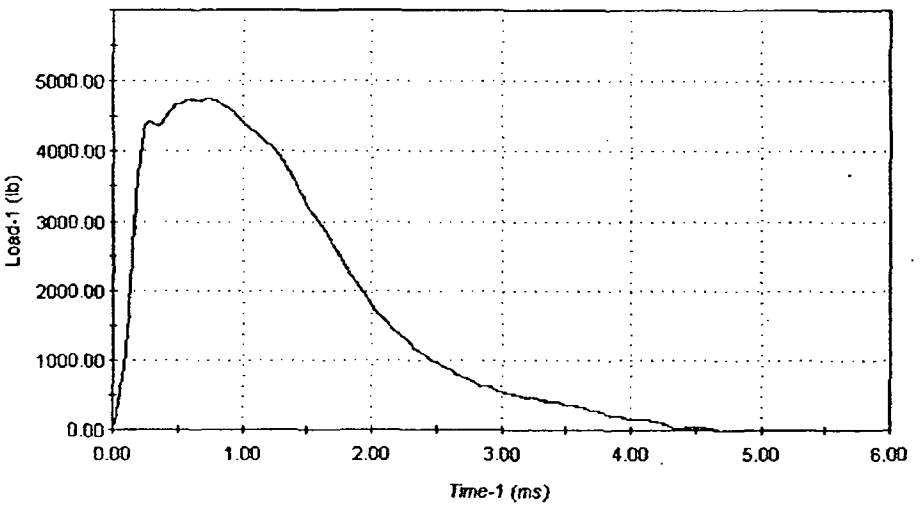

HH8, 25°F

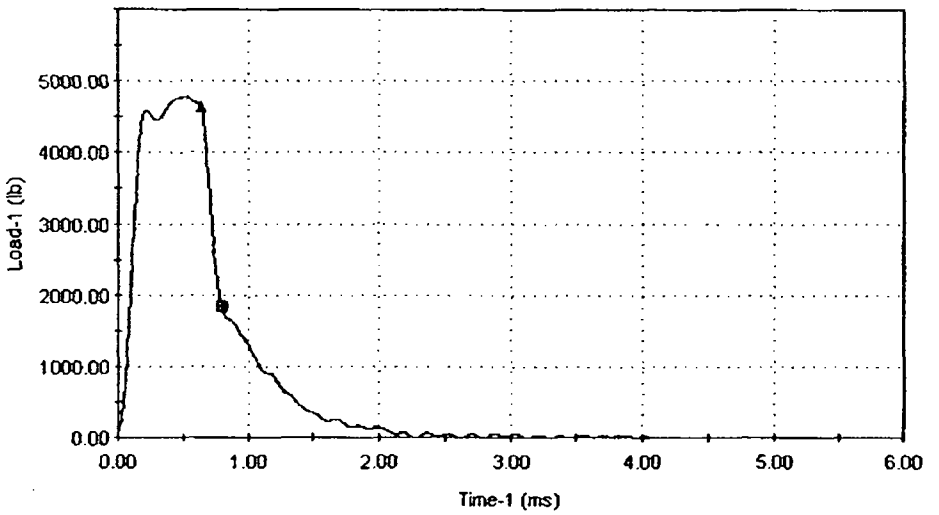

HH15, 50°F

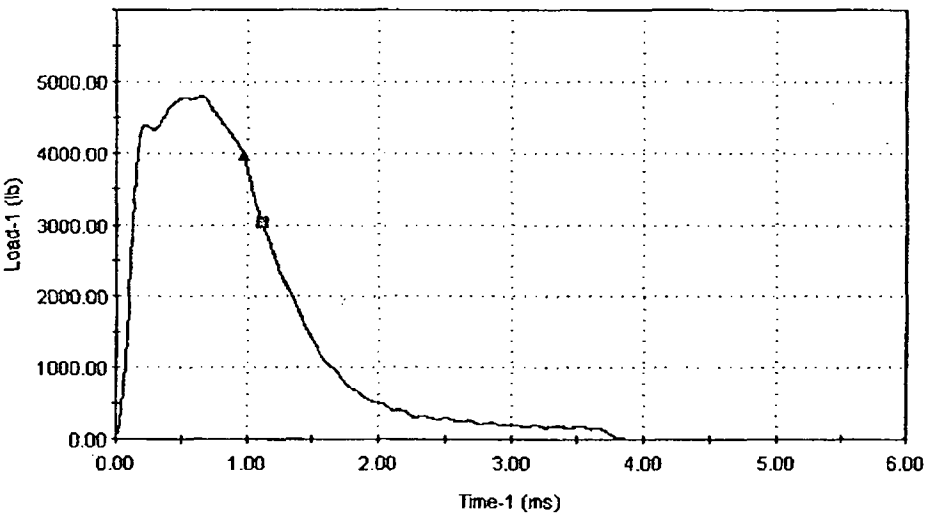

HH9, 75°F

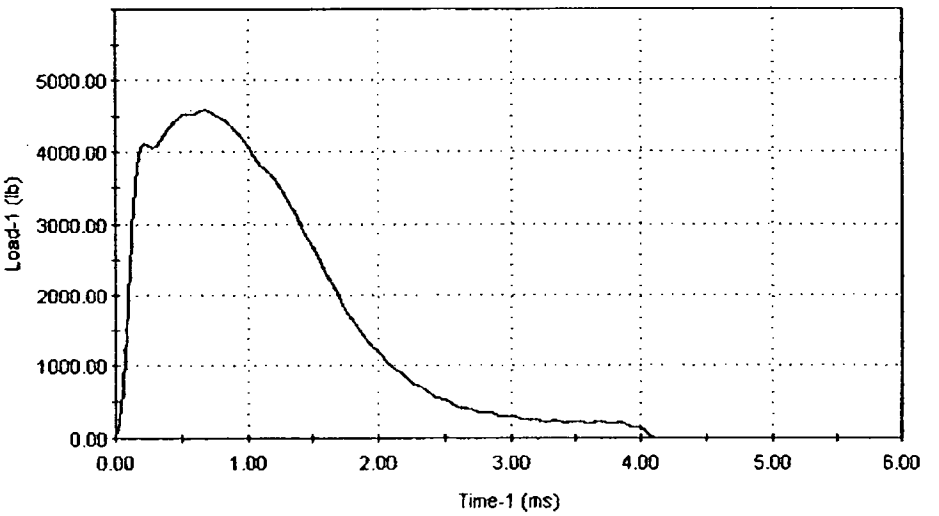

HH12, 125°F

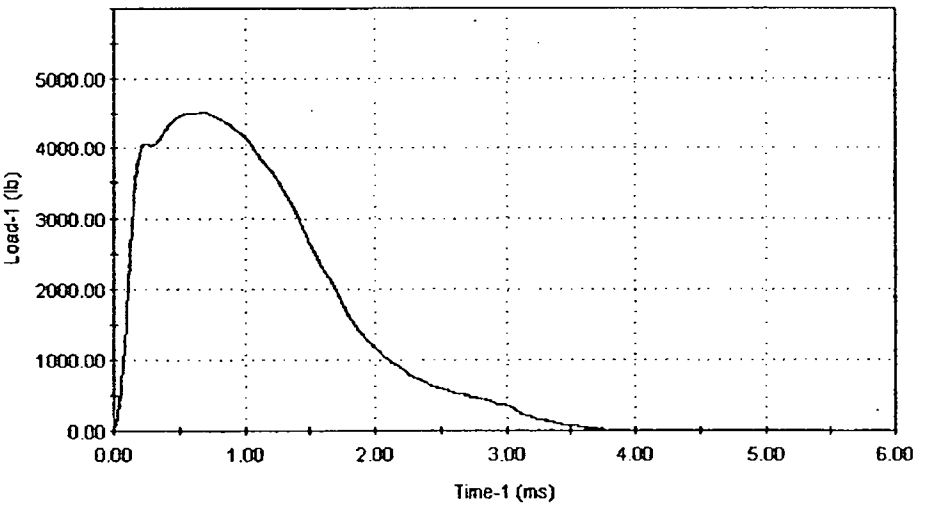

HH6, 150°F

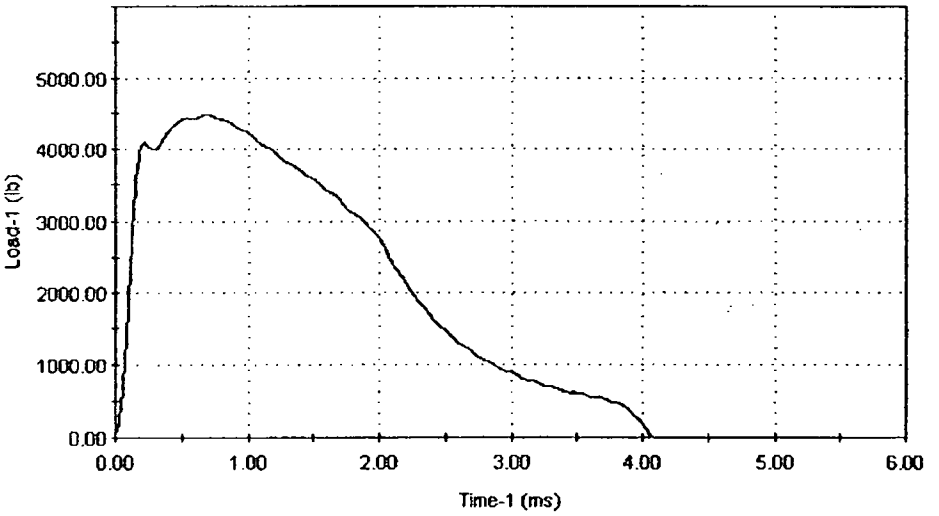

HH13, 175°F

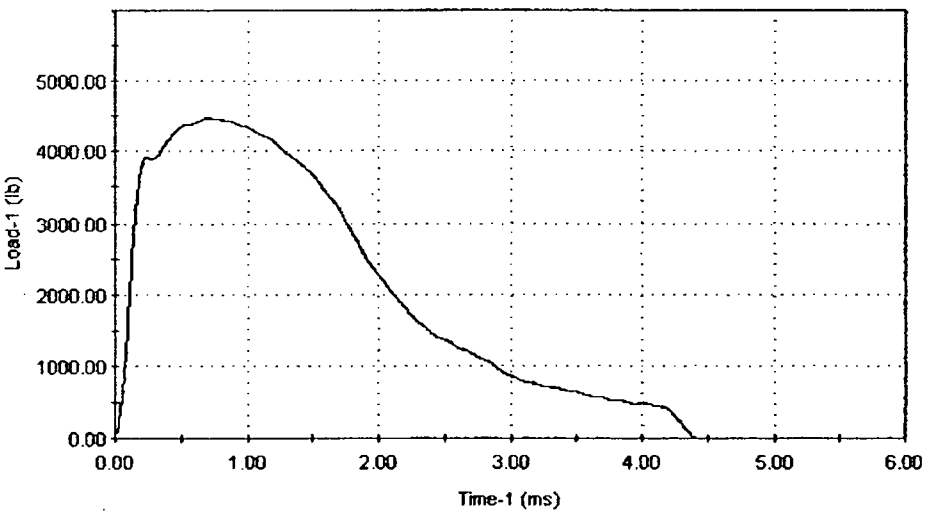

HH1, 200°F

APPENDIX C

CHARPY V-NOTCH PLOTS FOR CAPSULE U USING SYMMETRIC HYPERBOLIC TANGENT CURVE-FITTING METHOD

Contained in Table C-1 are the upper shelf energy values used as input for the generation of the Charpy V-notch plots using CVGRAPH, Version 4.1. The definition for Upper Shelf Energy (USE) is given in ASTM E185-82, Section 4.18, and reads as follows:

> "*upper shelf energy level* – the average energy value for all Charpy specimens (normally three) whose test temperature is above the upper end of the transition region. For specimens tested in sets of three at each test temperature, the set having the highest average may be regarded as defining the upper shelf energy."

If there are specimens tested in set of three at each temperature Westinghouse reports the set having the highest average energy as the USE (usually unirradiated material). If the specimens were not tested in sets of three at each temperature Westinghouse reports the average of all 100% shear Charpy data as the USE. Hence, the USE values reported in Table C-1 and used to generate the Charpy V-notch curves were determined utilizing this methodology.

The lower shelf energy values were fixed at 2.2 ft-lb for all cases.

Table C-1 Upper Shelf Energy Values Fixed in CVGRAPH [ft-lb]

Material	Unirradiated (ft-lbs)	Capsule V (ft-lbs)	Capsule Y (ft-lbs)	Capsule U (ft-lbs)
Intermediate Shell Plate R2507-1 (Long.)	138	139	133	140
Intermediate Shell Plate R2507-1 (Trans.)	98	105	105	104
Weld Metal (heat # 90209)	98	93	101	97
HAZ Material	155	137	137	129

CAPSULE U

CVGRAPH 4.1 Hyperbolic Tangent Curve Printed at 10:20:10 on 04-02-2003

Page 1

Coefficients of Curve 1

A = 71.09	B = 68.9	C = 66.82	T0 = 49.21

Equation is: CVN = A + B * [tanh((T - T0)/C)]

Upper Shelf Energy: 140 Fixed Temp. at 30 ft-lbs: -10.4 Temp. at 50 ft-lbs: 21.7 Lower Shelf Energy: 2.19 Fixed

Material: PLATE SA533B1 Heat Number: NR 62 067-1 Orientation: LT

Capsule: U Total Fluence:

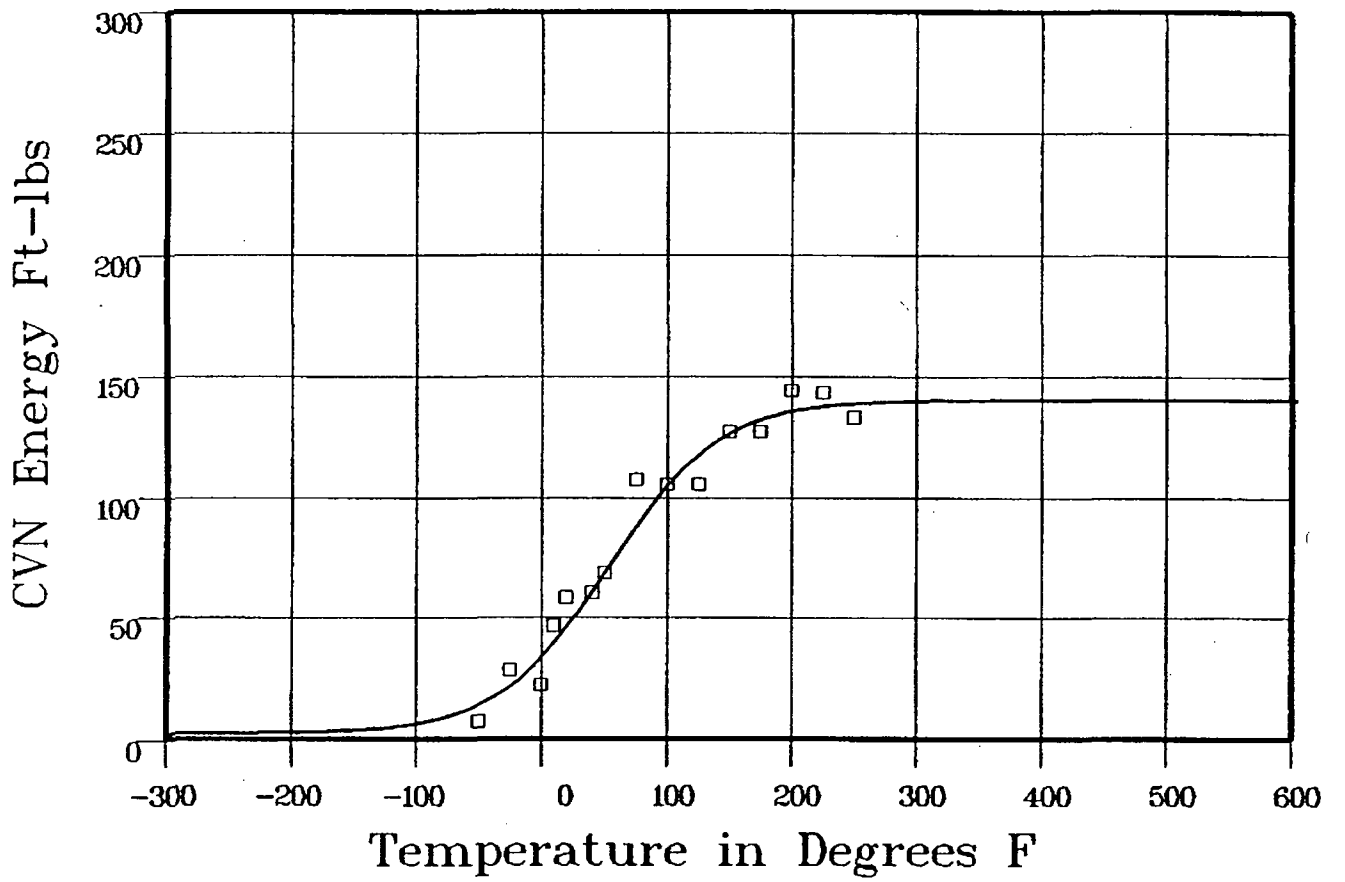

Data Set(s) Plotted

Plant: ST2 Cap: U Material: PLATE SA533B1 Ori: LT Heat #: NR 62 067-1

Charpy V-Notch Data

Temperature	Input CVN Energy	Computed CVN Energy	Differential
-50	7	14.92	-7.92
-25	28	23.31	4.68
0	22	35.74	-13.74
10	46	41.93	4.06
20	58	48.75	9.24
40	60	63.81	-3.81
50	68	71.71	-3.71
75	107	90.97	16.02
100	105	107.35	-2.35

**** Data continued on next page ****

CAPSULE U

Page 2

Material: PLATE SA533B1 Heat Number: NR 62 067-1 Orientation: LT

Capsule: U Total Fluence:

Charpy V-Notch Data (Continued)

Temperature	Input CVN Energy	Computed CVN Energy	Differential
125	105	119.52	-14.52
150	127	127.68	-.68
175	127	132.79	-5.79
200	144	135.85	8.14
225	143	137.63	5.36
250	133	138.66	-5.66

SUM of RESIDUALS = -10.69

CAPSULE U

CVGRAPH 4.1 Hyperbolic Tangent Curve Printed at 10:24:13 on 04-02-2003

Page 1

Coefficients of Curve 1

A = 40.37	B = 39.37	C = 71	T0 = 42.18

Equation is: L.E. = A + B * [tanh((T - T0)/C)]

Upper Shelf L.E.: 79.75 Temperature at L.E. 35: 32.4 Lower Shelf L.E.: 1 Fixed

Material: PLATE SA533B1 Heat Number: NR 62 067-1 Orientation: LT

Capsule: U Total Fluence:

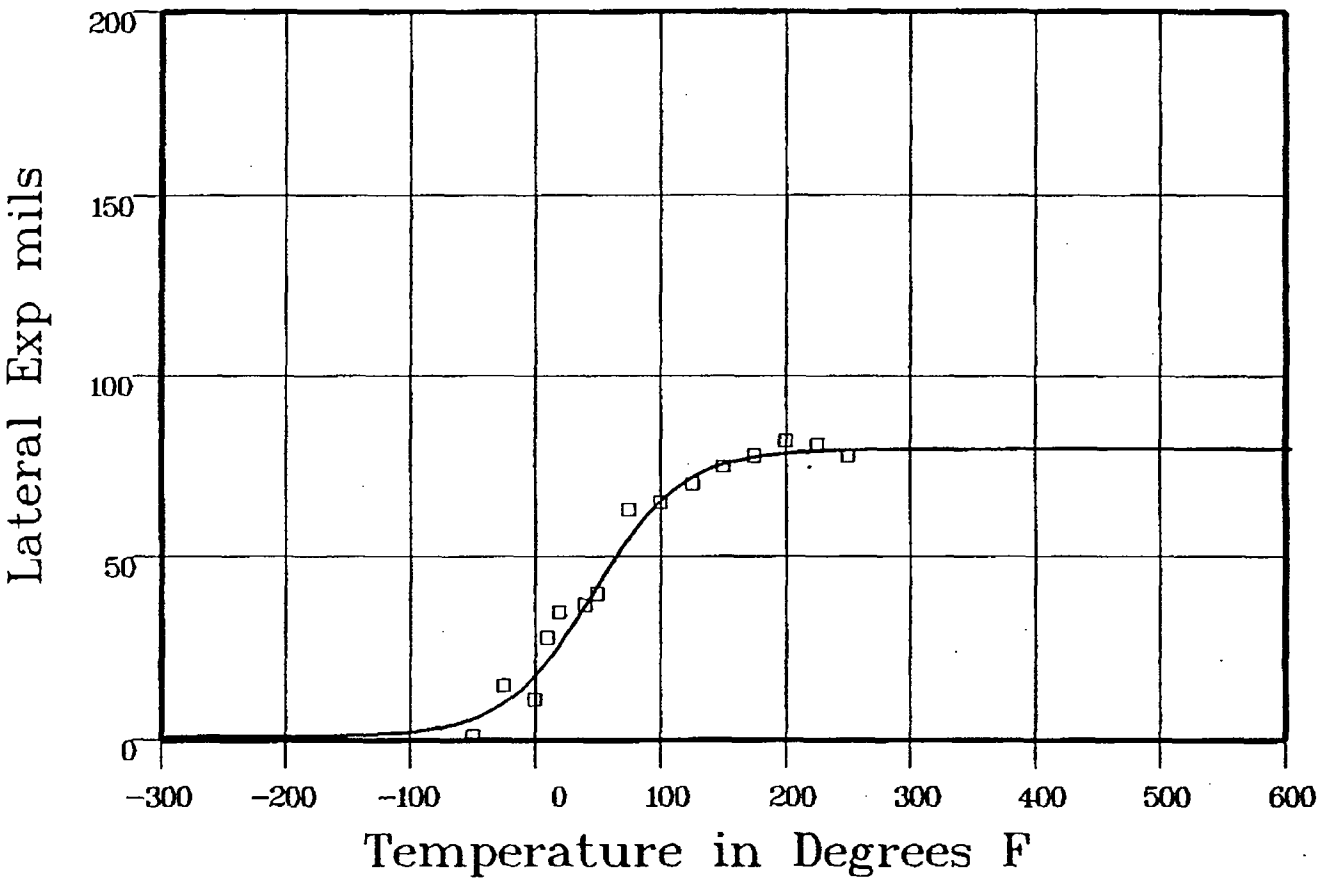

Data Set(s) Plotted

Plant: ST2 Cap: U Material: PLATE SA533B1 Ori: LT Heat #: NR 62 067-1

Charpy V-Notch Data

Temperature	Input Lateral Expansion	Computed L.E.	Differential
-50	1	6.46	-5.46
-25	15	11.31	3.68
0	11	19.39	-8.39
10	28	23.65	4.34
20	35	28.45	6.54
40	37	39.16	-2.16
50	40	44.69	-4.69
75	63	57.37	5.62
100	65	66.83	-1.83

**** Data continued on next page ****

CAPSULE U

Page 2

Material: PLATE SA533B1 Heat Number: NR 62 067-1 Orientation: LT

Capsule: U Total Fluence:

Charpy V-Notch Data (Continued)

Temperature	Input Lateral Expansion	Computed L.E.	Differential
125	70	72.78	-2.78
150	75	76.14	-1.14
175	78	77.92	.07
200	82	78.83	3.16
225	81	79.29	1.7
250	78	79.52	-1.52

SUM of RESIDUALS = -2.87

CAPSULE U

CVGRAPH 4.1 Hyperbolic Tangent Curve Printed at 10:25:32 on 04-02-2003

Page 1

Coefficients of Curve 1

A = 50	B = 50	C = 56.52	T0 = 55.77

Equation is: Shear% = A + B * [tanh((T - T0)/C)]

Temperature at 50% Shear: 55.7

Material: PLATE SA533B1 Heat Number: NR 62 067-1 Orientation: LT

Capsule: U Total Fluence:

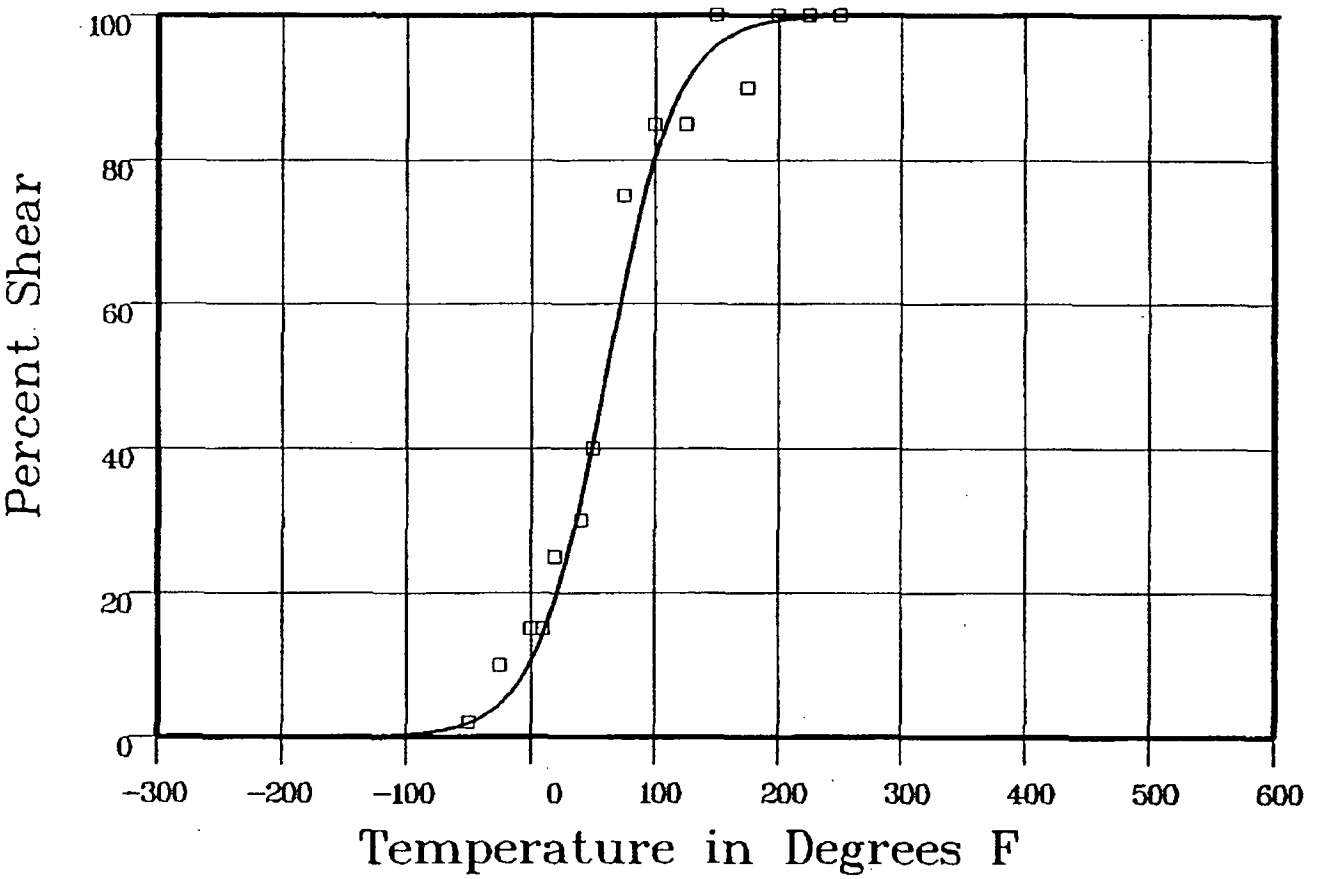

Data Set(s) Plotted

Plant: ST2 Cap: U Material: PLATE SA533B1 Ori: LT Heat #: NR 62 067-1

Charpy V-Notch Data

Temperature	Input Percent Shear	Computed Percent Shear	Differential
-50	2	2.31	-.31
-25	10	5.42	4.57
0	15	12.19	2.8
10	15	16.52	-1.52
20	25	21.99	3
40	30	36.39	-6.39
50	40	44.9	-4.9
75	75	66.37	8.62
100	85	82.7	2.29

**** Data continued on next page ****

CAPSULE U

Page 2

Material: PLATE SA533B1 Heat Number: NR 62 067-1 Orientation: LT

Capsule: U Total Fluence:

Charpy V-Notch Data (Continued)

Temperature	Input Percent Shear	Computed Percent Shear	Differential
125	85	92.05	-7.05
150	100	96.55	3.44
175	90	98.54	-8.54
200	100	99.39	.6
225	100	99.74	.25
250	100	99.89	.1

SUM of RESIDUALS = -3.03

CAPSULE U

CVGRAPH 4.1 Hyperbolic Tangent Curve Printed at 10:27:19 on 04-02-2003

Page 1

Coefficients of Curve 1

A = 53.09	B = 50.9	C = 100.51	T0 = 71.43

Equation is: CVN = A + B * [tanh((T - T0)/C)]

Upper Shelf Energy: 104 Fixed Temp. at 30 ft-lbs: 22.2 Temp. at 50 ft-lbs: 65.3 Lower Shelf Energy: 2.19 Fixed

Material: PLATE SA533B1 Heat Number: NR 62 067-1 Orientation: TL

Capsule: U Total Fluence:

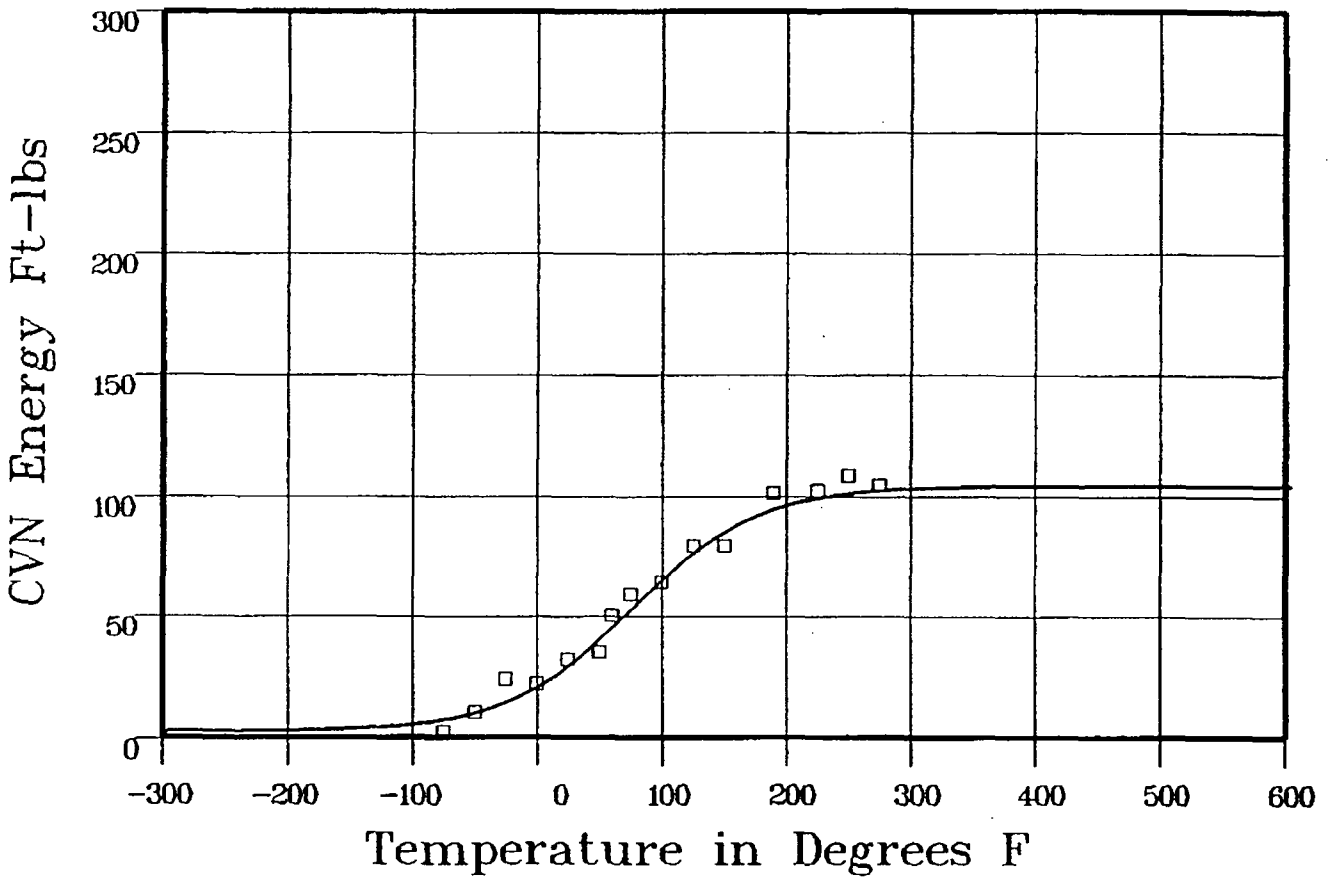

Data Set(s) Plotted

Plant: ST2 Cap: U Material: PLATE SA533B1 Ori: TL Heat #: NR 62 067-1

Charpy V-Notch Data

Temperature	Input CVN Energy	Computed CVN Energy	Differential
-75	2	7.44	-5.44
-50	10	10.54	-.54
-25	24	15.22	8.77
0	22	21.99	0
25	32	31.12	.87
50	35	42.4	-7.4
60	50	47.33	2.66
75	59	54.9	4.09
100	64	67.18	-3.18

**** Data continued on next page ****

CAPSULE U

Page 2

Material: PLATE SA533B1 Heat Number: NR 62 067-1 Orientation: TL

Capsule: U Total Fluence:

Charpy V-Notch Data (Continued)

Temperature	Input CVN Energy	Computed CVN Energy	Differential
125	79	77.91	1.08
150	79	86.36	-7.36
190	101	95.2	5.79
225	102	99.42	2.57
250	108	101.16	6.83
275	104	102.25	1.74

SUM of RESIDUALS = 10.49

CAPSULE U

CVGRAPH 4.1 Hyperbolic Tangent Curve Printed at 10:21:24 on 04-02-2003

Page 1

Coefficients of Curve 1

A = 34.58	B = 33.58	C = 91.43	T0 = 80.85

Equation is: L.E. = A + B * [tanh((T - T0)/C)]

Upper Shelf L.E.: 68.17 Temperature at L.E. 35: 81.9 Lower Shelf L.E.: 1 Fixed

Material: PLATE SA533B1 Heat Number: NR 62 067-1 Orientation: TL

Capsule: U Total Fluence:

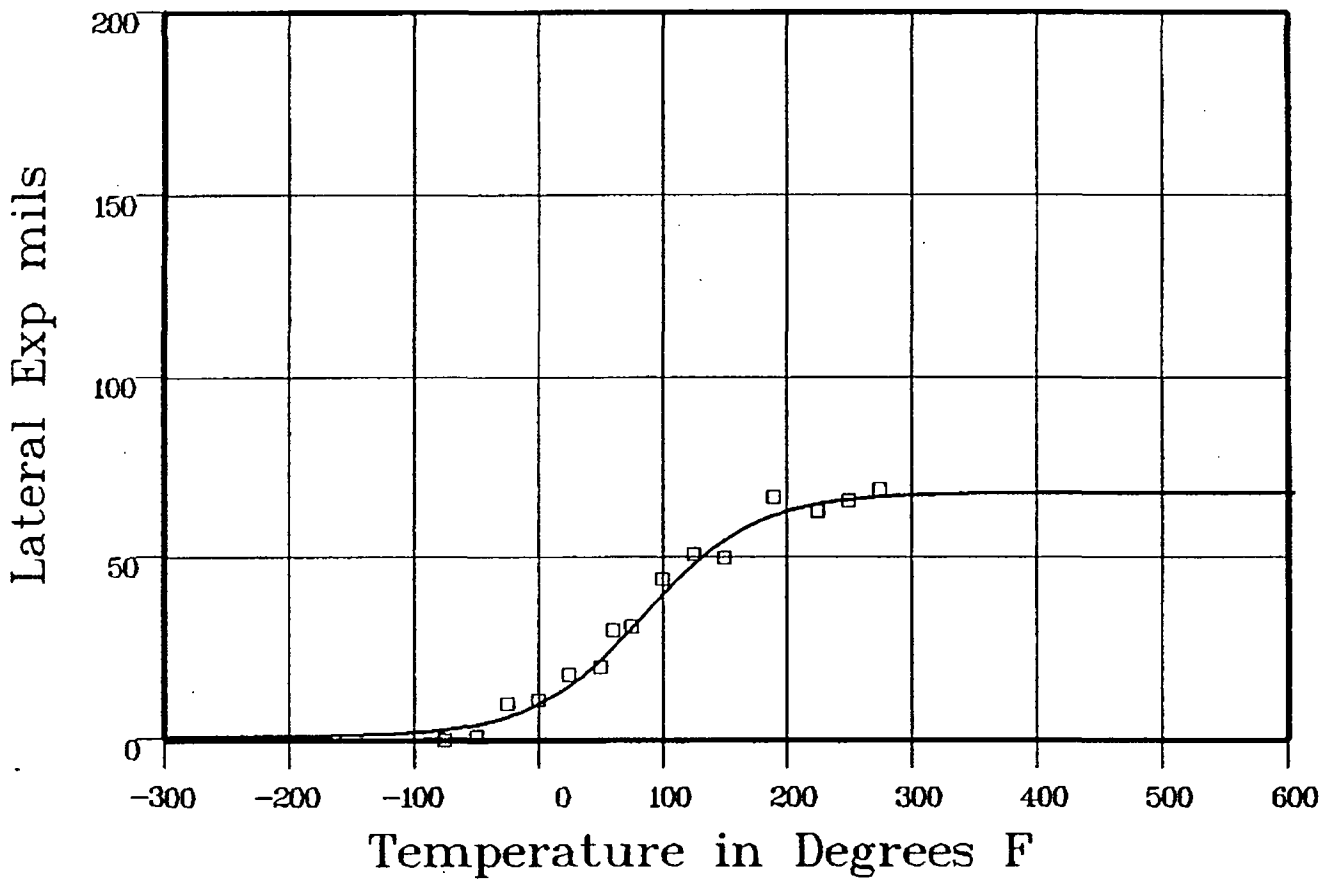

Data Set(s) Plotted

Plant: ST2 Cap.: U Material: PLATE SA533B1 Ori.: TL Heat #: NR 62 067-1

Charpy V-Notch Data

Temperature	Input Lateral Expansion	Computed L.E.	Differential
-75	0	3.15	-3.15
-50	1	4.63	-3.63
-25	10	7.03	2.96
0	11	10.78	.21
25	18	16.28	1.71
50	20	23.66	-3.66
60	30	27.05	2.94
75	31	32.43	-1.43
100	44	41.51	2.48

**** Data continued on next page ****

CAPSULE U

Page 2

Material: PLATE SA533B1 Heat Number: NR 62 067-1 Orientation: TL

Capsule: U Total Fluence:

Charpy V-Notch Data (Continued)

Temperature	Input Lateral Expansion	Computed L.E.	Differential
125	51	49.64	1.35
150	50	56.04	-6.04
190	67	62.51	4.48
225	63	65.41	-2.41
250	66	66.55	-.55
275	69	67.22	1.77
			SUM of RESIDUALS = -2.95

CAPSULE U

CVGRAPH 4.1 Hyperbolic Tangent Curve Printed at 10:29:54 on 04-02-2003

Page 1

Coefficients of Curve 1

A = 50	B = 50	C = 62.16	T0 = 89.35

Equation is: Shear% = A + B * [tanh((T - T0)/C)]

Temperature at 50% Shear: 89.3

Material: PLATE SA533B1 Heat Number: NR 62 067-1 Orientation: TL

Capsule: U Total Fluence:

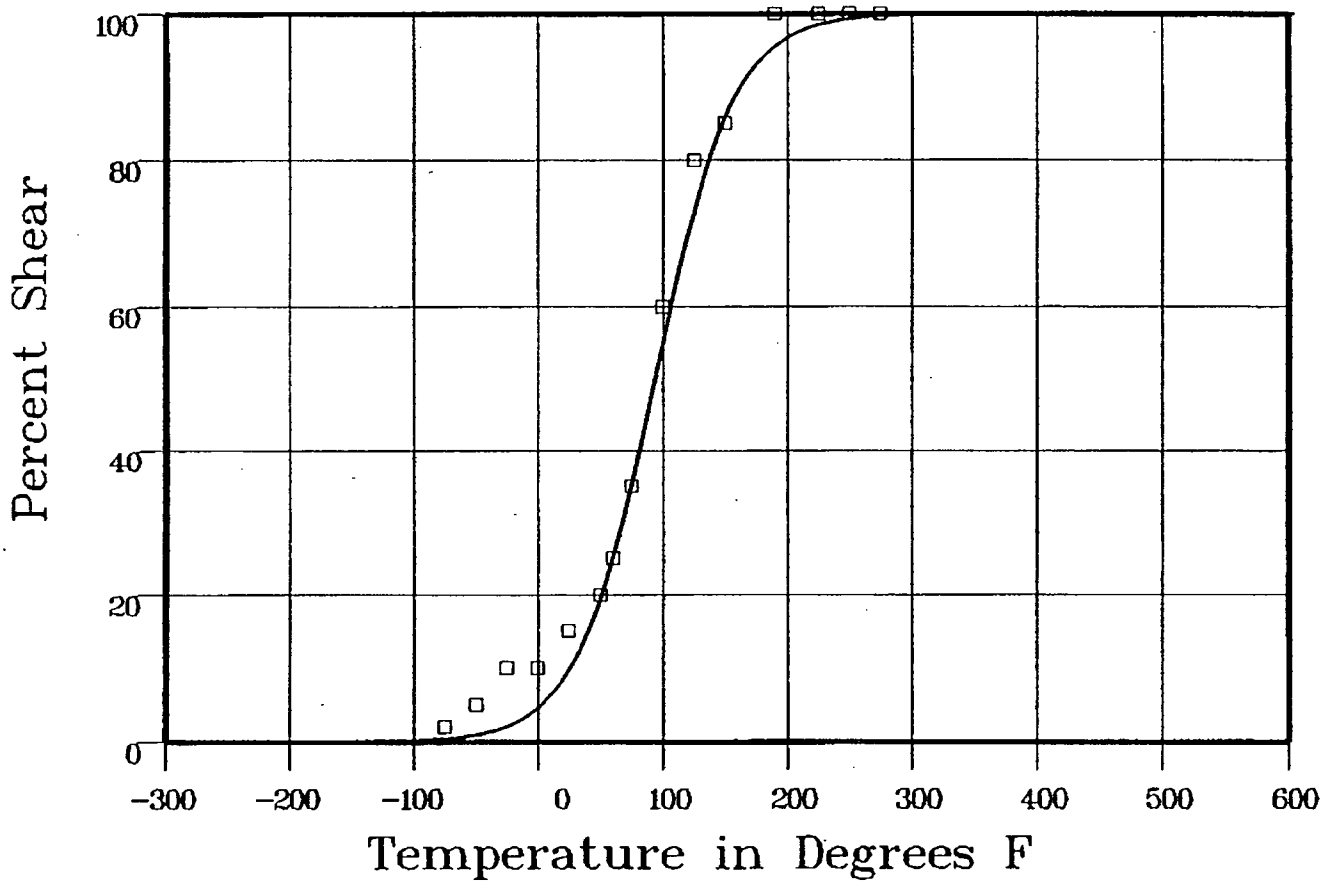

Data Set(s) Plotted

Plant: ST2 Cap: U Material: PLATE SA533B1 Ori: TL Heat #: NR 62 067-1

Charpy V-Notch Data

Temperature	Input Percent Shear	Computed Percent Shear	Differential
-75	2	5	1.49
-50	5	1.11	3.88
-25	10	2.46	7.53
0	10	5.34	4.65
25	15	11.19	3.8
50	20	21.99	-1.99
60	25	27.99	-2.99
75	35	38.65	-3.65
100	60	58.47	1.52

**** Data continued on next page ****

CAPSULE U

Page 2

Material: PLATE SA533B1 Heat Number: NR 62 067-1 Orientation: TL

Capsule: U Total Fluence:

Charpy V-Notch Data (Continued)

Temperature	Input Percent Shear	Computed Percent Shear	Differential
125	80	75.89	4.1
150	85	87.55	-2.55
190	100	96.22	3.77
225	100	98.74	1.25
250	100	99.43	.56
275	100	99.74	.25

SUM of RESIDUALS = 21.65

CAPSULE U

CVGRAPH 4.1 Hyperbolic Tangent Curve Printed at 10:32:58 on 04-02-2003

Page 1

Coefficients of Curve 1

A = 49.59	B = 47.4	C = 61.7	T0 = 33.01

Equation is: CVN = A + B * | tanh((T - T0)/C) |

Upper Shelf Energy: 97 Fixed Temp. at 30 ft-lbs: 5.8 Temp. at 50 ft-lbs: 33.5 Lower Shelf Energy: 2.19 Fixed

Material: WELD Heat Number: 90209 Orientation:

Capsule: U Total Fluence:

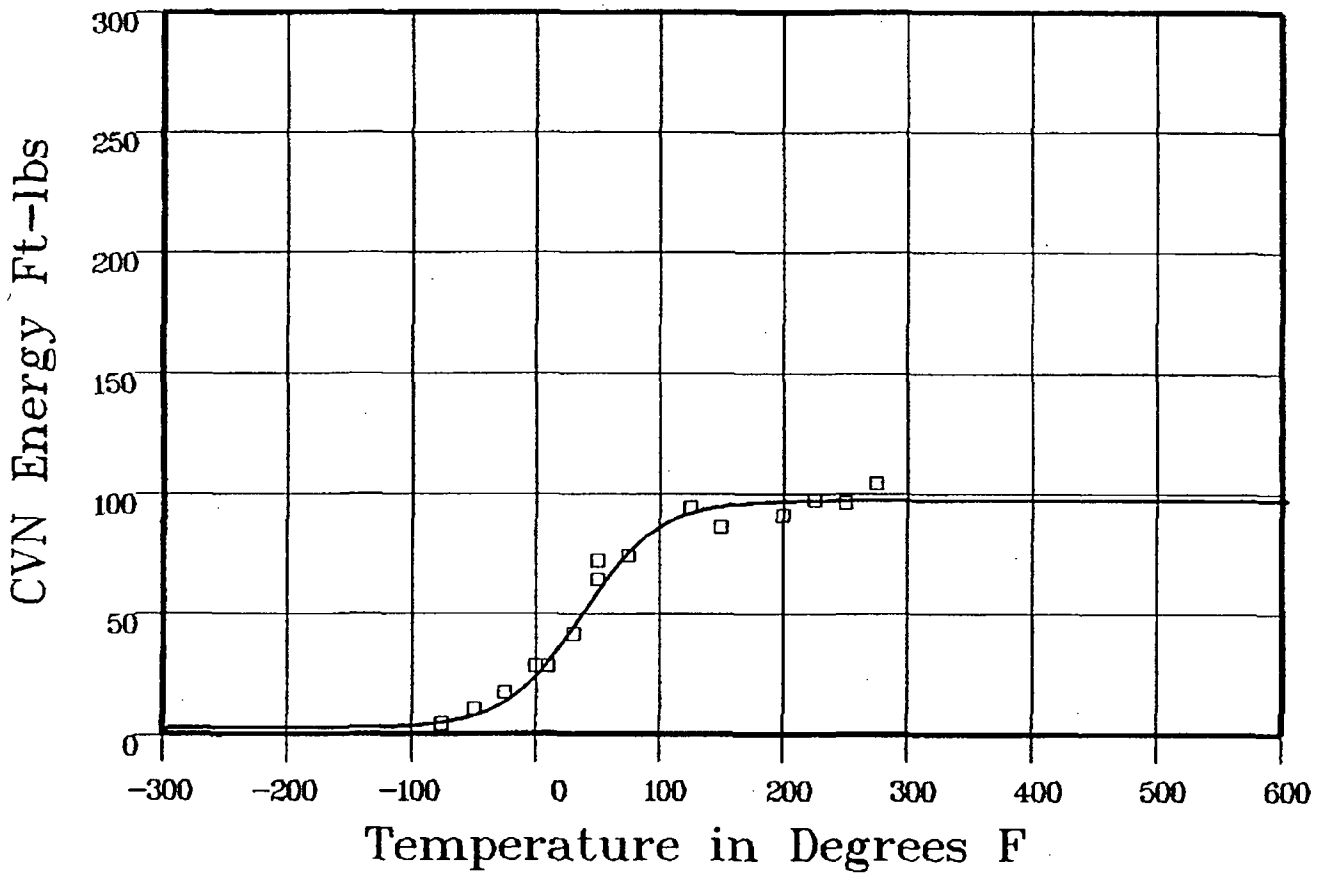

Data Set(s) Plotted

Plant: ST2 Cap.: U Material: WELD Ori.: Heat #: 90209

Charpy V-Notch Data

Temperature	Input CVN Energy	Computed CVN Energy	Differential
-75	4	4.97	-.97
-50	10	8.22	1.77
-25	17	14.74	2.25
0	28	26.4	1.59
10	28	32.69	-4.69
30	41	47.28	-6.28
50	64	62.32	1.67
50	72	62.32	9.67
75	74	77.64	-3.64

**** Data continued on next page ****

CAPSULE U

Page 2

Material: WELD Heat Number: 90209 Orientation:

Capsule: U Total Fluence:

Charpy V-Notch Data (Continued)

Temperature	Input CVN Energy	Computed CVN Energy	Differential
125	94	92.42	1.57
150	86	94.9	-8.9
200	91	96.57	-5.57
225	97	96.81	.18
250	96	96.91	-.91
275	104	96.96	7.03
		SUM of RESIDUALS =	-5.22

CAPSULE U

CVGRAPH 4.1 Hyperbolic Tangent Curve Printed at 10:36:56 on 04-02-2003

Page 1

Coefficients of Curve 1

A = 34.04	B = 33.04	C = 57.95	T0 = 33.75

Equation is: L.E. = A + B * [tanh((T - T0)/C)]

Upper Shelf L.E.: 67.08 Temperature at L.E. 35: 35.4 Lower Shelf L.E.: 1 Fixed

Material: WELD Heat Number: 90209 Orientation:

Capsule: U Total Fluence:

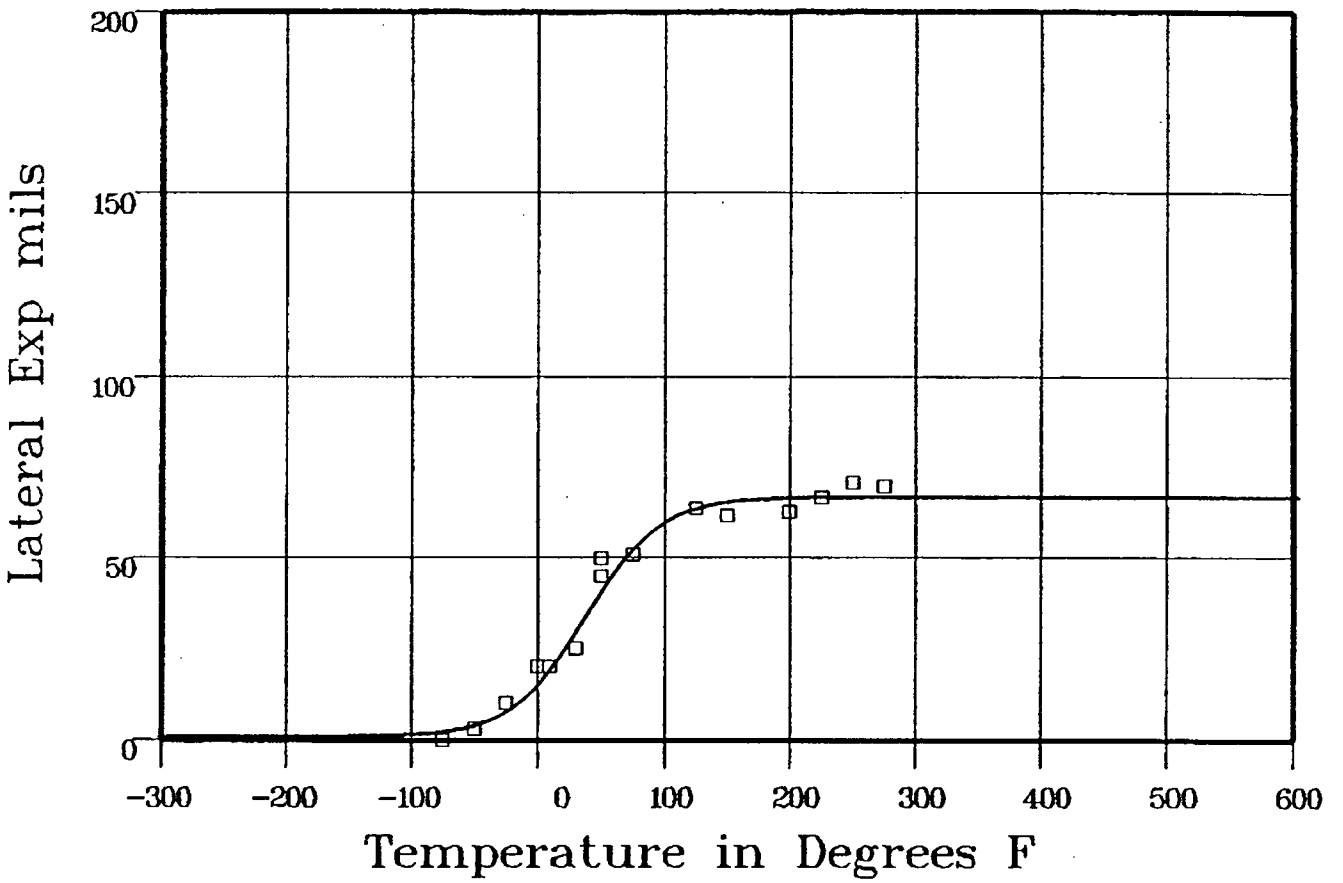

Data Set(s) Plotted

Plant: ST2 Cap.: U Material: WELD Ori.: Heat #: 90209

Charpy V-Notch Data

Temperature	Input Lateral Expansion	Computed L.E.	Differential
-75	0	2.51	-2.51
-50	3	4.47	-1.47
-25	10	8.68	1.31
0	20	16.71	3.28
10	20	21.21	-1.21
30	25	31.9	-6.9
50	45	43.07	1.92
50	50	43.07	6.92
75	51	54.25	-3.25

**** Data continued on next page ****

CAPSULE U

Page 2

Material: WELD Heat Number: 90209 Orientation:

Capsule: U Total Fluence:

Charpy V-Notch Data (Continued)

Temperature	Input Lateral Expansion	Computed L.E.	Differential
125	64	64.36	-.36
150	62	65.9	-3.9
200	63	66.86	-3.86
225	67	66.99	0
250	71	67.04	3.95
275	70	67.06	2.93

SUM of RESIDUALS = -3.14

CAPSULE U

CVGRAPH 4.1 Hyperbolic Tangent Curve Printed at 10:39:52 on 04-02-2003

Page 1

Coefficients of Curve 1

A = 50	B = 50	C = 74.3	T0 = 13.59

Equation is: Shear% = A + B * [tanh((T - T0)/C)]

Temperature at 50% Shear: 13.5

Material: WELD Heat Number: 90209 Orientation:

Capsule: U Total Fluence:

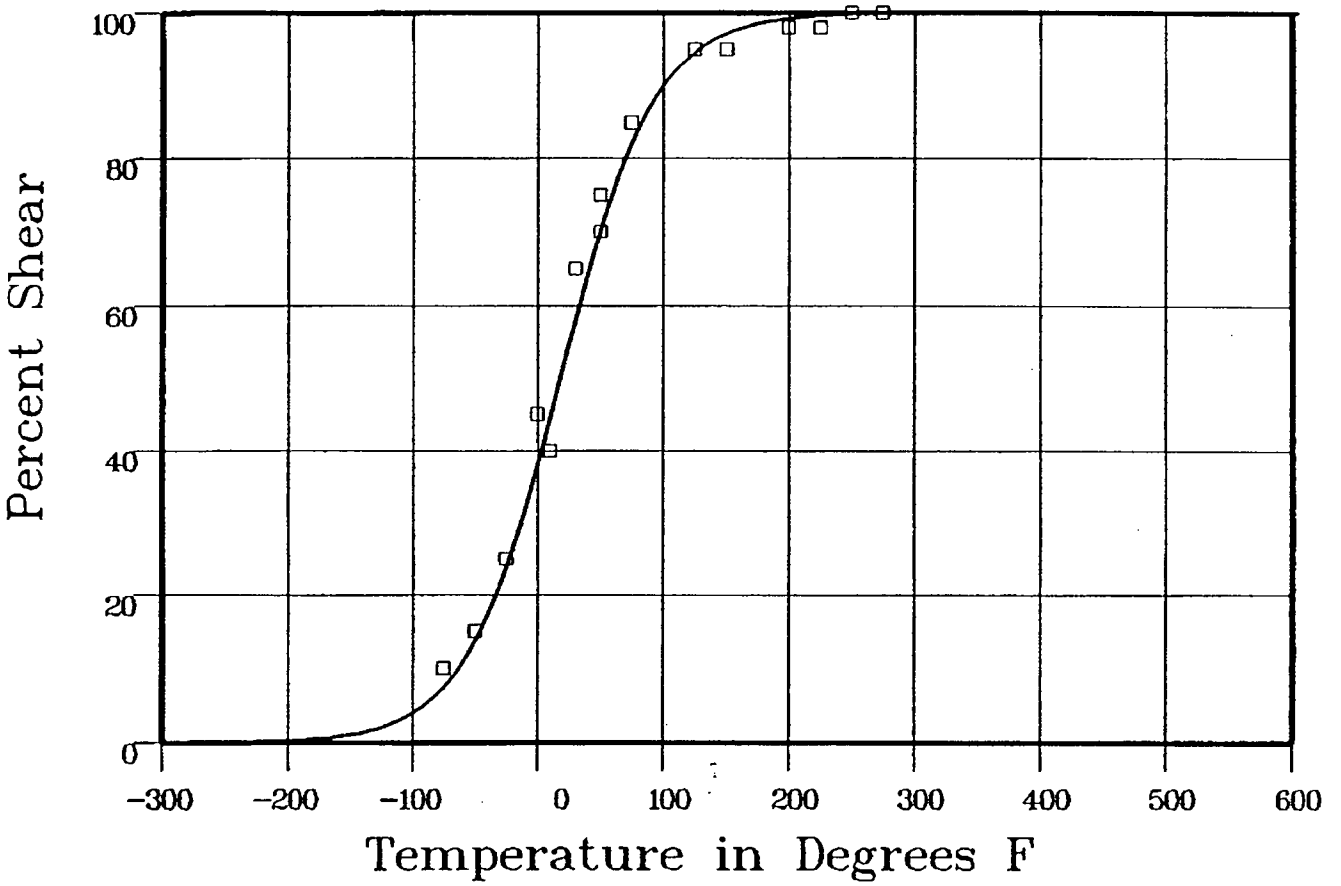

Data Set(s) Plotted

Plant: ST2 Cap: U Material: WELD Ori: Heat #: 90209

Charpy V-Notch Data

Temperature	Input Percent Shear	Computed Percent Shear	Differential
-75	10	8.43	1.56
-50	15	15.29	-.29
-25	25	26.13	-1.13
0	45	40.95	4.04
10	40	47.58	-7.58
30	65	60.86	4.13
50	70	72.7	-2.7
50	75	72.7	2.29
75	85	83.92	1.07

**** Data continued on next page ****

CAPSULE U

Page 2

Material: WELD Heat Number: 90209 Orientation:

Capsule: U Total Fluence:

Charpy V-Notch Data (Continued)

Temperature	Input Percent Shear	Computed Percent Shear	Differential
125	95	95.25	-.25
150	95	97.51	-2.51
200	98	99.34	-1.34
225	98	99.66	-1.66
250	100	99.82	.17
275	100	99.91	.08

SUM of RESIDUALS = -4.12

CAPSULE U

CVGRAPH 4.1 Hyperbolic Tangent Curve Printed at 10:50:24 on 04-02-2003

Page 1

Coefficients of Curve 1

A = 65.59	B = 63.4	C = 116.25	T0 = -21.22

Equation is: CVN = A + B * [tanh((T - T0)/C)]

Upper Shelf Energy: 129 Fixed Temp. at 30 ft-lbs: -95 Temp. at 50 ft-lbs: -50.4 Lower Shelf Energy: 2.19 Fixed

Material: HEAT AFFD ZONE Heat Number: Orientation:

Capsule: U Total Fluence:

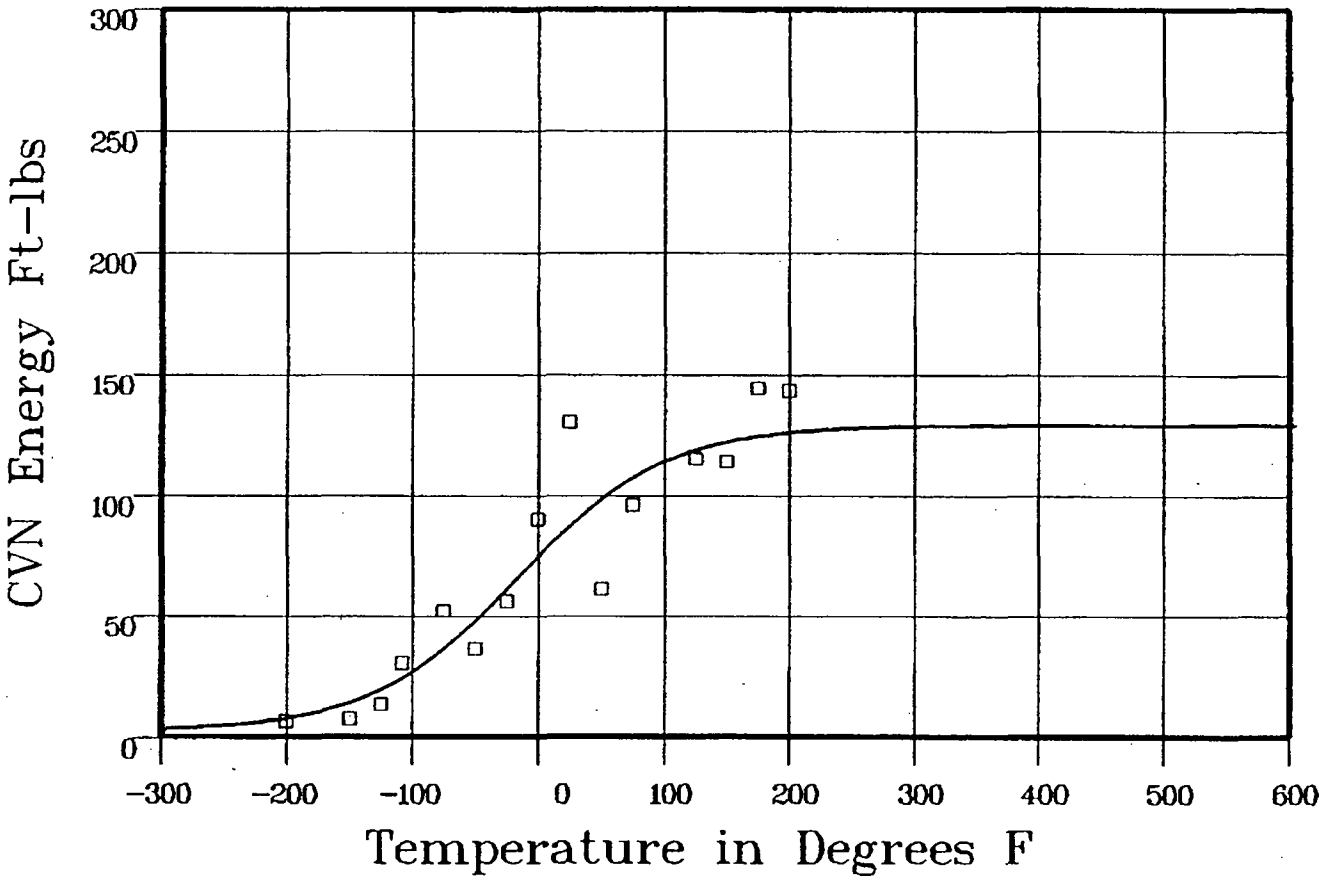

Data Set(s) Plotted

Plant: ST2 Cap: U Material: HEAT AFFD ZONE Ori: Heat #:

Charpy V-Notch Data

Temperature	Input CVN Energy	Computed CVN Energy	Differential
-200	6	7.79	-1.79
-150	7	14.67	-7.67
-125	13	20.41	-7.41
-108	30	25.46	4.53
-75	52	38.2	13.79
-50	36	50.22	-14.22
-25	56	63.54	-7.54
0	90	77.04	12.95
25	130	89.56	40.43

**** Data continued on next page ****

CAPSULE U

Page 2

Material: HEAT AFFD ZONE Heat Number: Orientation:

Capsule: U Total Fluence:

Charpy V-Notch Data (Continued)

Temperature	Input CVN Energy	Computed CVN Energy	Differential
50	61	100.21	-39.21
75	96	108.66	-12.66
125	115	119.51	-4.51
150	114	122.66	-8.66
175	144	124.8	19.19
200	143	126.24	16.75

SUM of RESIDUALS = 3.95

CAPSULE U

CVGRAPH 4.1 Hyperbolic Tangent Curve Printed at 10:53:21 on 04-02-2003

Page 1

Coefficients of Curve 1

A = 32.81	B = 31.81	C = 70.44	T0 = -26.25

Equation is: L.E. = A + B * [tanh((T - T0)/C)]

Upper Shelf L.E: 64.62 Temperature at L.E. 35: -21.3 Lower Shelf L.E: 1 Fixed

Material: HEAT AFF'D ZONE Heat Number: Orientation:

Capsule: U Total Fluence:

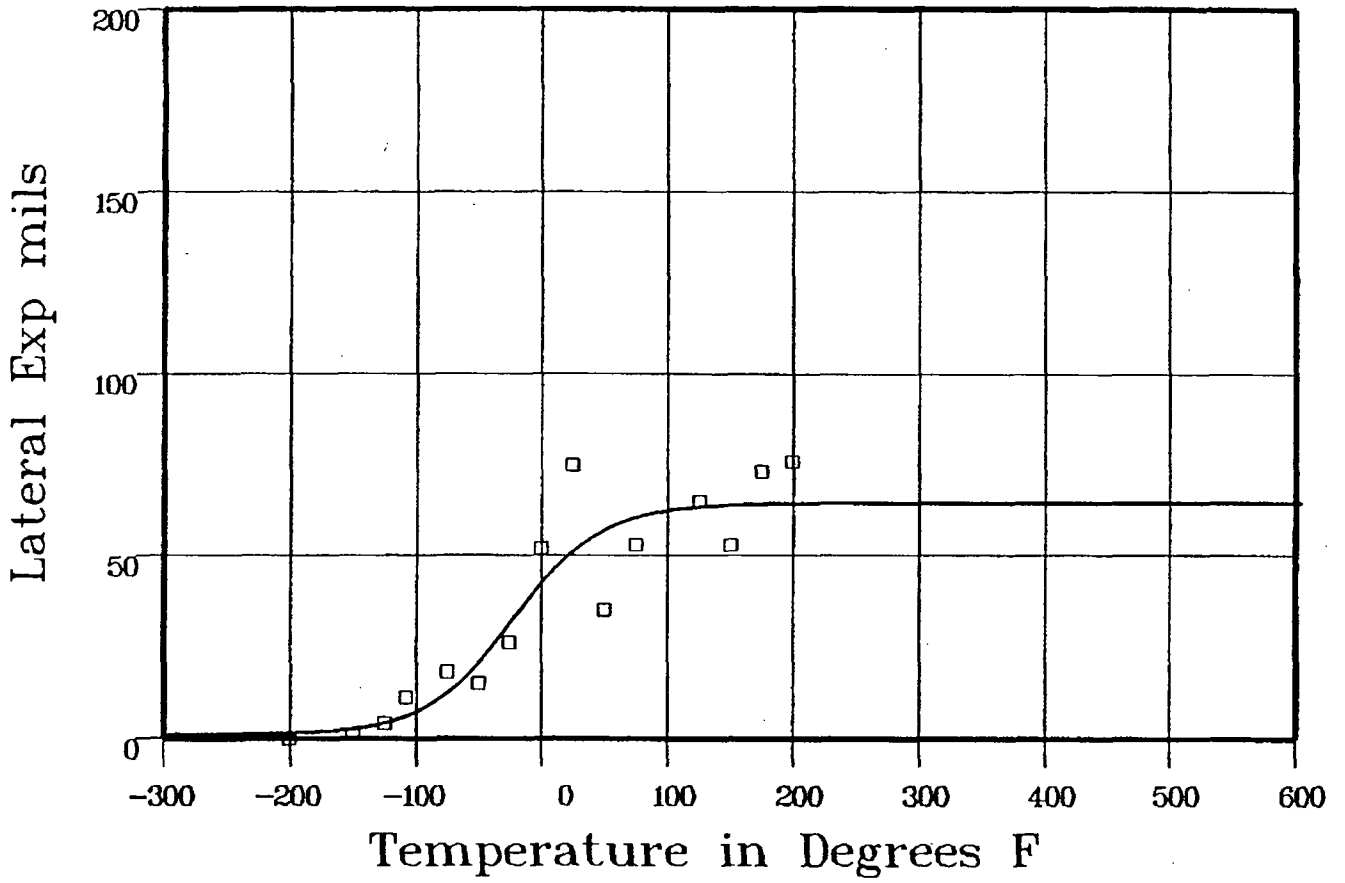

Data Set(s) Plotted

Plant: ST2 Cap: U Material: HEAT AFF'D ZONE Ori: Heat #:

Charpy V-Notch Data

Temperature	Input Lateral Expansion	Computed L.E.	Differential
-200	0	1.45	-1.45
-150	1	2.84	-1.84
-125	4	4.63	-.63
-108	11	6.68	4.31
-75	18	13.74	4.25
-50	15	22.47	-7.47
-25	26	33.37	-7.37
0	52	44.14	7.85
25	75	52.58	22.41

**** Data continued on next page ****

CAPSULE U

Material: HEAT AFFD ZONE Heat Number: Orientation:

Capsule: U Total Fluence:

Charpy V-Notch Data (Continued)

Temperature	Input Lateral Expansion	Computed L.E.	Differential
50	35	58.07	-23.07
75	53	61.22	-8.22
125	65	63.76	1.23
150	53	64.19	-11.19
175	73	64.41	8.58
200	76	64.52	11.47

SUM of RESIDUALS = -1.14

CAPSULE U

CVGRAPH 4.1 Hyperbolic Tangent Curve Printed at 10:56:43 on 04-02-2003

Page 1

Coefficients of Curve 1

A = 50	B = 50	C = 82.12	T0 = -27.18

Equation is: Shear% = A + B * [tanh((T - T0)/C)]

Temperature at 50% Shear: -27.1

Material: HEAT AFF'D ZONE Heat Number: Orientation:

Capsule: U Total Fluence:

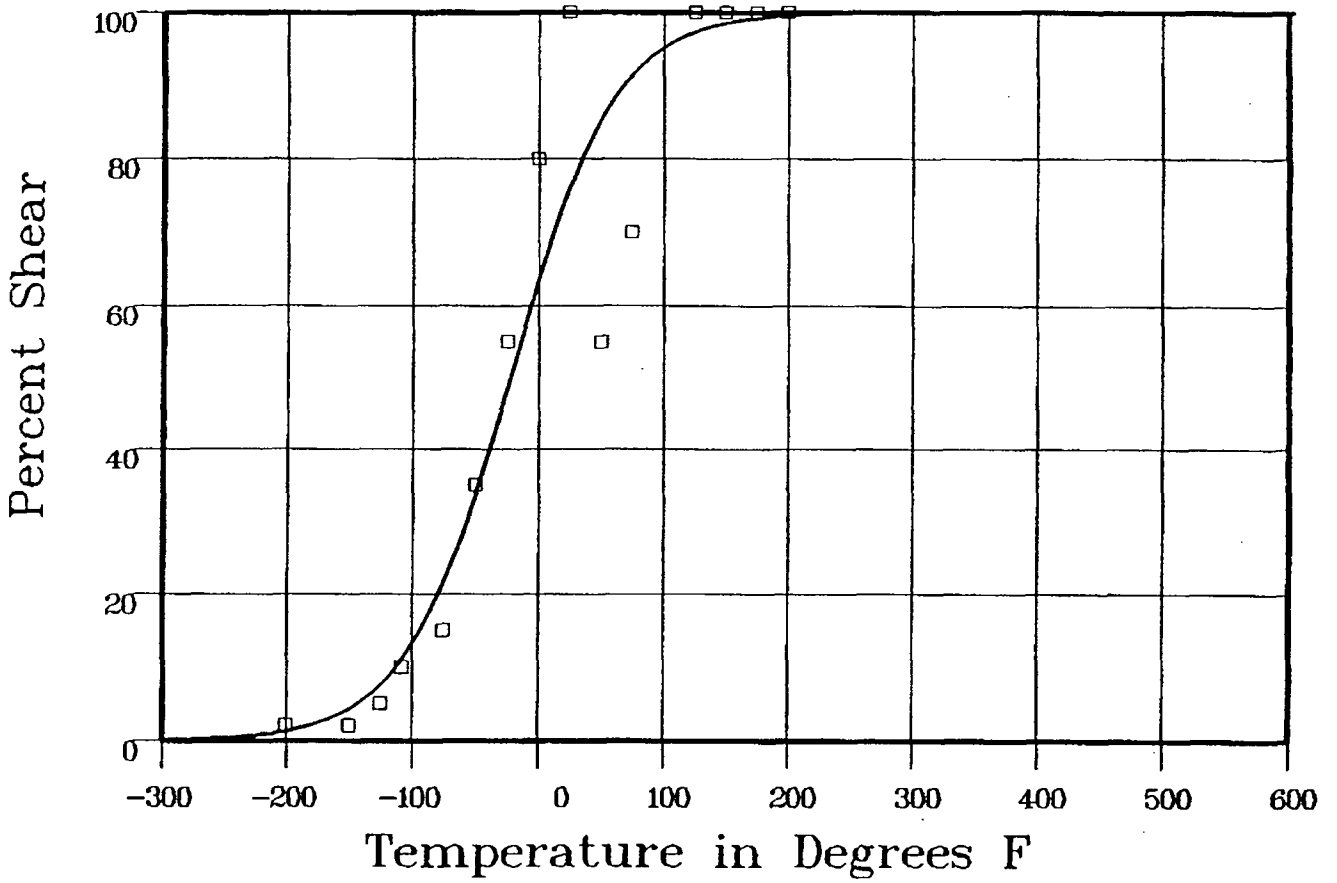

Data Set(s) Plotted

Plant: ST2 Cap: U Material: HEAT AFF'D ZONE Ori: Heat #:

Charpy V-Notch Data

Temperature	Input Percent Shear	Computed Percent Shear	Differential
-200	2	1.46	.53
-150	2	4.78	-2.78
-125	5	8.45	-3.45
-108	10	12.26	-2.26
-75	15	23.78	-8.78
-50	35	36.45	-1.45
-25	55	51.33	3.66
0	80	65.97	14.02
25	100	78.08	21.91

**** Data continued on next page ****

CAPSULE U

Page 2

Material: HEAT AFF'D ZONE Heat Number: Orientation:

Capsule: U Total Fluence:

Charpy V-Notch Data (Continued)

Temperature	Input Percent Shear	Computed Percent Shear	Differential
50	55	86.75	-31.75
75	70	92.33	-22.33
125	100	97.6	2.39
150	100	98.68	1.31
175	100	99.27	.72
200	100	99.6	.39

SUM of RESIDUALS = -27.86

APPENDIX D

SOUTH TEXAS UNIT 2 SURVEILLANCE PROGRAM CREDIBILITY EVALUATION

INTRODUCTION:

Regulatory Guide 1.99, Revision 2, describes general procedures acceptable to the NRC staff for calculating the effects of neutron radiation embrittlement of the low-alloy steels currently used for light-water-cooled reactor vessels. Position C.2 of Regulatory Guide 1.99, Revision 2, describes the method for calculating the adjusted reference temperature and Charpy upper-shelf energy of reactor vessel beltline materials using surveillance capsule data. The methods of Position C.2 can only be applied when two or more credible surveillance data sets become available from the reactor in question.

To date there has been three surveillance capsules removed from the South Texas Unit 2 reactor vessel. To use these surveillance data sets, they must be shown to be credible. In accordance with the discussion of Regulatory Guide 1.99, Revision 2, there are five requirements that must be met for the surveillance data to be judged credible.

The purpose of this evaluation is to apply the credibility requirements of Regulatory Guide 1.99, Revision 2, to the South Texas Unit 2 reactor vessel surveillance data and determine if the South Texas Unit 2 surveillance data is credible.

EVALUATION:

Criterion 1: Materials in the capsules should be those judged most likely to be controlling with regard to radiation embrittlement.

The South Texas Unit 2 reactor vessel consists of the following beltline region materials:

- Intermediate Shell Plates R2507-1, 2, 3
- Lower Shell Plates R3022-1, 2, 3
- Intermediate & Lower Shell Longitudinal Weld Seams (Heat # 90209),
- Intermediate to Lower Shell Circumferential Weld Seam (Heat # 90209).

At the time when the South Texas Unit 2 surveillance program material was selected it was believed that copper and phosphorus were the elements most important to embrittlement of the reactor vessel steels. The intermediate shell plate R2507-1 had one of the highest initial RT_{NDT} and the lowest USE of all plate materials in the beltline region. In addition, the intermediate shell plate R2507-1 had approximately the same copper and phosphorus content as the other beltline plate materials. Therefore, based on the highest initial RT_{NDT} and the lowest USE, the intermediate shell plate R2507-1 was chosen for the surveillance program.

The weld material in the South Texas Unit 2 surveillance program was made of the same wire as all the reactor vessel beltline welds, thus it was chosen as the surveillance weld material.

Hence, Criterion 1 is met for the South Texas Unit 2 reactor vessel.

Criterion 2: Scatter in the plots of Charpy energy versus temperature for the irradiated and unirradiated conditions should be small enough to permit the determination of the 30 ft-lb temperature and upper shelf energy unambiguously.

Based on engineering judgment, the scatter in the data presented in these plots is small enough to permit the determination of the 30 ft-lb temperature and the upper shelf energy of the South Texas Unit 2 surveillance materials unambiguously. Hence, the South Texas Unit 2 surveillance program meets this criterion.

Criterion 3: When there are two or more sets of surveillance data from one reactor, the scatter of ΔRT_{NDT} values about a best-fit line drawn as described in Regulatory Position 2.1 normally should be less than 28°F for welds and 17°F for base metal. Even if the fluence range is large (two or more orders of magnitude), the scatter should not exceed twice those values. Even if the data fail this criterion for use in shift calculations, they may be credible for determining decrease in upper shelf energy if the upper shelf can be clearly determined, following the definition given in ASTM E185-82.

The functional form of the least squares method as described in Regulatory Position 2.1 will be utilized to determine a best-fit line for this data and to determine if the scatter of these ΔRT_{NDT} values about this line is less than 28°F for welds and less than 17°F for the plate.

Following is the calculation of the best-fit line as described in Regulatory Position 2.1 of Regulatory

Guide 1.99, Revision 2. In addition, the recommended NRC methods for determining credibility will be followed. The NRC methods were presented to industry at a meeting held by the NRC on February 12 and 13, 1998. At this meeting the NRC presented five cases. Of the five cases, Case 1 ("Surveillance data available from plant but no other source") most closely represents the situation listed above for South Texas Unit 2 surveillance weld metal and plate materials.

TABLE D-1

Calculation of Chemistry Factors using South Texas Unit 2 Surveillance Capsule Data

Material	Capsule	Capsule f[a]	FF[b]	ΔRT_{NDT}[c]	$FF * \Delta RT_{NDT}$	FF^2
Intermediate Shell	V	0.23	0.60	16.39	9.83	0.36
Plate R2507-1	Y	1.21	1.05	33.96	35.66	1.10
(Longitudinal)	U	2.40	1.24	27.48	34.08	1.54
Intermediate Shell	V	0.23	0.60	11.86	7.12	0.36
Plate R2507-1	Y	1.21	1.05	35.26	37.02	1.10
(Transverse)	U	2.40	1.24	40.18	49.82	1.54
				SUM:	173.53	6.00
	$CF_{R2507-1} = \Sigma(FF * RT_{NDT}) + \Sigma(FF^2) = (173.53) \div (6.00) = \mathbf{28.9°F}$					
Surveillance Weld	V	0.23	0.60	-7.6	-4.64	0.30
Material[d]	Y	1.21	1.05	4.08	4.28	1.10
	U	2.40	1.24	20.64	25.59	1.54
				SUM:	25.23	3.00
	$CF_{Surv.\ Weld} = \Sigma(FF * RT_{NDT}) \div \Sigma(FF^2) = (25.23) \div (3.01) = \mathbf{8.4°F}$					

Notes:

(a) f = fluence. See Table 6.2-3, [x 10^{19} n/cm^2, E > 1.0 MeV].

(b) FF = fluence factor = $f^{(0.28 - 0.1 * \log f)}$.

(c) ΔRT_{NDT} values are the measured 30 ft-lb shift values taken from Appendix C, herein [°F].

The scatter of ΔRT_{NDT} values about the functional form of a best-fit line drawn as described in Regulatory Position 2.1 is presented in Table D-2.

Table D-2:
South Texas Unit 2 Surveillance Capsule Data Scatter about the Best-Fit Line for Surveillance Forging Materials.

Material	Capsule	CF ($Slope_{best\ fit}$)	FF	Measured ΔRT_{NDT}	Predicted ΔRT_{NDT}	Scatter ΔRT_{NDT} (°F)	<17°F (Base Metals) or <28°F (Weld)
Intermediate Shell Plate R2507-1 (Longitudinal)	V	28.9	0.60	16.39	17.63	-1.24	Yes
	Y	28.9	1.05	33.96	30.35	3.61	Yes
	U	28.9	1.24	27.48	35.84	-8.36	Yes
Intermediate Shell Plate R2507-1 (Transverse)	V	28.9	0.60	11.86	17.63	-5.77	Yes
	Y	28.9	1.05	35.26	30.35	4.91	Yes
	U	28.9	1.24	40.18	35.84	4.34	Yes
Vessel Beltline Welds (Heat # 90209)	V	8.4	0.60	-7.6	5.04	-12.64	Yes
	Y	8.4	1.05	4.08	8.82	-4.74	Yes
	U	8.4	1.24	20.64	10.42	10.22	Yes

Table D-2 indicates that no data point falls outside the +/- 1σ of 17°F scatter band for the intermediate shell plate R2507-1 surveillance data. In addition, no data points fall outside the +/- 1σ of 28°F scatter band for the surveillance weld data. Therefore, the intermediate shell plate R2507-1 and the weld data is deemed credible per the third criterion.

Criterion 4: The irradiation temperature of the Charpy specimens in the capsule should match the vessel wall temperature at the cladding/base metal interface within +/- 25°F.

The capsule specimens are located in the reactor between the core barrel and the vessel wall and are positioned opposite the center of the core. The test capsules are in baskets attached to the neutron pad. The location of the specimens with respect to the reactor vessel beltline provides assurance that the reactor vessel wall and the specimens experience equivalent operating conditions such that the temperatures will not differ by more than 25°F. Hence, this criterion is met.

Criterion 5: The surveillance data for the correlation monitor material in the capsule should fall within the scatter band of the database for that material.

The South Texas Unit 2 surveillance program does not contain correlation monitor material. Therefore, this criterion is not applicable to the South Texas Unit 2 surveillance program.

CONCLUSION:

Based on the preceding responses to all five criteria of Regulatory Guide 1.99, Revision 2, Section B and 10 CFR 50.61, the South Texas Unit 2 surveillance plate and weld data is credible.